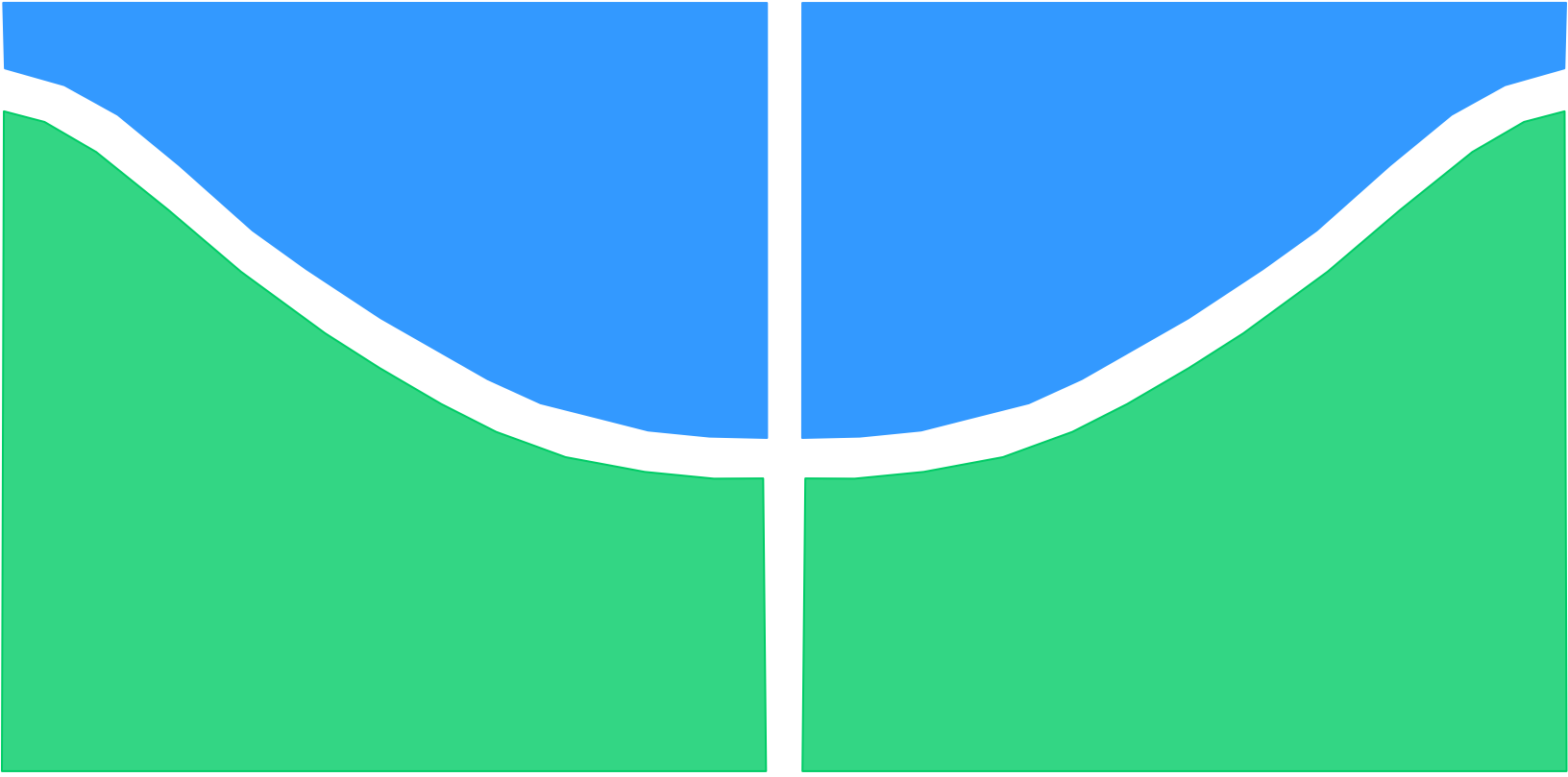

METHODOLOGY TO IDENTIFY WELD STABILITY IN THE GAS METAL ARC WELDING PROCESS

Por,

Elina Mylen Montero Puñales, MSc.

UNIVERSIDADE DE BRASÍLIA, UnB

Brasília, 2025

Faculdade de Tecnologia

Departamento de Engenharia Mecânica

Programa de Pós-Graduação em Sistemas Mecatrônicos

UNIVERSIDADE DE BRASÍLIA

Faculdade de Tecnologia
Departamento de Engenharia Mecânica
Programa de Pós-Graduação em Sistemas Mecatrônicos

Tese apresentado ao Programa de Pós-graduação em Sistemas Mecatrônicos, como parte dos requisitos necessários à obtenção do título de Doutor.

Orientador: Sadek C. Absi Alfaro, PhD

ABSTRACT

The Gas Metal Arc Welding (GMAW) process is widely employed in industrial production due to its efficiency and versatility. As a result, significant efforts are directed toward selecting the most suitable parameters to ensure high weld quality. One of the most critical and extensively studied factors affecting quality is process stability. This research proposes a comprehensive methodology for analyzing welding data to detect instability and develop a corresponding stability indicator. The approach emphasizes sensor fusion, integrating information from multiple sources—including acoustic signals, images, and current measurements—collected during the welding process. Various parameter configurations were explored to evaluate the three primary metal transfer modes. A detailed statistical analysis was conducted, and advanced techniques such as image processing, acoustic signal analysis, and machine learning were employed to support the evaluation and classification of process stability.

Keywords: GMAW; quality index; process stability, welding

TÍTULO EM PORTUGUÊS:

Metodologia para Identificar a Estabilidade da Soldagem no Processo de arco elétrico com gás de proteção GMAW

RESUMO

O processo de soldagem a arco com gás e eletrodo metálico (GMAW) é amplamente utilizado na produção industrial devido à sua eficiência e versatilidade. Por isso, grandes esforços são direcionados à seleção dos parâmetros mais adequados para garantir a qualidade da solda. Um dos fatores mais críticos e amplamente estudados que influenciam essa qualidade é a estabilidade do processo. Este trabalho propõe uma metodologia abrangente para a análise de dados de soldagem visando identificar instabilidades e desenvolver um indicador de estabilidade correspondente. A abordagem adotada enfatiza a fusão sensorial, integrando informações provenientes de múltiplas fontes — sinais acústicos, imagens e medições de corrente — captadas durante o processo de soldagem. Diversas configurações de parâmetros foram exploradas para avaliar os três principais modos de transferência metálica. Foi realizada uma análise estatística detalhada, e aplicaram-se técnicas avançadas como processamento de imagens, análise de sinais sonoros e algoritmos de aprendizado de máquina para apoiar a avaliação e classificação da estabilidade do processo.

Palavras-chave: GMAW; índice de qualidade; estabilidade do processo; soldagem

Index

Figures index

Tables index

Abbreviations list

GMAW	Gas Metal Arc Welding
MAG	Metal Active Gas
MIG	Metal Inert Gas
CTWD	Contact tip-to-work- piece distance
IVcc	Regularity index
ΔFcc	Cutting frequency index
FFT	Fast Fourier Transform
SPL	Sound Pressure Level
S	Amplitude of the sound signal over time
Po	Reference Acoustic Pressure (20 uPa)
ξ	Integration time variable
t	Start time

T	Integration Time Range
SD	Standard Deviation
bkg	Background welding current
pkv	Peak welding current
Ipa	Input parameters a lteration

1 Introduction

GMAW (Gas Metal Arc Welding) is a widely adopted welding process known for its high production efficiency, operational reliability, and suitability for automation. It employs a continuously fed consumable electrode and a shielding gas to establish an electric arc with the workpiece. Depending on the type of shielding gas used—either inert or active—the process is classified as Metal Inert Gas (MIG) or Metal Active Gas (MAG) welding, respectively. With appropriate parameter settings, GMAW can be applied in various welding positions and across a broad range of metallic materials.

A central feature of the process is the metal transfer mode, which determines how molten droplets are transferred from the wire to the weld pool. This behavior is directly influenced by key process parameters such as current (amperage), voltage, wire stick-out, and welding speed. The three main modes of metal transfer are short-circuit, globular, and spray. Due to the complex interplay among these parameters and the sensitivity of the arc behavior to small perturbations, the process exhibits highly dynamic and nonlinear characteristics. In many operational scenarios, this complexity results in behavior that is difficult to predict, often modeled as stochastic or governed by nonlinear dynamics.

Hence, significant efforts are devoted to selecting the appropriate procedures to ensure the highest quality. Quality, in this context, can be defined as meeting a client's product requirements. In the specific case of welding, the primary goal is to achieve a weld bead that closely aligns with the specified requirements. Welding quality can be monitored at two stages: online, while the welding process is in progress, and offline, after obtaining the welded bead.

The offline evaluation considered geometric factors such as proper penetration, reinforcement, and the dimensional consistency of the welded parts. Destructive tests can be carried out; they consist of taking samples of weldments to evaluate metallic continuity, mechanical strength, and other critical factors for ensuring adequate performance in service. In some cases, these tests result in the destruction of the tested specimen. On the other hand, Wu et al. (C. Wu, Polte, & Rehfeldt, 2001) affirm that online quality control allows cost savings by reducing

defects in the production line. For this purpose, sensors for visual imaging, sound acquisition, infrared thermography, and ultrasonic inspection have been implemented.

One concept that is strongly correlated to the online quality is the control of the process stability. According to Ponomarev (Ponomarev, 1997), the stability of the GMAW process is evaluated online by three factors: metallic transfer regularity, arc stability, and the operational behavior of the welding process. Meneses (L. Y. H. Meneses, 2013) also ensures that the higher the transfer stability, the higher the penetration and the less the amount of spatter.

However, these models do have certain limitations. They are typically designed to function within a specific metal transfer mode and lack the flexibility to be generalized. A significant proportion of them are primarily geared towards the short-circuit transfer mode and offline evaluation. Relatively few proposals incorporate sensory fusion techniques to integrate process signals such as sound, images, and current data. Furthermore, there is a shortage of models harnessing the potential of new data analysis and machine learning techniques.

To address these limitations, a novel quality index has been developed, leveraging concepts from machine learning. This proposed index, powered by artificial intelligence, enables real-time monitoring of the welding process, facilitating the detection of defects and the assessment of its stability. It utilizes acoustic monitoring, image processing, statistical modeling, and data analysis algorithms to achieve its objectives.

1.1 General objective

The primary aim of this study is to propose a stability index for the GMAW (Gas Metal Arc Welding) process by employing a combination of statistical methods, image processing algorithms, and machine learning techniques.

1.2 Specific objectives

- Modeling the geometrical characteristics of the weld bead to find the optimum voltage parameters, wire feed speed, and welding speed.

- Configure the necessary equipment to obtain the digital sound, image, and current signals.
- Develop a data processing methodology for data integration, feature extraction, and identification of stability process characteristics.
- Develop an algorithm of image processing, tools, and methodology to measure the drop detachment and the transference mode.
- Develop an algorithm to calculate the frequency and sound pressure characteristics.
- Develop a stability index using the features extracted from the data behavior.
- Develop a machine learning model that implements the quality index for stability evaluation.

1.3 Potential applications.

- This work develops a stability index that can be applied in the industry for real-time monitoring of the welding process.

- It can also be used for welder training, laboratory research, and process modeling.

1.4 Justificative

The GMAW process exhibits stochastic and nonlinear behavior, which contributes to the complexity of modeling it accurately. Developing a quality indicator to support the adjustment of process parameters and achieve the expected welding performance remains a challenging task..

In the last years with the increase of the technologies, the solutions with machine learning have increased, which has made it possible to implement new solutions in real-time. Also, there are great possibilities to integrate and process several signals simultaneously.

1.5 Summary of results

PUÑALES, Elina Mylen Montero; BESTARD, Guillermo Álvarez. Estudio de las técnicas de inteligencia artificial empleadas en la evaluación de la calidad del proceso de soldadura. In:

TALLER INTERNACIONAL DE CIBERNÉTICA APLICADA, 21–23 feb. 2017, La Habana, Cuba. La Habana: Revista Electrónica CUJAE, 2017.

Preprocessing of data obtained in the GMAW welding process using machine learning techniques (result presented in conference IV Conferencia Internacional de Soldadura y Unión de Materiales - ICONWELD 2018 (Montero Puñales, Elina Mylen; Absi Alfaro, 2018))

Stability on the GMAW Process, Elina Mylen Montero Puñales and Sadek Crisóstomo Absi Alfaro, submitted: August 29th, 2019 Reviewed: November 5th, 2019 Published: January 14th, 2021, DOI: 10.5772/intechopen.90386

PUNALES, Elina Mylen Montero; BESTARD, Guillermo Alvarez; ALFARO, Sadek. Improving weld stability in Gas Metal Arc Welding: a data-driven and machine learning approach. Crystals, ISSN 2073-4352. Fator de impacto: 2.4. Qualis A3. Seção: Crystalline Metals and Alloys. Edição especial: Fatigue and Fracture of Welded Structures. Manuscript ID: crystals-3544966, 2025

PUNALES, Elina Mylen Montero; BESTARD, Guillermo Alvarez; CARIBÉ, Guilherme; ALFARO, Sadek. Melhorando a estabilidade da soldagem em GMAW: uma abordagem baseada em dados. In: ENCONTRO DE PÓS-GRADUAÇÃO NA UNB GAMA, 1., 2025, Brasília. Brasília: UnB Gama, 2025.

1.6 Work organization

The present work is structured into well-defined chapters, each of which addresses a specific stage of the research process and contributes to the overall development of the study. Below is a description of the content covered in each chapter.

Chapter 2 presents a comprehensive literature review of the GMAW (Gas Metal Arc Welding) process. It includes a detailed compilation of the factors that influence process stability, an analysis of previously proposed stability indexes, and a critical synthesis of the main findings in the field. This chapter establishes the theoretical foundation upon which the present research is developed.

Chapter 3 details the data acquisition procedures and the development of the open-loop control system used in the experiments. It describes the tools, sensors, and configurations applied to capture synchronized signals of current, sound, and images, as well as the methodology adopted to ensure experimental consistency and reproducibility. This chapter lays the technical groundwork for subsequent analyses.

Chapter 4 is dedicated to the presentation and analysis of the experimental results. It includes a thorough discussion of the findings obtained through multisensory data processing, the application of feature extraction techniques, and the construction of the proposed stability index. The chapter also covers the development and performance evaluation of a machine learning model aimed at classifying the stability of the welding process.

Finally, the **Bibliographic References** section compiles all relevant sources used throughout the research. This includes scientific articles, technical books, theses, patents, and other documents that support the theoretical and methodological basis of the study.

2 Literature review

2.1 Stability Control in the GMAW process

This chapter presents a detailed literature review that supports the theoretical foundation of the present research. The objective is to examine the key aspects related to the stability of the Gas Metal Arc Welding (GMAW) process, with emphasis on the variables that influence arc behavior and weld quality.

We begin by discussing the concept of stability control in GMAW and the operational characteristics of the process. Subsequently, we analyze the factors that affect arc stability, including current and voltage waveforms, droplet transfer control, and spatter generation. The chapter also reviews existing stability indexes and statistical techniques for disturbance identification.

Further sections explore the role of acoustic signal monitoring and the application of machine learning methods in welding quality evaluation. Finally, a synthesis of recent research highlights the most relevant contributions from the last five years, identifies innovative techniques, and outlines areas that require further investigation.

To carry out this research, the following have been used: the database Periódicos Capes (available in the central library of the Brasilia University); keywords related to the subject to be investigated were defined (welding, GMAW, quality index, MIG/MAG, process stability); publications in major journals such as the Journal of Materials Processing Technology (A1), Soldagem & Inspeção (B2), International Journal of Advanced Manufacturing Technology (B1), Welding Journal (A1), Materials and Manufacturing Processes (B1).

The literature search was conducted in English, Portuguese, and Spanish and a total of 284 documents were recovered, of which 75 were used in the bibliometric analysis. The work covers a time frame of the last 20 years in general and the last decade more specifically. The distribution of papers by years is indicated in Figure 1. The number of applications has been increasing over the last 10 years.

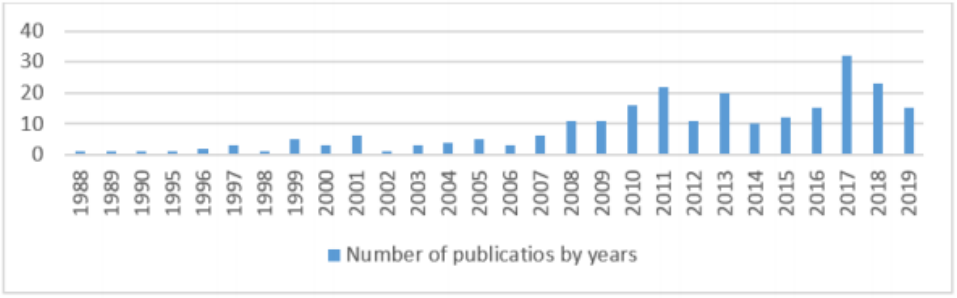

Figure 1 Number of publications per year (Total 284).

2.2 GMAW process operation

GMAW process is characterized by producing an arc between a consumable electrode that is constantly fed, protective gas and the piece to be welded, as represented in Figure 2.

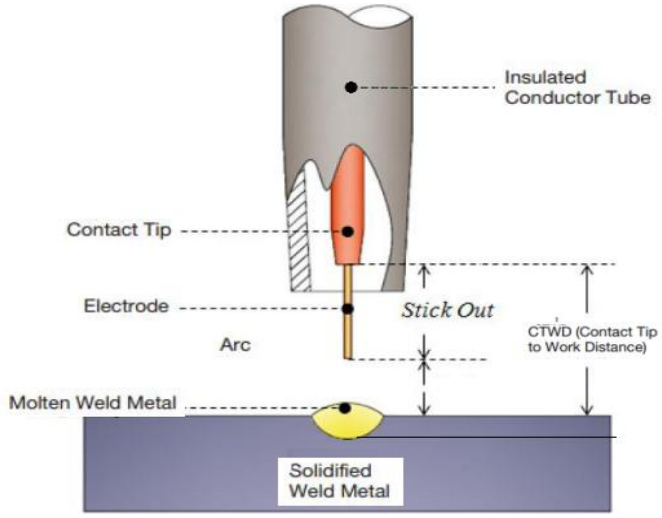

Figure 2 Basic diagram of the MIG / MAG process (Modified from (Pinto Lopera, 2016))

- Conductor Tube**:** It is a component of the welding torch that connects the torch body to the front end. It guides the welding wire, conducts the electrical current, and channels the shielding gas towards the contact tip and nozzle region.

- Nozzle: A non-conductive component located at the tip of the welding torch in GMAW. Its main function is to direct and evenly distribute the shielding gas over the weld pool and arc area, preventing contamination from atmospheric gases.

- Contact Tip: It is a torch device that has the function of guiding and supplying voltage to the wire.
- Electrode: It is the consumable copper-coated steel electrode that melts with the electric arc and transfers to the melting pool.
- Workpiece: composed of the metal bodies to be joined by the weld.
- CTWD (Contact Tip to Work Distance): It is often confused with the distance between the contact tip and the workpiece, which coincides when the nozzle front cut is also the same as the contact tip front cut.
- Stick out: Is the length of free wire after it has passed through the contact tip.

The gas composition aims to stabilize the arc and protect the welding material from atmospheric gases such as nitrogen and oxygen, which can cause fusion defects, porosity, and weld metal embrittlement if they come in contact with the electrode, the arc, or the welding metal. Depending on whether the gas is inert (Ar ou He) or active (CO2, or mixtures including N2 or O2), it can be classified as Metal Active Gas (MAG) or Metal Inert Gas (MIG).

The weld bead geometry depends directly to the parameters that govern the process. The Figure 3 outlines these geometric parameters in the cross-section of a weld bead. The most important parameters affecting penetration and geometry in the GMAW process are welding current, arc voltage, torch travel speed or welding speed, stick out, torch tilt, and the diameter of the electrode.

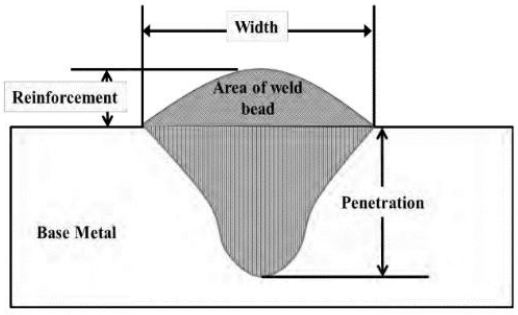

Figure 3 Weld bead geometric characteristics (Margarita et al., 2013)

According to (Guillermo Alvarez Bestard, 2017) the process parameters of GMAW can be divided into five basics groups (as shows Figure 4):

- Fixed, that can't be modified by the operator and it is defined in the process design.
- Adjustable online, that can be modified during the process.
- Adjustable offline, that can be modified only before starting the process.
- Quantifiable online, which is measurable during the process.
- Quantifiable offline, which is measurable only after the process ended.

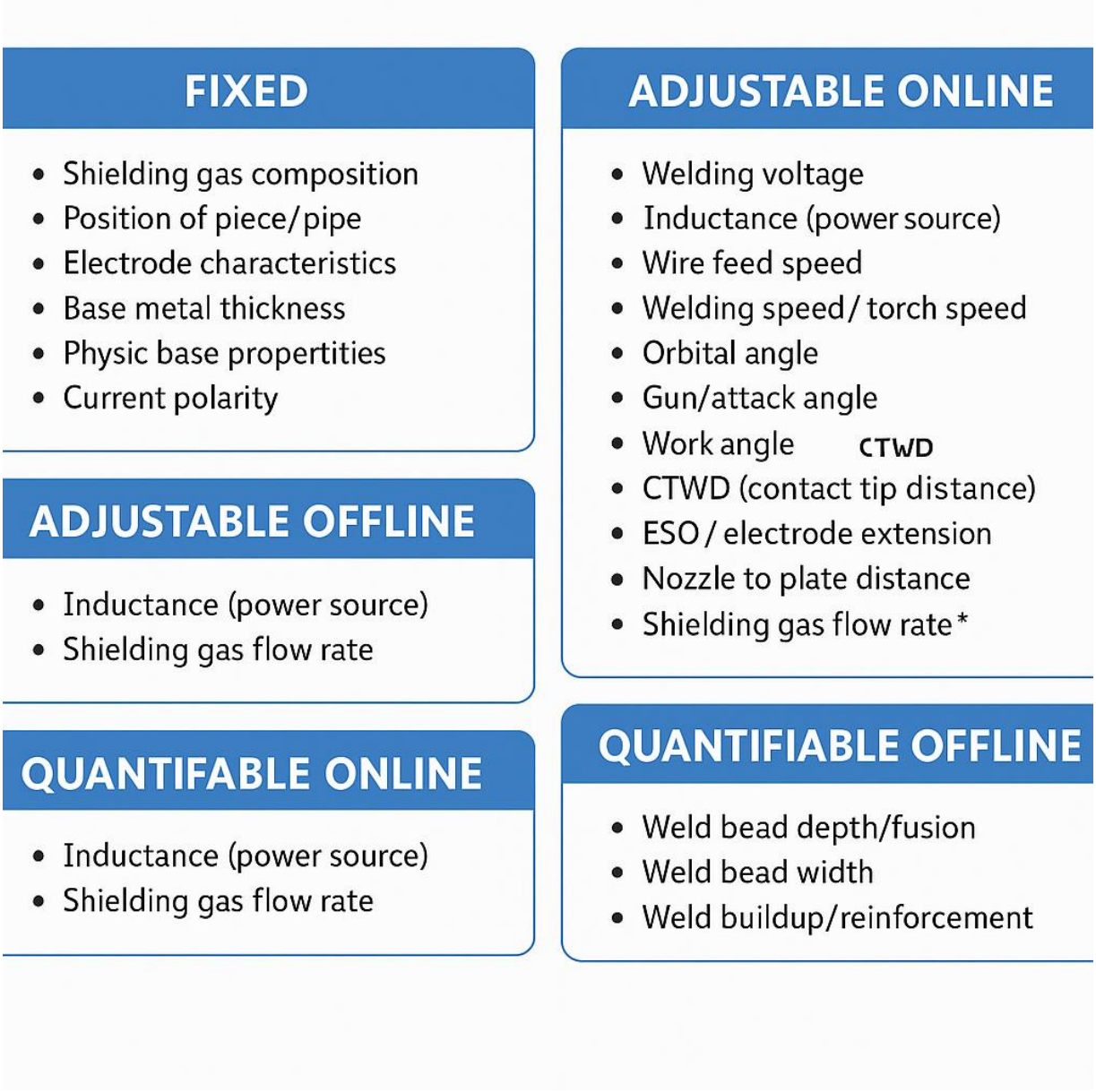

Figure 4 Classifications of GMAW parameters (Guillermo Alvarez Bestard, 2017)

2.3 Factors that affect the stability

The operational behavior plays a key role in the stability of the process. If the gas is not supplied accurately, the protective effect will be affected; nitrogen, oxygen, and water vapor enter the welding region and direct contacts with the arc and melting metals, reducing the arc

stability and forming a variety of welding defects. In the same way presence of grease, paint, dust, humidity and extreme temperature produce a variation on the welding voltage.

But arc stability is directly influenced by the parameters of the process. A relationship exists between arc length and process stability. Increasing the arc length (due to an increase in the contact tip to work distance) leads to a destabilization of the process, producing variations in welding current and arc voltage. When the voltage is too low, the arc becomes short and the droplet may not detach properly or contact the molten pool (Hermans & Den Ouden, 1999)

The parameter's wire feed speed also has an influence. By increasing the feed rate of the wire, the diameter of the drop decreases; very high or lower values coincide with the most unstable conditions. But the degree of this influence depends on the shielding gas used and the welding voltage.

Furthermore, the variation of the current affects the metallic transfer regularity and the transfer regularity reflects the stability of the process. Then it can be said that these factors are going to be influenced by the dynamic behavior of the GMAW welding process, particularly by the physical variations during the different transfer modes. Consequently, to understand how these factors influenced the stability, it is necessary to delve into the characteristics of the metal transfer.

The metal transfer has a direct influence on the stability of the arc and the final geometry of the weld bead. The metal transfer is controlled by several parameters such as current, voltage, electrode diameter, and shielding gas composition. It directly influences the way that metal droplets are transferred; the uniformity and the volume of the drop, and variations in arc length.

The three first transfer modes are short circuit, globular, and spray. In addition to these modes of transfer, there are others classified as free-flight transfer modes which happen when the arc voltage is high and includes repelled globular; projected spray; streaming spray, and rotating spray. The present study focuses on the three first natural modes of transference.

Spray transfer is characterized by small, uniform droplets with diameters close to the size of the electrode. This transfer mode is achieved using high current intensities and voltages. For carbon steel, typical spray transfer occurs within a current range of 150 to 500 A and voltages from 24 to 40 V. However, for materials such as aluminum, higher values are usually required due to their thermal conductivity and electrical properties. The process is known for its high arc stability, high current levels, deep penetration in the workpiece, and high detachment frequency. Voltage and welding current oscillograms do not vary significantly, as shown in Figure 5.

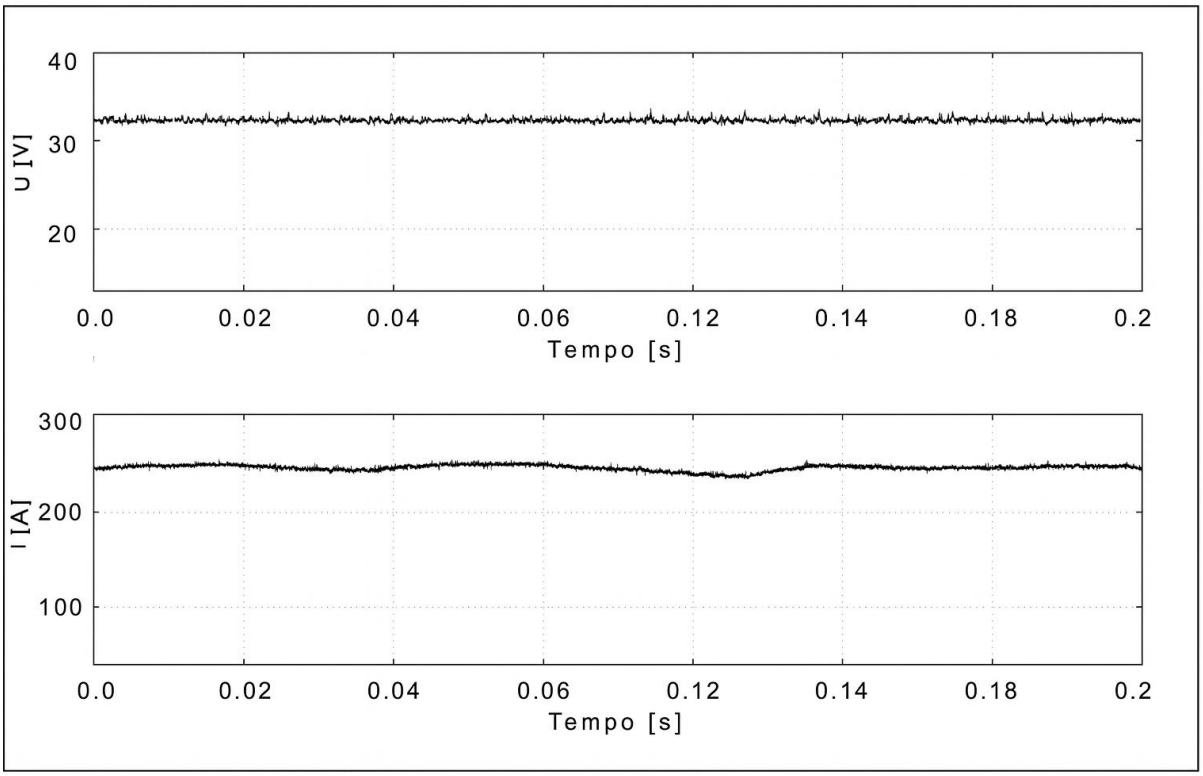

Figure 5 Waveform factors Spray transfer mode (FIGUEIREDO, 2000)

In the globular transfer, the drop grows until exceeding the size of the electrode and the detachment occurs by the action of the gravitational force. Typical parameters in globular transfer are Voltage 20 to 36V, Current Intensity 70 to 255A. It has been unwanted in the industry for its instability and high grade of spatter. During this transfer mode, the output currents are kept oscillating depending on the detachment of the drop, as shown in Figure 6.

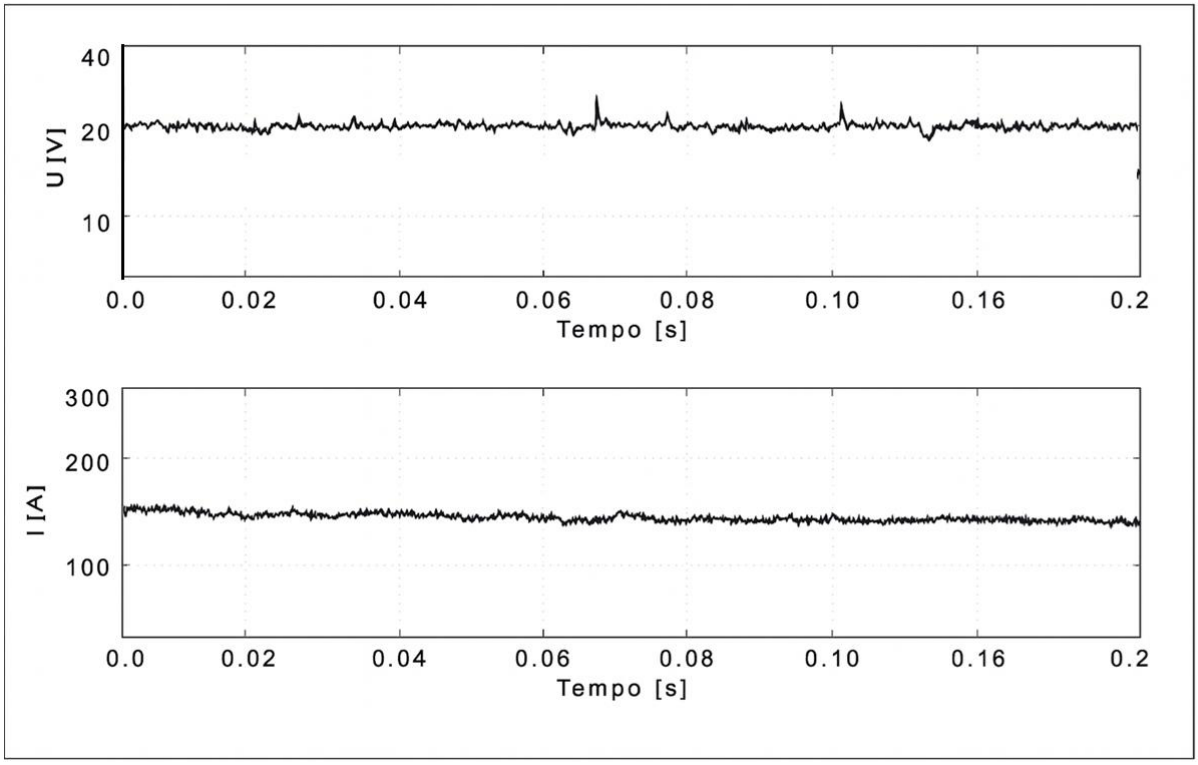

Figure 6 Waveform factors Globular transfer mode (FIGUEIREDO, 2000).

The pulsed transfer is considered a particular case of spray transfer but is characterized by great stability that is achieved by controlling the process variables, in particular the current. The welding equipment generates two levels of current, in the first, the base current (Ib) is kept low so that there is no transfer, but only the onset of wire fusion; in the second, the peak current (Ip) is higher than the globular transition current causing the transfer, under optimal operating conditions, of a single drop. Typical parameters in pulsed transfer are Voltage 20 to 30 V, Current Intensity 100 to 300A, as shown in Figure 7.

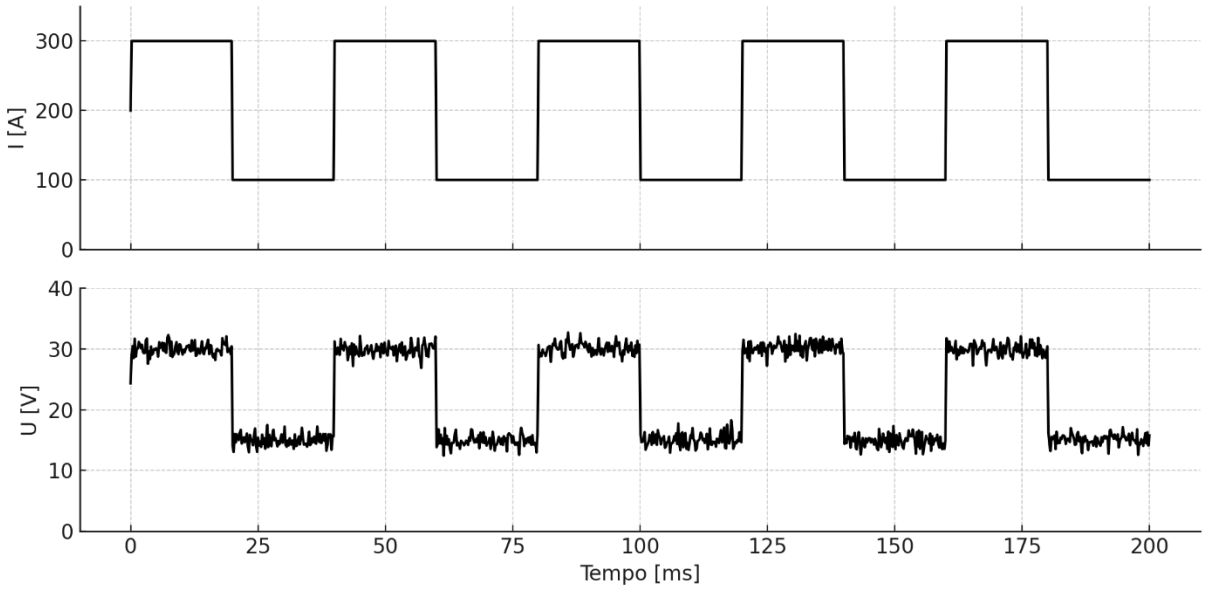

Figure 7 Waveform factors (modified from (CHÁVEZ, 2014))

Another parameter that influences the stability of the process is the transition current, which changes the frequency and diameter of the transferred drops.

In the case of a given current of short-circuiting transition, the droplet transfer exists in the form of short-circuiting, and the welding is stable. When the welding current increases, the droplet transition changes from the short-circuiting mode to the mixed mode, so the welding process and electric signal become unstable.

On the other hand, the globular - spray transition current has great instability; a greater number of spatters and the arc is no longer extinguished. Studies show that with the increase of CO2 in the gas mixture an increase of the transition current is produced.

Finally, a peculiarity of the short circuit transfer mode is the existence of regular contact between the electrode and the workpiece. Typical short circuit parameters are Voltage 16 to 22V: Current intensity 50 to 150A. When the short circuit occurs, the arc is extinguished establishing two characteristic phases: the arcing period and the short-circuit period. Droplet growth occurs in the arcing period, whereas, during the contact period the metal is transferred. Also, the voltage and current oscillate to high and low at the same frequency of the metal transfer (see Figure 8).

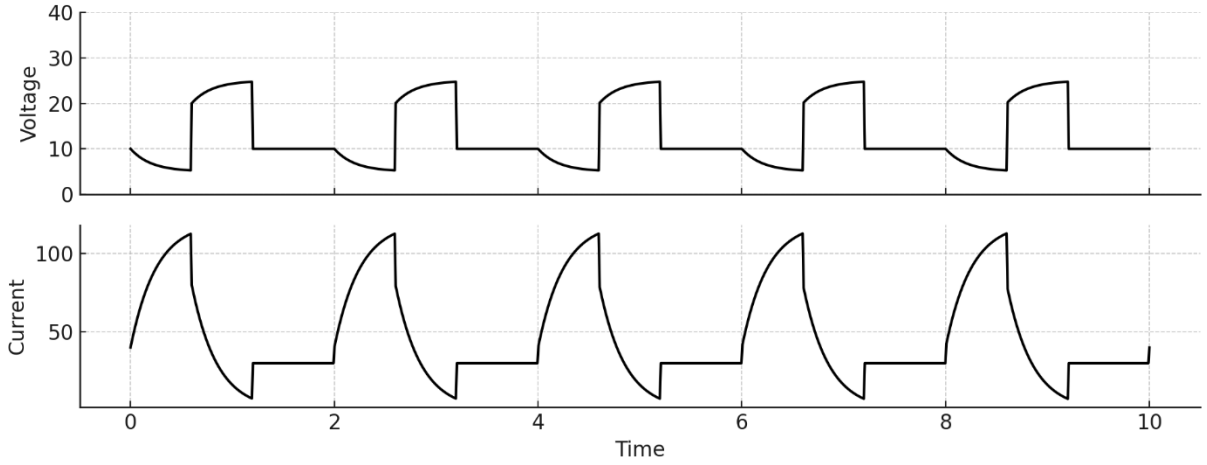

Figure 8 Waveform factors (modified from (Mita, Sakabe, & Yokoo, 1988))

Furthermore, exists a relationship between the waveform factor of the short circuit and the arc stability. Some parameters (relating to time and current) used to quantify stability are easy to calculate from the waveform factor, as the short circuit time, the arcing time, the transfer period, and the short-circuit frequency. Mita et al. (Mita et al., 1988) also affirm that the correlation between those parameters and the stability becomes weaker with increasing current.

2.4 Summary of stability indexes

Using the above-mentioned concepts, several indexes have been proposed to infer the stability and quality of the welding process. They were calculated using image processing techniques, acoustic monitoring, and analysis of the electrical signals. Figure 9 shows the percentage of papers classified by transfer modes and it was found that the highest percentage of indexes focused on the short circuit transfer mode.

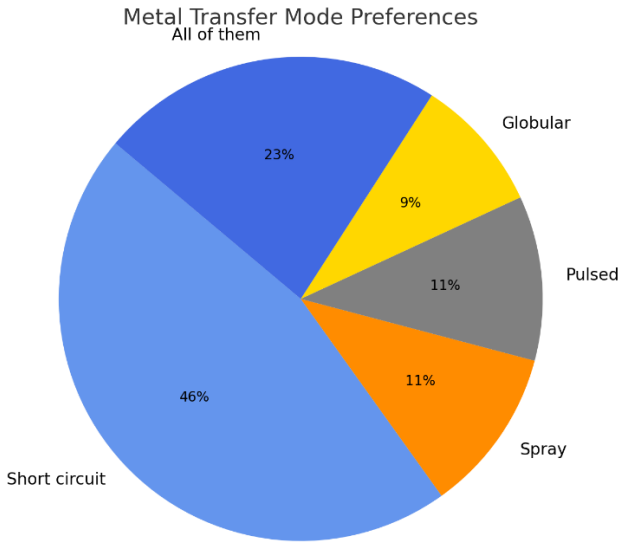

Figure 9 Papers classified by transfer modes

2.5 Statistical analysis to identify disturbances

Knowing that a signal behaves according to a stochastic process, it is possible to determine a probabilistic model and apply some algorithms to process this signal. Hence, several works have focused on the study of the electrical signals at the moment of disturbance, using a statistical treatment.

Adolfsson and Bahrami (Adolfsson & Bahrami, 1999) calculate the variance of weld voltage (every 1024 signals). The study validates the hypothesis that the instability of the process (caused by disturbances) correlates with a decrease in the variance of the weld voltage; similarly, the short-circuit transfer rate decreased; conversely, no decrease occurs in the estimated variance of the weld current. The results obtained were used in the development of an online fault detection algorithm. This work shows a promising stability index, but is only oriented to short circuit transfer mode and was not extended to other transferences modes. Note that the moments of disturbance were caused by making cuts in the workpiece and not varying input variables of the process such as wire feed speed, welding speed, and contact tip-to-work- piece distance (CTWD), which also influence the stability.

Luksa (Luksa, 2006), calculates the mean value of the short circuit; the variance of welding current; the time of arc burning and the short circuit frequency values (every 2200 signals samples). He identifies two types of disturbances those caused by external factors such as grease and paint that affect the gas shield of the welding arc and a second group caused by variations in the wire extension. As was mentioned in previous work the author indicates that the variance of weld voltage decreased in the disturbance moment. But he also affirms that the short-circuit rates increase and optimal process stability can also occur during step disturbance, which contradicts the results found by (Adolfsson & Bahrami, 1999). An interesting contribution of this work is the study of the correct data window size since very large or small data window size can lead to erroneous stability results.

Finally, Wu et al. (C. S. Wu, Gao, & Hu, 2007) used statistical process control (SPC), creating a sequential chart of the welding voltage and current (every 2000 signals). Coinciding with the index previously presented, a decrease in the estimated variance of the welding voltage occurs during the disturbance step. They also understand as a result an increase in the kurtosis for both the welding voltage and current. The results were generalized for the three main transferences modes and used in the construction of an SPC.

2.6 Arc stability

We consider a stable process when the variables have the quality of keeping in balance, not varying, or staying in the same state for a while. But, in the case of the short circuit, the current and voltage variables keep oscillating and the arc opens and closes continuously. Them, when the stability of a short-circuiting welding process is considered it cannot be treated as arc stability since in this case, the arc is essentially unstable: The cyclic repetition of this unstable system is what makes the process viable, the regularity of this behavior being an indication of process stability.

In 1988, the authors Mita et al. (Mita et al., 1988) enunciated the correlation between the stability of the arc and standard deviation of the arcing time; the standard deviation of short current, and the average value of short circuit frequency. They used linear regression to prove this correlation and to create a new stability index. They showed that short circuit frequency is

influenced by several welding parameters mainly the wire feed rate and the arc voltage. Also, affirm that the stability of the process grows when the standard deviation of the short circuit frequency decreases. Although, the proposed index was tested in all current ranges and the authors conclude that good arc stability can be obtained in all transfer modes.

Hermans and Ouden (Hermans & Ouden, 1999) propose a criterion for arc stability (equation 1), based on the short circuit frequency using the relationship between the arc time and the short circuit time. To do this, they analyzed the behavior of the weld pool taking images with a high-speed camera. The authors concluded that the moment in which the oscillation frequency of the welding pool and the short circuit frequency are synchronized is reached the greatest stability.

Ogunbiyi and Norris (Ogunbiyi & Norrish, 1997) perform a summary of several criteria presented by other authors and proposes three indexes to calculate the stability of the metal transfer. Transfer index (Equation 2, Table 1), transfer stability index (Equation 3, Table 1), and dip consistency index (Equation4, Table 1), highlighting the correlation between the metal transfer modes, the arc stability, and the current waveform. The study confronts the three main modes of metal transfer, an advantage to other studies. They calculate the indexes based on the relationship between minimum, mean, and maximum welding current. The indexes and the mathematical formulation is presented in Table 1. They also use the voltage waveform to predict the mode of metal transfer because more variations are observed in the voltage moving from spray to short circuit transfer. They perform a generalization and propose a new index Power Ratio (PR) (Equation 5, Table 1), used for identification of the metal transfer mode and arc stability. Finally, an online monitoring system was created capable of predicting the status of the process.

Simpson (Simpson, 2008) presents a stability index using an image processing method known as signature images. This index is calculated successively from the comparison of two images of dimensional histograms of the voltage and current data, allowing the detection of faults for the three main modes of metal transfer. Although it is a method of image processing that does not require high-speed cameras, instead, a good data acquisition system must work in real-

time. Therefore, it can be considered as a cheap and feasible method to implement in the industry

Finally, the group Laprosolda of the Federal University of Uberlândia, Brazil [12,13] in a similar approximation, based on numerical and statistical techniques, propose two indexes for the short circuit transfer mode. The Regularity index (IVcc) (Equation 6, Table 1) criteria for quantifying the short-circuit transfer stability in the MIG/MAG welding process. Taking into account the constancy of the short-circuit and open-arc times and Cutting frequency index (ΔFcc) (Equation 7, Table 1) criteria to determine the voltage regulation range that guarantees greater stability of metal transfer in GMAW short circuit. Using wire-electrode diameter; wire feed rate; drop diameter as a function of the wire diameter. They address metal transfer behavior (especially regarding the correlation between the stability of transfer mode and the welding defects). The use of these indices allowed the authors to test the correlation between the inductance; the regularity of the metallic transfer and the influence of the variation in the contact tip to work distance (CTWD), with 3 different types of gases. In addition, the proposed indices have been widely used in other studies some of them are discussed below.

Sousa (2010) (Souza, 2010) presents work related to mapping the droplet transfer modes to help welders in the choice of the best welding setting parameters needed. The maps were proposed for spray and short circuit transfer modes. They used the IVcc and ΔFcc parameters to allow focusing voltage range and to obtain transfer regions with proper operating characteristics for the short circuit mode. The study demonstrates that the index has the characteristic of decreasing and then again increasing its value with increasing welding voltage. As smaller index values indicate better stability, it appears that the process has poor stability at very low and very high voltages.

Meneses (2013) (L. Y. H. Meneses, 2013) presents an implementation of a model that represents the GMAW process in orbital welding. She also developed a study of metal transfer control, to achieve a high level of quality of welded joint in different conditions. The mentioned indices were used to make evaluating the hypothesis possible so that more short circuits had greater stability in the process. That allows users to choose a correct parameter

setting depending on their needs, to obtain a stable transfer with appropriate welding conditions.

Costa (2014) (Costa, 2014) performed the validation of the stability on the welding process for the short circuit transfer mode. The regularity index (IVcc) and Cutting frequency (Fcc) were used and this was able to identify the tension levels that result in greater transfer regularity, lower level of spatter, higher deposition efficiency, and better surface quality of the weld bead. In the next step, they used the deposition performance; allowed to estimate the amount of material lost by slag and fumes, along with the amount of generated spatter. It was also able to evaluate the effects of the feed rate and the influence of the type of protection gas on the behavior of short circuits. Finally, he developed a thermal efficiency analysis where he concludes that there is no relationship between the values of thermal efficiency and the regularity of transfer.

Silva et al. (Correia, Gonçalves, Da Cunha, & Ferraresi, 2005) define that welding quality is related to the bead characteristics, enclosing presence of defects (surface finishing, spattering, cracking, porosity, the degree of penetration, excessive reinforcement, etc.), mechanical proprieties (strength, toughness, hardness, etc.) and chemical composition. But they also affirm that quality is a relative property. To describe quality quantitatively is a hard task. Good or bad quality is a function of the requirements for a particular application. Them, to say that a weld has the required quality, it is necessary to compare the geometry obtained with that requested in the project specifications.

In the same way as the lower standard deviation in the drop detachment, several shorts per second and standard deviation of the voltage values are stability indicators, they do not ensure the best quality. A clear example would be the case that the gas is not properly supplied, the drop detachment and sound pressure may have values that indicate a stable behavior but the final geometry will be completely deformed and far from the desired quality.

Concluding, those indices are powerful tools to determine the stability in the GMAW process and can be monitored in real-time. The short circuit frequency is one of the most suitable parameters to determine stability in the short circuit transference mode, either by correlating it

with the oscillation frequency of the weld pool or by calculating its standard deviation. The so-called Vilarinho index developed by the group Laprosolda has been widely adopted in Brazil and it is the index of stability for short circuit transfer of which the largest number of references were found.

2.7 Analysis of current and voltages waveforms

The analysis of current and voltage waveforms are used in the same way as an indicator of stability. Power spectral density and time-frequency analysis methods were used; allowed the decomposition in time and frequency of the waveforms.

Adolfsson and Bahrami (Adolfsson & Bahrami, 1999) used spectral domain analysis of measurement data to detect differences in the power spectral densities of the weld voltage and current in disturbance moments. It made possible the creation of an algorithm that detects changes in the frequencies and that enables the detection of faults. They also affirm that a decrease in the variance was reflected in a decrease in the area in the power spectral density. This work was discussed previously in section 2.3.1.

Also, Huang et al. (Huang, Wang, Zhou, Zhou, & Fang, 2017) used Hilbert–Huang transforms (HHT) and time-frequency entropy to estimate the stability of short-circuiting gas metal arc welding. Demonstrating that, when the welding is more stable, the time-frequency entropy increases. To obtain the results, the authors made variations in the input variables such as current, voltage, and welding speed; demonstrating that it is possible to use this technique to define the parameters that provide more stability. Finally, the results can be used to perform the process classification in a stable and non-stable arc. It would be interesting in future works to get an integration of these techniques with supervised machine learning algorithms to perform stability classification.

Chu et al. (Y.X.Chu, S.J.Hu, W.K.Hou, P.C.Wang, 2004), perform an analysis of power spectral density of the current and voltage signals also for processes with short circuit transfer mode using Fourier transformation to do that. To determine if the testing processes were stable, a correlation was made between the weld bead geometry and the voltage and current values. They affirm that the welding process with a unique frequency corresponds to uniform

welds and good weld surface quality, enabling the detection of stable ranges and areas with defects.

Cayo and Alfaro (E. H. Cayo & Alfaro, 2009) make a comparison between time domain and frequency domain to define which is most appropriate to calculate the stability of the S-GMAW welding process. Applying the two methods to the welding arc sound, the time domain was found the most appropriate technique. They also demonstrate that the acoustical ignitions frequency and short circuits frequency decrease in regions of instability. The results obtained can be used for the development of an online system to identify regions of disturbances.

Macías et al. (Macías, Roca, Fals, Fernández, & de la Parte, 2010) use image processing to analyze the image generated by the time-frequency diagram obtained from acoustic monitoring. Proving that the minimum standard deviation of the metal transfer weld indicates that the process is stable, as previously mentioned. The authors did not implement online monitoring but highlight the existing flexibility in terms of image processing and online signal processing. It should be noted that in future works, the authors integrate their results into a neural network with artificial intelligence to predict stability in the process.

Then, it can be concluded that power spectral density is a powerful method for the quantification of stability and allows identify faults in the process through the detection of changes in the waveform frequency. Besides, being possible to correlate the power spectral frequency with the quality of the geometry of the weld bead.

The current and voltage signals have also been used to create cyclograms that show the welding voltage as a function of welding current to obtain a process stability indicator. Cyclograms are a novel method for stability analysis in the welding process. They constitute a visual representation by graphs of the voltage values as a function of the current, see Figure 10. It has been widely used as a stability indicator for the short circuit transfer mode.

According to Moinuddin and Sharma (Moinuddin & Sharma, 2015), using the cyclograms it is possible to represent characteristics of droplet detachment and arc burning stage. The authors also carried out an analysis of probability density distribution of arc voltage, weld bead, and

microstructure analysis for various welding conditions, allowing to extend the stability study to spray transfer mode. The study showed that there is a strong correlation between the microstructure and the stability of the arc. Besides, the different types of electrodes and their electrical conductivity capacity having the greatest influence on the resulting microstructure in a welded bead. A stable arc produces greater penetration and improves melting efficiency. The authors mention that the study can be expanded taking into account other parameters such as electrode type, electrode extension, shield protection gas, welding speed, and other current modes such as pulsed.

Cayo (E. Cayo, 2008) uses the cyclograms to detect defects in the weld reflected in the arc and current-voltage signals. The cyclograms were used to analyze areas of instability, three disturbances were created, a variation of the stand of, presence of grease and absence of protection gas. Each type of defect showed changes in the cyclograms, allowing them to analyze the changes in voltage and current. One of the advantages of the cyclograms is that it provides a visual result that allows a quick analysis of the values obtained in the process. Again a powerful stability indicator is shown but it has been oriented only to the analysis of the short circuit transfer mode.

Suban (Suban, 2001) uses this index to determine a more stable short-circuit material transfer. As a result, open arc, short circuit, and spray transfer moments are identified depending on the type of gas used. Also, the author performs an analysis of the probability distribution of voltage and current using Fourier analysis. Among the conclusions, the authors emphasize that with pure CO2, more stability is achieved. This method is simple and can be implemented in real-time

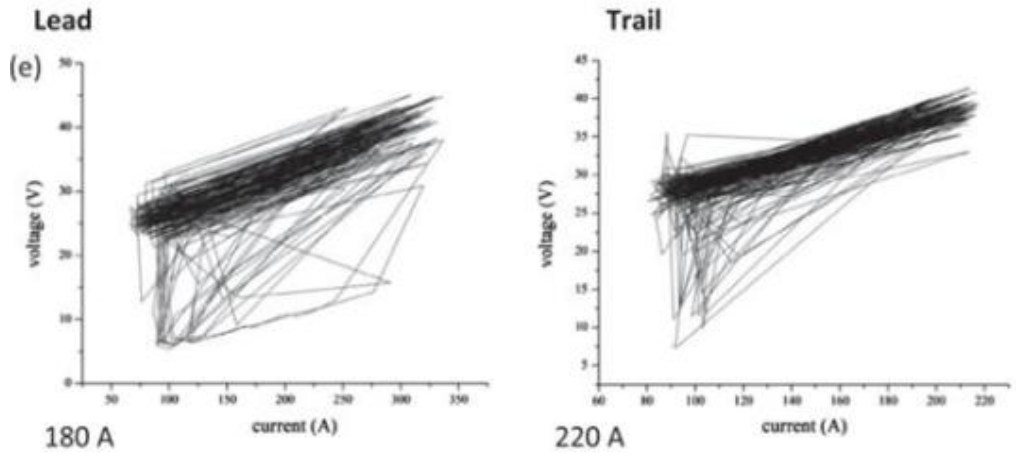

Figure 10 Representation of the cyclograms (modified from (Moinuddin & Sharma, 2015))

2.8 Control of droplet size

The control of droplet size ensures transfer stability. For measuring this variable, image processing, laser shadowing, and sound processing techniques are generally used. The appropriate control ensures proper transfer mode; increases the quality of welding and decreases the number of defects. Large drops do not represent a suitable condition.

The transfer of the drop is dependent on welding current and arc voltage waveforms influenced by gravity force, electromagnetic force, plasma drag force, and surface tension. Suban (Suban, 2001) ensures that to maximize stability the time between the transfer of two subsequent drops should always be the same.

Mousavi and Haeri (2011) [23,24] demonstrate that exists a relationship between droplet detachment and statistical parameters of current, assuring that lesser standard deviation and coefficient to variation were considered to be of uniform droplet detachment and arc length uniformity.

Soderstrom and Mendez (Soderstrom & Mendez, 2008) use high-speed laser shadowgraphs and Fast Fourier Transform (FFT) of the voltage signal for droplet diameter and detachment frequency measurement. Found that exists a relationship between average droplet diameter

and current for the different diameter electrodes. Also, affirm that increase of CO2 above critical levels causes erratic detachment.

Then it can be concluded that there is a correlation between the waveform of the current and the detachment of the drop. A lower coefficient of variation in the mean of the welding current represents uniformity in the detachment frequency. Additionally, for variable transfer time, the welding arc tends to be unstable and the current signals exhibit irregular behavior. In the case of short circuit transfer mode, it is recommended to detach one dropper short. Equally, Pal et al. (Pal & Pal, 2011) affirm that in the pulsed welding processes the droplet detaches it must be in correspondence with the pulses and the droplet diameter close to that of the electrode wire. Finally, adequate control and study of the metallic transfer allow guaranteeing the quality in the geometry of the welded bead.

2.9 Spattering Index

The amount of spatters generated during the welding process has been another indicator widely used, the spatters are a product of instability in the arc and should be minimized. The largest amount of study is developed in the short circuit area. The moment when the short circuit occurs and the arc is reset is when the largest number of spatters are produced. Also, if the mean of the short circuit time is irregular, more spatters will be generated.

Silva et al. (Silva, Ferraresi, & Scotti, 2000) propose a criterion for the spattering index correlating spattering rate (S – Equation 1, Table 2) and the deposition rate (D – Equation 2, Table 1). The purpose was to demonstrate that the correct control of these indicators allows choosing appropriate parameters for any specific welding application.

On the other hand, Kang and Rhee (Kang & Rhee, 2001) develop statistical regression models to predict the amount of spatter in the short circuit transfer for GMAW. Showing, in the same way, that voltage and welding current waveforms can be satisfactorily used to predict the presence of spatters. Kang et al. (Kang, Kim, Ahn, & Rhee, 2003) in a similar work using four different linear and nonlinear regression models composed of the waveform factors to develop the spatter prediction model. Demonstrating that the amount of spatter is dependent on the number of arc extinctions when the welding voltage is below the optimal. In another study,

models were developed for evaluating the spatter rate based on the conventional feed-forward multilayer perceptrons with the error back-propagation as the learning algorithm to estimated spatter rate.

Lastly, Fernandes et al. (Fernandes, de Menezes Júnior, Vilarinho, & Scotti, 2010) propose a Spatter Index (Equation 7, Table 2) relating in a mathematical equation the weight of the spatter collected in the box, and weight of the weld bead. Using the calculated value of the spatter index, they propose a new index of stability (Equation 8, Table 1) that enhances the electrical stability of the process and the weight of spatter generated during welding. The proposed method is efficient as soon as the collection of spatters is carried out correctly. It is suitable for a laboratory environment but can hardly be implemented in the industry since it depends on the collection device. However, the results obtained can be generalized in an automatic learning model and implemented for the control of spatters.

Table 1 Summary of Arc Stability Indexes.

Objective	gas	Transfer mode	Equation	Measured parameters and Variables
Calculate Short Circuit frequency	CO_2	Short Circuit	short circuit frequency $Fs = \frac{1}{(ta+tc)}$ (1)	When *ta* is arc time and *tc* Short circuit time
Identification of the metal transfer mode and arc stability	Ar+Co2 Ar+He+CO_2	Globular Spray Short Circuit	Transfer index $TI = 1 - \frac{I_{min}}{I_{mean}}$ (2) Transfer stability index $TSI = 1 - \frac{I_{max}}{I_{mean}}$ (3) Dip consistency index DCI $DCI = 1 - \frac{V_{bk}}{V_{mean}}$ (4) Power ratio $PR = \frac{I_{bk} \cdot V_{bk}}{I_{mean} * V_{mean}}$ (5)	I mean =average of the welding current I max =maximum value of the current Imin= lowest value of the current. V mean =average of the voltage Vbk =average of all the voltage Ibk =average of all the current
Metal Transfer Regularity	Ar+CO2	Short Circuit	Regularity index $IVcc = \frac{\sigma tcc}{tcc} + \frac{\sigma tab}{tab}$ (6) Cutting frequency index $Fcc = \frac{Valim*(d)^2}{(k*d)^3}$ (7)	σtcc = standard deviation of the short-circuit time; σtab = standard deviation of open arc time, tcc = average of the short-circuit time; tab = average open arc time. d = wire-electrode diameter; Valim = wire feed rate; k = constant to estimate the drop diameter

Table 2 Summary of Transfer Stability Indexes.

Objective	gas	Transfer mode	Equation	Measured parameters and Variables
Calculate Spattering Index	CO2 Globular Spray Short Circuit		spattering index $SI = \frac{S}{-} * 100$ (%) (1) spattering rate S = (Felect or Fwire) – D. (2) Deposition rate D = 3,6 x (Mfcp – Micp) / tarc (3) Covered electrode fusion rate Felect = 3,6 x (Miel – Mfel) / tarc . (4) Penetration index PI = (p / t) x 100 [%]. (5) The convexity index CI = (r / w) x 100 [%]. (6)	The penetration index (PI) was defined by relating the depth of the weld bead (P) to the sheet thickness CI was defined as a relationship between the bead reinforcement (r) and the bead width (w), in percentage. where p is the weld penetration [mm], t is the joint thickness [mm], r is the bead reinforcement [mm], w is the bead width [mm], S is the spattering rate [kg/h], D is the deposition rate [kg/h], Felect is the covered electrode fusion rate [kg/h], Miel is the initial mass of the covered electrode, before welding [g], Mfel is the final mass of the covered electrode, after welding [g], tarc is the arc duration time [s], Fwire is the wire fusion rate [kg/h], ϕ is the wire diameter [mm], fwire is the wire feed rate [m/min], γ is the steel density (7.85 x 103 g/mm3), Mfcp is the final mass of the test plate, after welding [g], Micp is the initial mass of the test plate, before welding [g] and de is the deposition efficiency [%].
Calculate Spatter Index Stability Index	CO2 Short Circuit		Spatter Index $F_{sp} = \frac{W_{SP}}{W_{SP}+W_{Bead}} * 100$ (7) Index of stability (SI) was defined as: $SI = \frac{K}{F_{SP}}$ (8)	W_{sp} is the weight of the spatter collected in the box, and W_{Bead} is the weight of the weld bead. Where K is an arbitrary constant, which was considered by the author be equal to 100

2.10 Acoustic monitoring

According to Grad et al. (Grad, Grum, Polajnar, & Slabe, 2004), the acoustic signal contains information about the transfer mode and the behavior of the arc. It is also possible to identify changes in arc dimensions and geometry; changes in arc intensity; metal transfer and oscillations of the molten pool.

Even according to Mota et al. (Mota, Mendes, Neto, & Vilarinho, 2013), it is possible to observe that the sound signal accompanies the electrical signal, specifically the voltage, concerning the moments of extinction and ignition of the arc. It is easy to see in Figure 11 the sound pulses from the moments of abrupt change in the voltage of the electric arc, and the time intervals between them follow the same pattern observed in the electric signal.

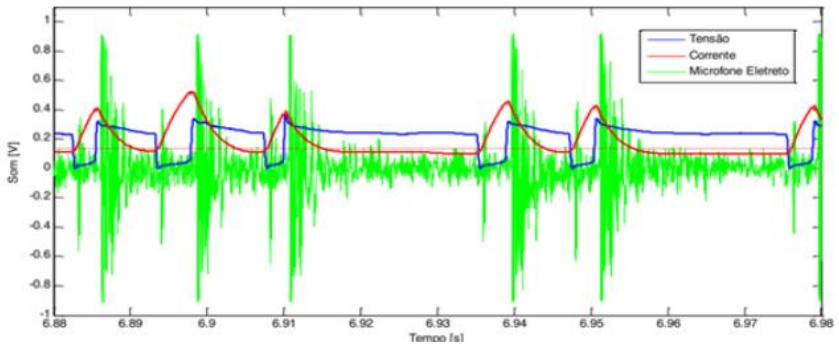

Figure 11 Comparison between sound and current signals (modified from (Mota et al., 2013))

Grum et al. (Grum, Bergant, & Polajnar, 2012) use the sound signal and the light signal to detect even the smallest deviations of arc behavior, as well as large deviations due to the material transfer mode and excessive/inadequate weld penetration. They propose a mathematical model using sound and light values. The authors demonstrated the existence of a correlation between light signals and the energy provided to the system. With the monitoring of sound, it was possible to identify oscillations in the arc that indicated instability. The model was developed for the short circuit transfer mode but was generalized for the spray transfer mode.

Cayo and Alfaro (Cayo & Alfaro, 2008) use the sound to define the difference between the transfer modes on the GMAW process. They use sound pressure and current signals to identify changes in the transfer mode and identifying defects. In the case of the Spray transfer mode, the drops are small and practically imperceptible during the acoustic analysis. Already in the case of the short circuit, it is possible to monitor the occurrence of each short and the reignition of the arc.

Roca et al. (Roca, Fals, Fernández, Macías, & De La Parte, 2009) also applied acoustic monitoring, and the results obtained were used for the training of a neural network. To perform the analysis, they obtain the standard deviations of the peak amplitudes of the sound at the moment in which the short circuit is made and they use as stability indicator. Equation 12, Table 1 shows the stability index previously established. The combination of statistical

technique, acoustic monitoring, and artificial intelligence allowed us to use online monitoring, considering it an efficient and non-destructive technique.

It can be summarized that the electrical and acoustic signals are correlated mainly in the short circuit transfer mode where it is possible to identify the detachment of the drop and the arc reignition. Besides, it is possible through sound monitoring to identify the transference modes. It is a method that is not expensive and that is feasible to implement in the industry. The combination of this method with machine learning techniques that allow prediction and classification are open for future works.

2.11 Machine Learning application for welding quality

Another trend that could be identified is the increase in research that integrates classical statistics techniques and novel machine learning algorithms. It is well known that with the increase of the computing processing capacities the data analysis, big data, and machine learning have had a significant boom since 2009. The welding area has not been oblivious to the use of such techniques; although it should be noted that in the area of stability, classical statistics is more commonly used as demonstrated in the present study.

Machine learning algorithms adapt to the stochastic and chaotic nature of the welding process better than classical mathematical models, allowing the creation of non-linear models with the ability to predict and adjust to new data.

Machine learning is intrinsically linked to artificial intelligence and recognized as a sub-area of it. Contemplates algorithms based on mathematical and statistical models that, through a historical data set, perform prediction, classification, and regression tasks (Sun, Yang, & Wang, 2017).It can be divided into two areas, supervised learning and unsupervised learning.

The supervised method allows the training through input data and its associated expected output, creating a model to predict and classify new data. Some of the best-known algorithms are Artificial Neural Networks, Support Vector Machine, Fuzzy Logic, Genetic Algorithms, and Decision Trees. In the area of welding, these models are predominant.

On the other hand, unsupervised methods only perform the analysis of input data whose behavior is unknown, it is mostly used to explore data, organize it, and find patterns. Examples are clustering algorithms such as K-Means, K medians, Hierarchical Clustering, Self-Organized Maps, and Based Density Clusters.

Neural networks were identified by (Kim, Son, Park, Kim, & Kim, 2005) as one of the most suitable techniques for the prediction of weld bead geometry and mechanical properties, its learning capacity makes it possible to create an efficient model that considers the stochastic nature of the process and the variables involved in it. Being a powerful tool to map the relationships between parameters.

Already in recent years, some interesting solutions have been presented. Ates (Ates, 2007) proposes a Multilayer Perceptron ANN throw spectroscopic analysis for the task of select the most adequate shielding gas, take into account chemical and metallurgical properties. As input (Ar, O2, and CO2) values were used for the training network and the outputs (tensile strength, elongation, impact strength, and hardness).

Another group of authors (Ghetiya & Patel, 2014) (S. W. Campbell, Galloway, & McPherson, 2012) present similar proposals, create models using a backpropagation neural network (BPN), to predict bead geometry, specifically the bead penetration in GMAW process. The models use wire feed rate, travel speed, and current signals as input and bead geometry, penetration, and reinforcement as output.

In the case of Campbell et al. (S. W. Campbell et al., 2012) decide to alternate with two shielding gases during the tests, causing variations in the travel speed and the heat input, the model was able to adapt to those changes with an acceptable prediction error. Meanwhile, Correia et al. (Correia et al., 2005) use GA techniques, in the determination of the optimal GMAW process parameters obtaining better deposition efficiency, penetration, width, and reinforcement. Malviya et Pratihar (Malviya & Pratihar, 2011) use Particle swarm optimization (PSO) population-based evolutionary computing techniques and neural networks for mappings the bead geometry for metal inert gas (MIG) welding process. The PSO allowed improving the performance of the backpropagation algorithm. They also used Fuzzy C-means

clustering and Entropy-based fuzzy clustering algorithms to decide the best structure of the network.

These powerful models can also be used in reverse mode to predict the parameters needed to obtain the desired geometry. Leading to a group of works that not only predict geometric characteristics but also optimize the parameters and controlling the process in real-time (Xiong, Zhang, Hu, & Wu, 2014) (Cruz, Torres, & Absi Alfaro, 2015) create a multilayer feedforward neural network trained with the back-propagation error algorithm for gas metal arc welding. Both models allowed the construction of a real-time controller.

Xiong et al (Xiong et al., 2014), also implements a second-order regression model, but affirm that the neural network model has better performance due to its great capacity of approximating any nonlinear processes. Already in the case of Cruz et al. (Cruz et al., 2015)complement the results obtained from the neural network with image processing and a control system developed with a fuzzy algorithm.

Welding defect detection has also benefited from these methods. Yonglun and Feng (Di, Yonglun, & Feng, 2000) use SOM unsupervised neural network for on-line detection of the weld defects. The classification allowed to separate the defect data from normal, also separate the instability data from other situations and perform the estimation of angular distortions, the input variables were plate length and width and the output was the deflection edge.

(Agapkin, Orlov, Persiantsev, & Dolenko, 2003) employed Hopfield-style neural networks to pre-process ultrasonic scanning data for nondestructive inspection of welded pipeline joints. Their model worked with image-based inputs, and the network was trained to detect high noise levels and inadequate acoustic coupling between the scanning probe and the test material. (Mirapeix, García-Allende, Cobo, Conde, & López-Higuera, 2007) applied principal component analysis (PCA) combined with a feedforward neural network trained via backpropagation to perform defect detection and classification through spectroscopic analysis of the welding arc. The monitoring system developed by the authors was capable of identifying defects such as lack of penetration, insufficient welding current, and reductions in

inert gas flow. (Souza et al., 2012) used ultrasound signals from weld inspections to train a neural network capable of identifying various discontinuities, including lack of penetration, inclusions, slag, and porosity.

2.12 Synthesis of the study and future research directions

To synthesize the study, it was conducted an analysis of the documentation obtained, the metadata of the document collection was exported to Information Systems Research (RIS) format and a bibliometric analysis was performed using the VOSViewer software. A graph with groups of the main authors and their relationship of co-authorship (taking five as a frequency of occurrence of the author's surname), is presented in Figure 12. It is possible to identify as the largest cluster the Chinese authors, followed by smaller groups of Brazilian and Indian authors, highlighting that there is little cooperation between those groups.

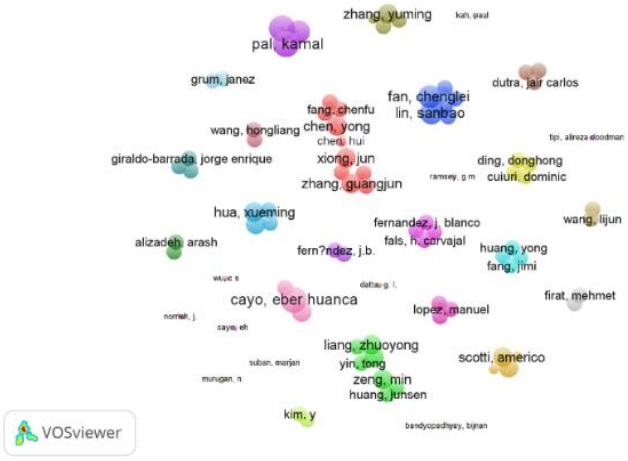

Figure 12 Authors and their relationship of co-authorship (two as a frequency of occurrence of the author's surname).

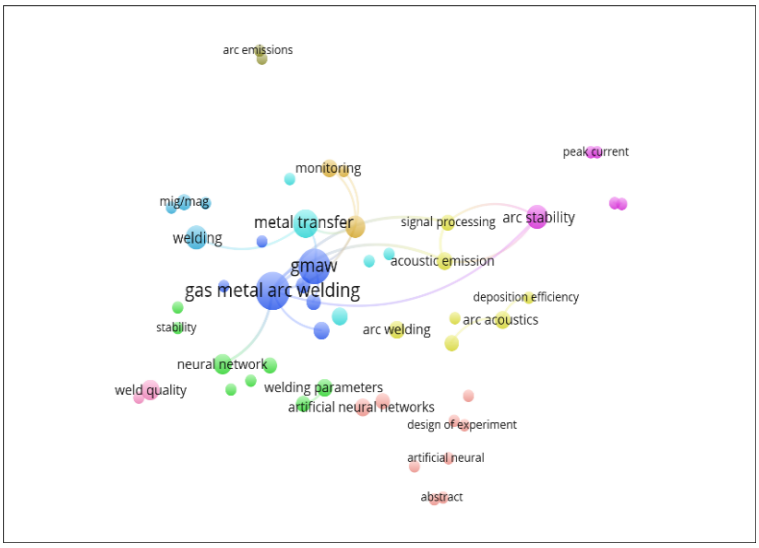

Figure 13 Cluster of terms (two as a frequency of occurrence of the term).

Figures 14 and 15 show a summary of the signals and methods used to measure or estimate the indexes. Consequently, the current and voltage signals are widely used, as well as, the camera in the image processing and the microphone for the analysis of acoustic signals.

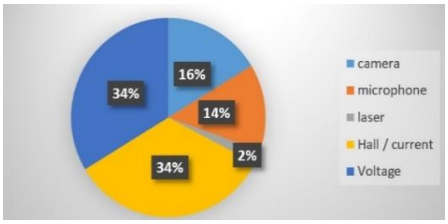

Figure 14 Sensors used to measure.

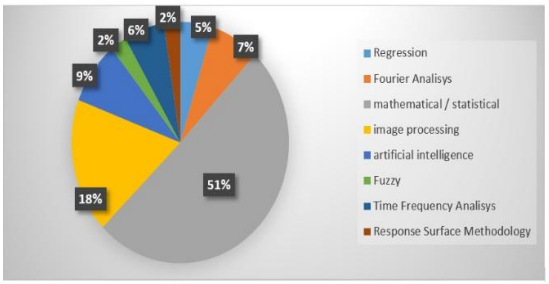

Figure 15 Methods used to estimate the indexes.

Figure 16 summarizes the parameters and variables used in the studies showing that among the most influential in the stability of the process can be mentioned current, voltage, wire feed speed, short circuit time, arcing time, and short circuit frequency.

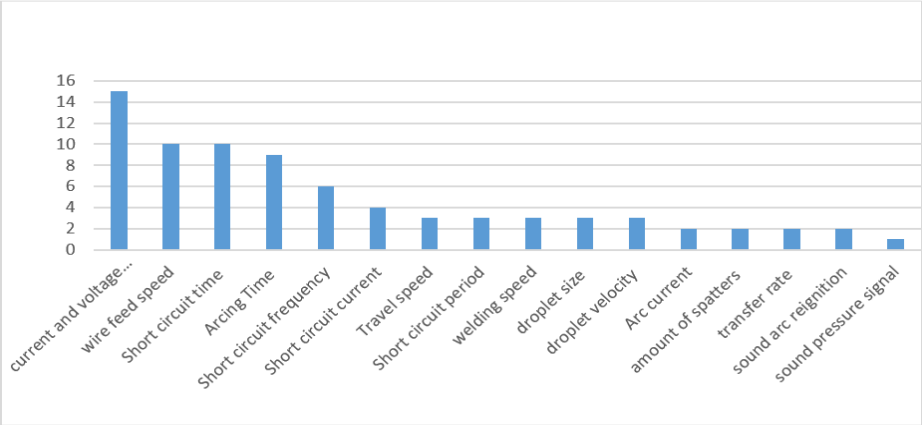

Figure 16 Parameters and variables used in the studies.

Also, it is possible to classify the indexes according to their purpose, those that are oriented to the monitoring of the metallic transfer, analysis of the stability of the arc, and the process in general. Figure 17 shows the percentage by group, Figure 18 shows the technique used to develop the indexes for those groups. It is important to emphasize that these concepts are widely correlated.

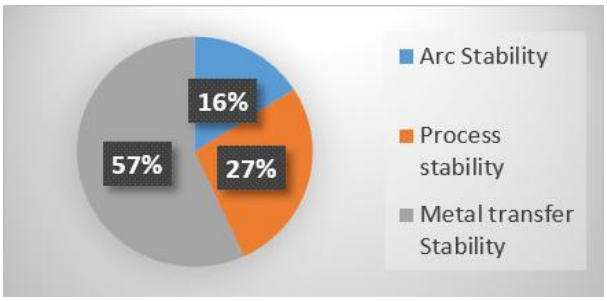

Figure 17 Percentage by the group.

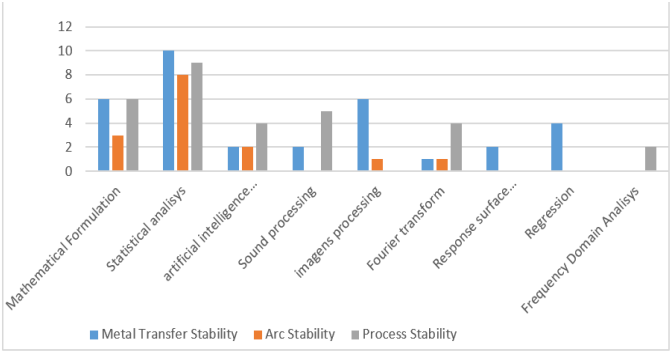

Figure 18 Techniques used to develop the indexes classified by groups.

Note that the highest percentage of investigation is aimed at the study of metal transfer stability. It is also evident that the main processing techniques to develop the indexes were the mathematical formulation and statistical methods. Although in the case of metal transfer, image processing is widely used, mainly to define the transfer mode and drop size.

Figure 19 shows a taxonomy that details the methods used to measure the stability of the welding process and the techniques associated with them. The techniques used were divided according to Weglowski (Weglowski, 2008) into traditional and non-traditional.

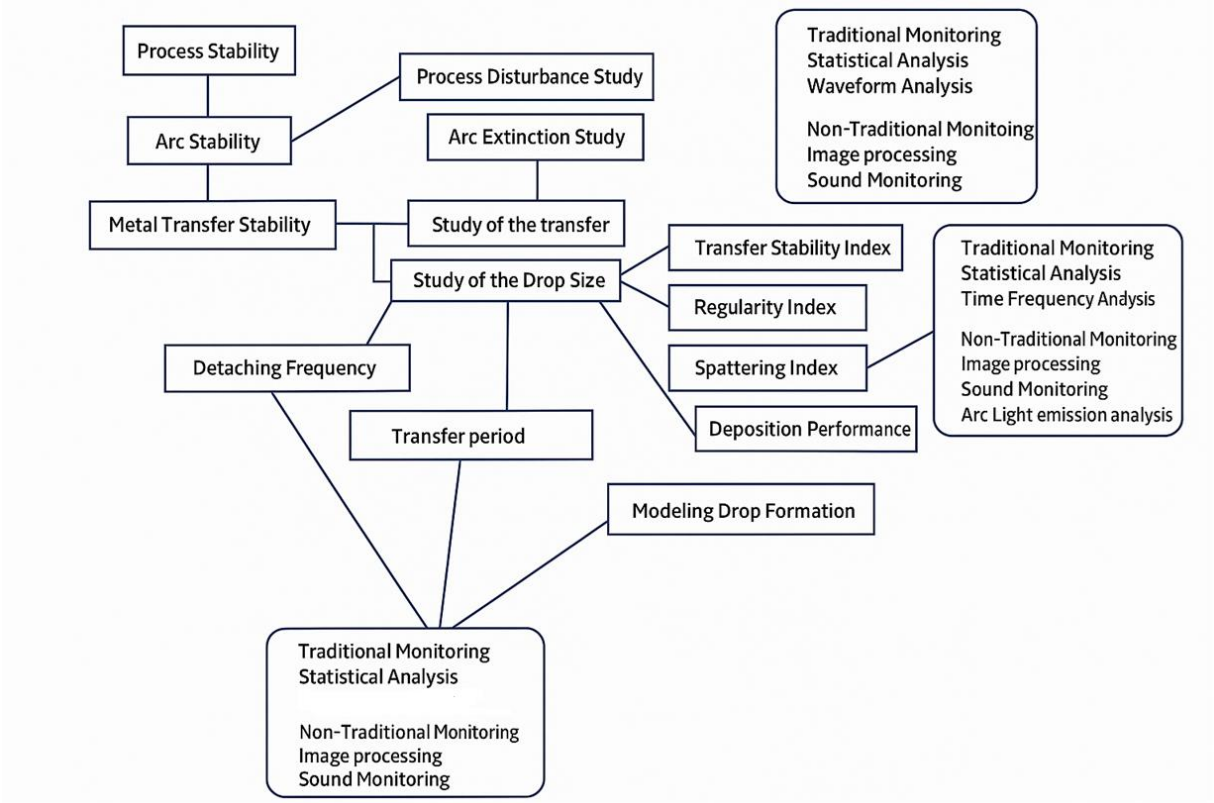

Figure 19 Classification of the main methods used for monitoring.

Finally, to find a trend and a possible vision of the direction of future studies, the following was analyzed:

2.12.1 Highlights of the works of the last five years

An analysis of the works in the field of stability in the last five years was made and allowed to find the following trends. There is a considerable increase in the study and application of works in pulsed GMAW (see Figure 20). This increase is caused by the known improvements in quality and productivity concerning regular metal gas arc welding (GMAW).

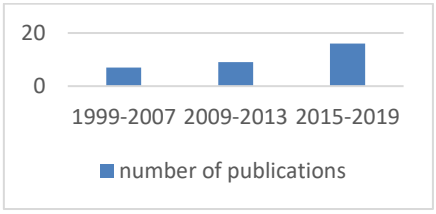

Figure 20 Number of publications for years in the area of pulsed GMAW.

2.12.2 Innovative Techniques

It is known that metal transfer has a direct influence on the stability of the process and the final quality of the welding. Consequently, it has been widely studied as demonstrated in the present review of the literature.

But innovative techniques continue to appear in this field with prospects of great interest. In this case, they were identified laser-enhanced gas metal arc welding (GMAW), a modification of GMAW, used to control the metallic transfer. A low power laser helps to obtain greater strength in the detachment of the drop.

Ultrasonic-wave-assisted arc welding has also been identified as a newly developed method that introduces high-power ultrasound into the arc and weld pool. This technique influences the thermal dynamics of the process, particularly the rate at which the plasma cools and heats.According to Fan et al (Fan, Xie, Yang, Lin, & Fan, 2017), it allows increasing the stability of the process.

2.12.3 Areas where further study is required

Very correlated with the study of acoustic monitoring is the analysis of the arc light emission. It is used to control the metallic transfer. A low power laser helps to obtain greater strength in the detachment of the drop. Weglowski (Węglowski, Huang, & Zhang, 2008) demonstrate that light emission has a linear correlation with the current. On another hand, Shao et al. (Shao, Wang, & Zhang, 2011) affirm that the light signal indicates the arc radiation intensity and the arc radiation is proportional to the power released been a relevant indicator of the energy supplied into the weld.

To a lesser extent and with little representation in the scientific literature, there are works related to the quantification of the emission of fumes. Yamamoto et al. (Yamamoto, Yamazaki, Suzuki, & Koshiishi, 2013) conclude that exists a relation between heat content, fume emission rate, and molten metal transfer mode, consequently the fume emission rate per unit weight of consumed wire increases with the increase in heat content.
But Meneses et al. (V. A. De Meneses, Gomes, & Scotti, 2014) proved that there is no correlation between the amount of spattering generated and the fume generation rate. Because

the regularity of the transfer did not show influence on the morphology, size, or composition of the fumes. Then the generation of fumes is not correlated with the stability of the process.

Finally, other techniques that can be developed are 3D computational modeling, simulation, spectroscopy, spectral analysis, and X-ray observation system.

2.13 Chapter considerations

In this chapter, we present a comprehensive exploration of reliable and precise methods for quantifying and assessing stability within the GMAW (Gas Metal Arc Welding) welding process. The primary focus of research efforts in this field has predominantly revolved around the examination of metallic transfer phenomena. Notably, the majority of stability indexes developed thus far have been tailored to the short-circuit transfer mode, indicative of its significance within the welding domain.

These indexes have been meticulously crafted through the analysis of crucial process signals encompassing current, voltage, sound, and light. The arsenal of techniques employed to refine these stability indexes encompasses mathematical formulation, statistical analysis, image processing, and the monitoring of acoustic signals and light spectrum variations. Each of these methodologies plays a pivotal role in enhancing our understanding of stability within the GMAW process.

Moreover, while various advanced techniques have been embraced, such as artificial intelligence and machine learning, it is noteworthy that their utilization remains relatively limited within this context. This observation opens up an intriguing avenue for future research, offering a promising trajectory to explore and exploit the potential of these cutting-edge technologies in the pursuit of further advancements in GMAW stability assessment.

3 Methods and tools

This chapter presents the methodology and tools used to support the development of a weld stability indicator for the GMAW process.

In this work, an experimental procedure is developed to obtain a stability indicator for the GMAW welding process. Figure 21 shows the general diagram of the work. See that in the first stage the acquisition and analysis of the data of the different sources of information and sensors are carried out. Subsequently, the data is integrated and correlated. In a final step, the data is processed using machine learning algorithms allowing the identification of patterns and stability rules. With these results, it was possible to create a stability and quality indicator for the GMAW welding process.

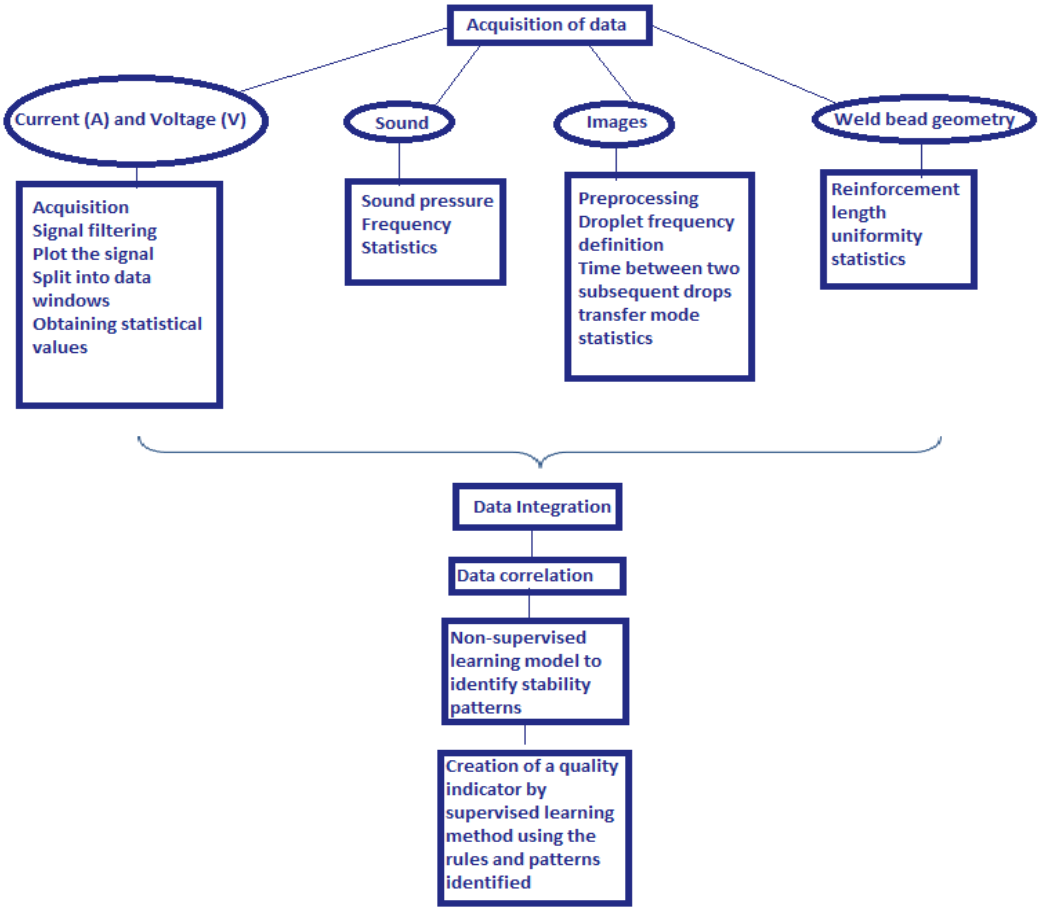

Figure 21 General diagram of the experimental procedure

The variables measured by the system are welding voltage, welding current, sound acoustic pressure signal, process images, and welded bead geometry. The components of the signal acquisition system are detailed below.

3.1 Data acquisition system

The following Figure 22 shows the distribution of the computer system and the hardware used in this research. The following briefly details each of the system devices used, the features they perform, as well as the materials used in the process.

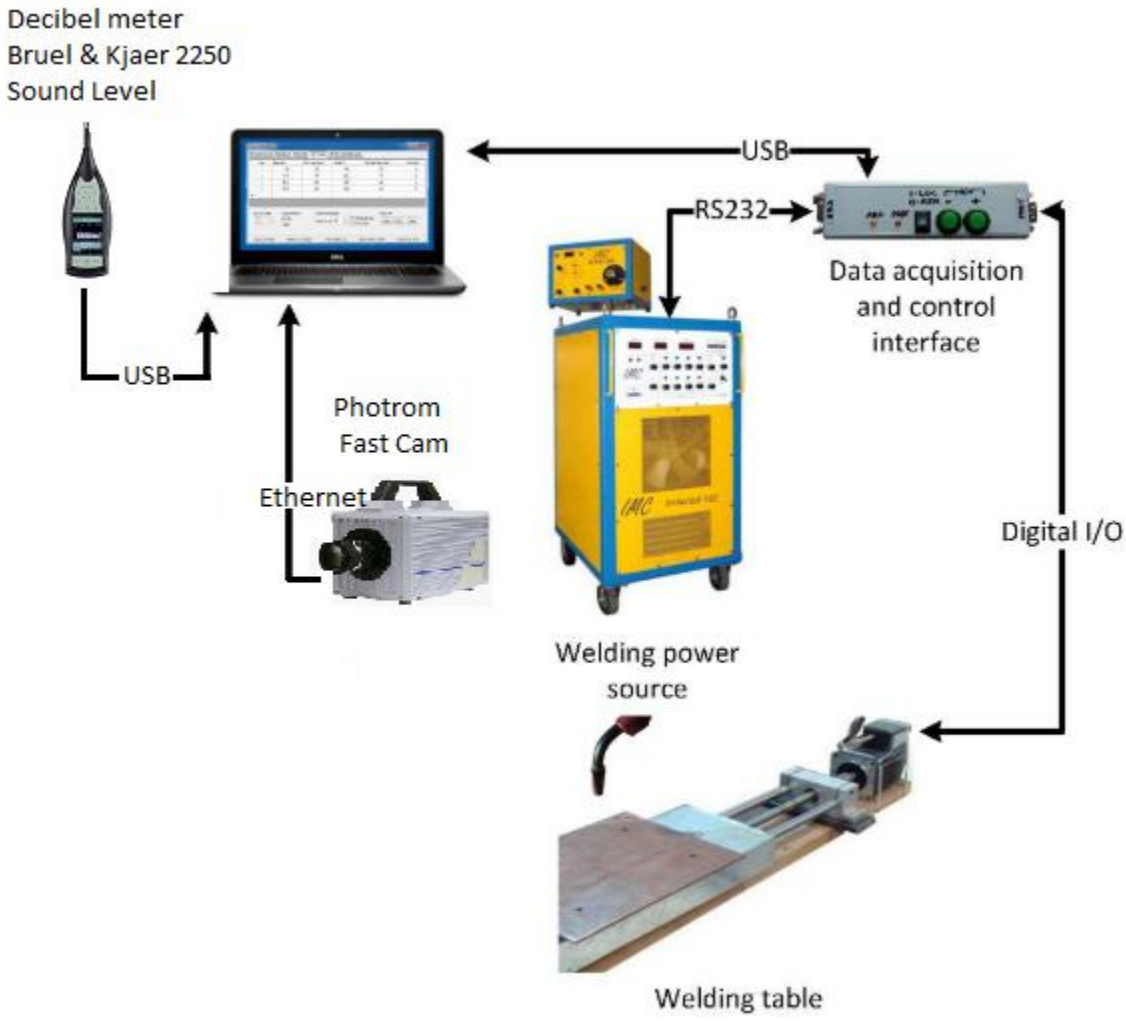

Figure 22 Data acquisition system: main components, welding table and instruments support (Modified from (Guillermo Alvarez Bestard, 2017))

3.1.1 Welding power source

The welding power source Inversal 450 is equipped with an RS232 interface for accessing operational parameters in real time. This interface allows the acquisition of effective welding voltage and current values with a sampling time of 2 milliseconds or less. The measurement system uses a 10-bit analog-to-digital converter (ADC), with an input range of 0 to 68 V for voltage—resulting in a resolution of approximately 0.07 V—and 0 to 450 A for current, providing a resolution of 0.44 A.

Importantly, the power source includes an internal digital filter, which processes and stabilizes the signal to minimize noise. As a result, the voltage and current values obtained correspond to filtered instantaneous readings or moving averages, providing a more reliable representation of the arc behavior in real time.

The welding process was carried out in the vertical position, with the torch remaining fixed in place. The control interface also manages the stepper motor driver responsible for moving the workpiece vertically. The welding speed is retrieved directly from the internal registers of the interface.(Guillermo Alvarez Bestard, 2017).

3.1.2 Flat welding table

The electro-mechanical system, integrated for a linear axis of 5 mm of movement by revolution and a stepper motor of 1.8 grades by step, is used to move the piece, keeping the welding torch fixed. This system, development by GRACO students (Franco, 2008) has a stepper motor controller circuit with signals for modifying the stepper time (speed) and the direction. Other signals show the status of the system and protect against overload. This structure supports 15 kg of load and 15 mm/s of maximum speed.

3.1.3 Process consumables

According to the availability of the laboratory, the materials used in this research were:

GMAW process under study, the gas shield was a 96% Ar + 4% O2 mixing gas. The gas flow rate used in the experiment was 15 L/ min. To perform the width modeling and reinforcement

of the weld bead, we used the solid wire of AWS A5.18 ER70S_6 class, with a diameter equal to 1 mm.

The specimens used in this experiment were made of standard carbon steel, commonly employed in industrial applications. For each sample, only a single welding pass was performed, resulting in the deposition of one weld bead along the surface of the plate. It is important to note that the pieces were not cut or sectioned after welding, in order to preserve the original conditions of the bead for subsequent geometric and visual.

3.1.4 User interface

The user interface system (Figure 23), development by GRACO student (Guillermo Alvarez Bestard, 2017) provides a tool to create the welding sequence. This includes the start and end positions, the stimulus that will be sent to the welding power source and the sampling period. The user starts the process and it stops automatically when the sequence ends, or when the sequence is stopped manually. It was set for a sampling time of 20 ms, three files are created in each experiment that store the system configuration, the stimulus sequence, and the measurements collected.

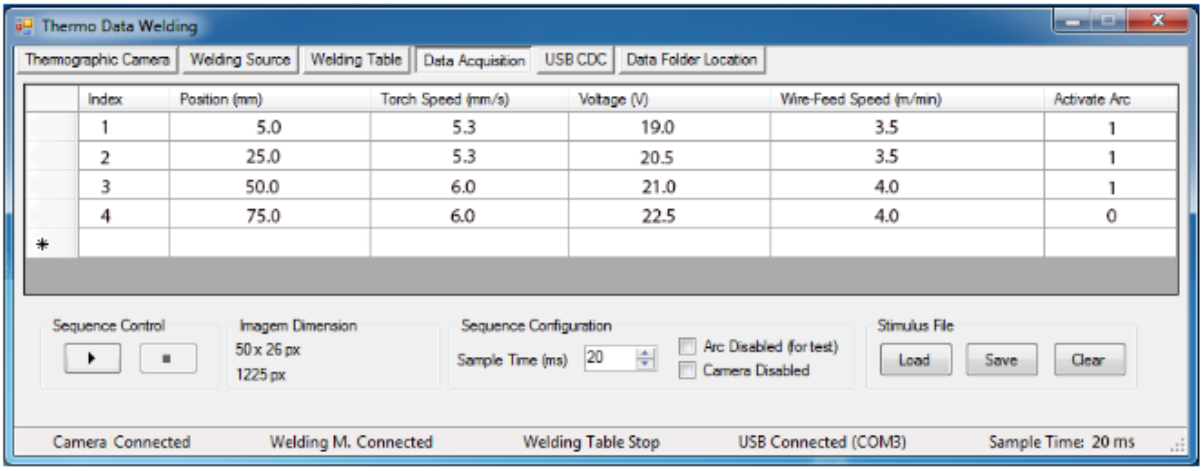

Figure 23 User interface system

3.1.5 Sound Level Meter

The sound analysis presented in this study is based on previous investigations by (CAYO, 2008) a GRACO-UNB student. The Brüel & Kjær Type 2250 decibel meter used in this project uses Equation 1 for the calculation of acoustic pressure level, which will be referred to below as Sound Pressure Level (SPL).

Equation 1

$$SPL = 20.Log\left[\sqrt{\frac{1}{\Delta t}\int_{t}^{t+\Delta t} P^2(\xi)d\xi}\Big/ p_o\right] \quad (9)$$

The pressure of the sound or sound pressure is the product of sound propagation. The energy caused by the sound waves generates a wave movement of the air particles, causing alternate variation in the static pressure of the air. The reason for these variations in atmospheric pressure that is produced in areas where the particles concentrate (concentration zones) and other areas are less saturated (refractive zones). The zone with the highest concentration of molecules has the highest density and the zones with the lowest concentration have the lowest density. Then, the acoustic pressure is defined as the instantaneous pressure difference and the static atmospheric pressure. The sound pressure is measured in multiples of pascals. These pressure variations originate from mechanical variations that may be longitudinal or transverse. When these mechanical variations are longitudinal and range from 20 Hz to 20 kHz. the human ear can perceive them as sound (CAYO, 2008).

To measure the sound pressure signal, a microphone is used, which is a transducer that changes the mechanical energy of acoustic waves in an electrical signal. The relationship between acoustic and electrical pressure variation is known as microphone sensitivity. Equation 2 presents equation 1 as a function of microphone sensitivity:

Equation 2

$$SPL = 20.Log\left[\sqrt{\frac{1}{\Delta t}\int_{t}^{t+\Delta t}\left(\frac{S(\xi)}{50E-3}\right)^2 d\xi}\Big/ p_o\right] \quad (10)$$

Where:

SPL: Sound Pressure Level

S: Amplitude of the sound signal over time

P: K Acoustic Pressure: Geometric Factor (experimentally-10E = 5)

Po: Reference Acoustic Pressure (20 uPa)

ξ: Integration time variable

t: Start time

T: Integration Time Range

The acquisition frequency used was 100 milliseconds (10 Hz).

3.1.6 Weld bead dimensions' measurement

To measure the geometry, images of the welded cord in the vertical and the horizontal were taken, a Photoshop script was used to measure the width and height every 1 mm, converting the image pixel scale into measurements in millimeters (as shows Figure 24).

To ensure accurate measurement, a millimeter-scale ruler was included in each photograph as a reference. From this reference, a scale factor was calculated, and measurements were adjusted accordingly. A baseline of 5 mm was adopted as a calibration step for consistency, and from that point, the entire bead length was analyzed in intervals of 1 mm to quantify both the bead width and height with precision.

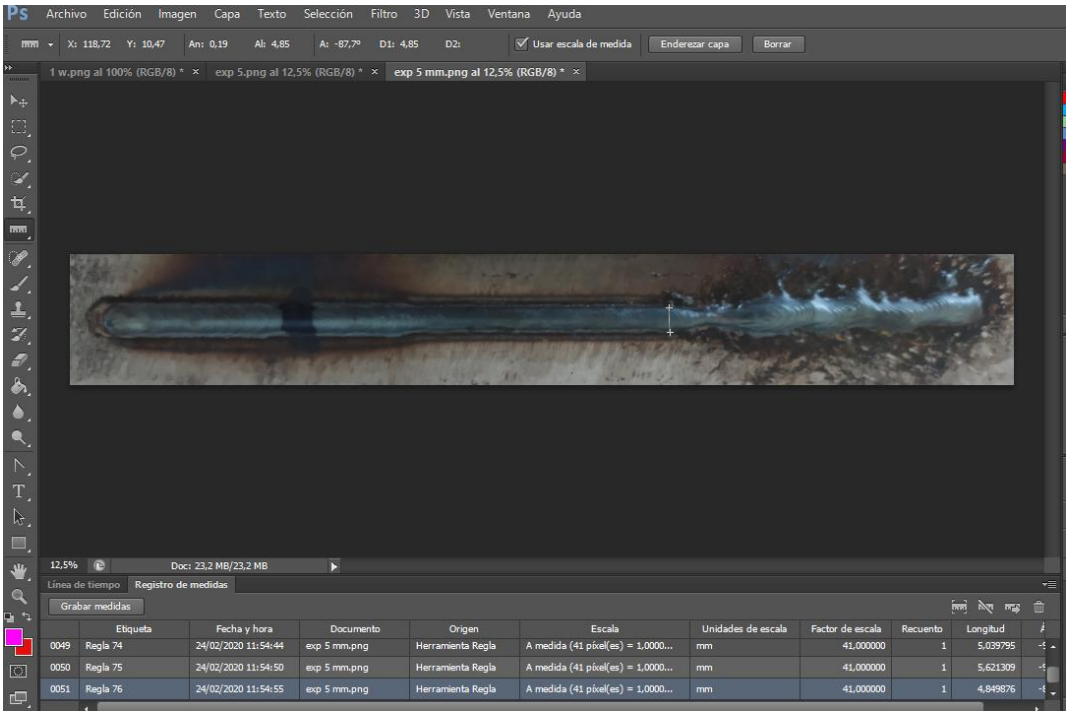

Figure 24 Weld bead dimensions' measurement

3.1.7 Image pre-processing

To obtain the images was used shadowgraph technique used an optical expander composed of a divergent lens and a convergent lens (see Figure 25). The system uses a He-Ne (Helium - Neon) laser. The divergent lens has a focal length of 40mm. The second lens is convergent, leaving the laser light with a constant beam. The distance between the second lens and the wire is 70 cm, and the distance between the camera and the wire is 40 cm.

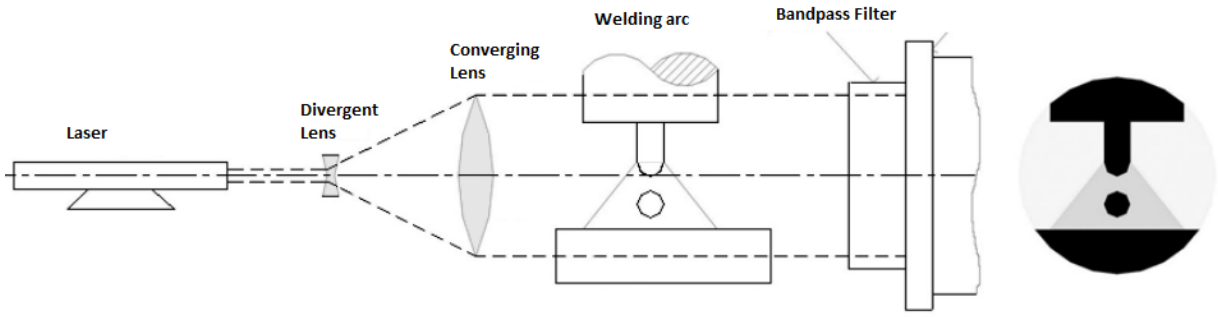

Figure 25 Assembly for application of shadowgraph technique (Modified from (Lopera, Alfaro, & Motta, 2012))

The Photron APX-RS high-frequency acquisition camera is used, provides full megapixel resolution images at frame rates up to 3,000 frames per second (fps). For the present work, the following configuration was used: frame rate 512 fps and resolutions of 512 x 512 pixels. Figure 26 shows an example of an image obtained using the high-speed camera and profiling method.

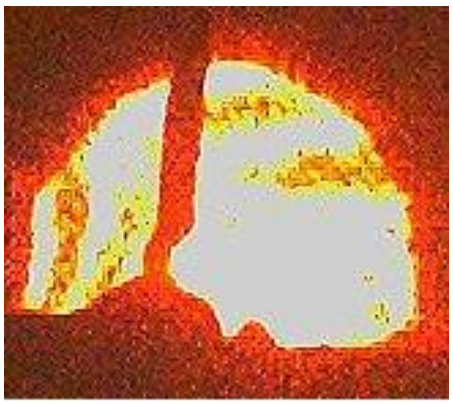

Figure 26 Example of an image obtained using the high-speed camera and profiling method

The data is transferred to the computer via Ethernet. For processing, a python program was developed using the OpenCV image library.

The images of each experiment are processed using various computer vision techniques to improve the image to increase the chances for the success of the subsequent processes. Filters were used for noise removal, isolate specific regions of the image, and binarize it. The operations were carried out directly on the pixels of the image working in the space domain.

The Gaussian filter mask was used, is a linear filter for smoothing, as follow:

$$I_A(i,j) = I * A = \sum_{h=-\frac{n}{2}}^{\frac{n}{2}} \sum_{k=-\frac{n}{2}}^{\frac{n}{2}} e^{-\frac{h^2+k^2}{2\sigma^2}} I(i-h, j-k)$$

(Pinto Lopera, 2016) (11)

$I_A(i,j)$: is the new pixel value;

A: is the square mask used;

*: indicates a discrete convolution;

I: it is the original image;

(h,k): are the row and column positions of the pixel in the mask;

(i,j) are the row and column positions of the pixel in the image;

n: is the number of rows (or columns) of the mask, is an odd number, so n/2 is the smallest integer in that relationship.

The median filter follows the same mathematical principle, used to soften the image, in this case, the convolution mask will have value 1.

In the case of the median filter the value of each pixel is replaced by the median of the gray levels of the image in its vicinity (limited by the size of the kernel), so to calculate the median of this region, the values are ordered in a vector in ascending order and then determined the median value (value of the central position of the vector) that is finally assigned to the pixel. This method is very effective in removing isolated pixels.

Finally, the images were binarized using Thresholding segmentation, a technique for segmenting homogeneous regions based on similarity characteristics. Thresholding segmentation aims to separate objects from the interest of the fund by applying a gray tone threshold *(T)* to the image *f(x,y)*, transforming it into a binary *g(x,y)* with the relation:

$$g(x,y) = \begin{cases} 0 & se\ f(x,y) < T \\ 1 & se\ f(x,y) \geq T \end{cases}$$ (Pinto Lopera, 2016) (12)

Below Figure 27 shows an example of the results obtained with the commented techniques:

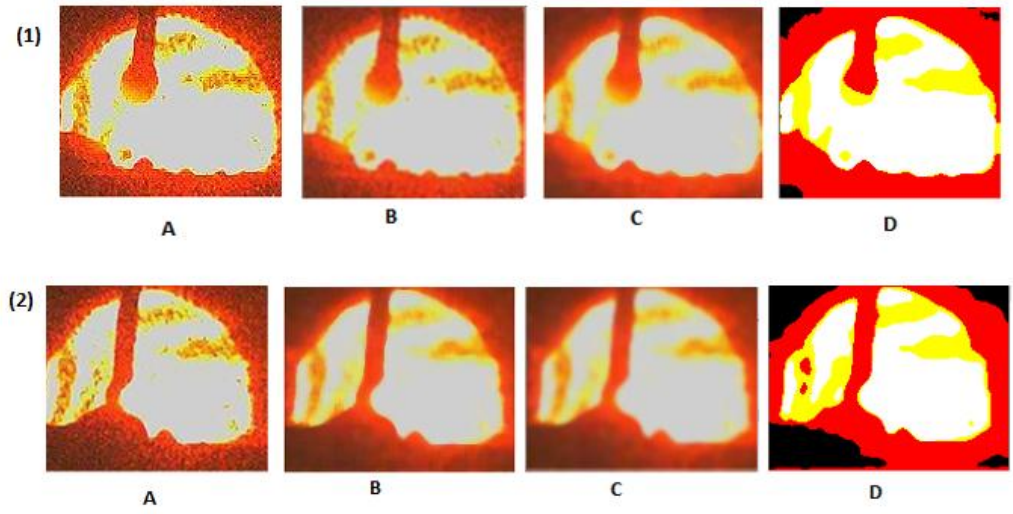

Figure 27 Example of the pre-process filters

The Figure shows two original images where A is the original image, B is the image with the median filter, C is the image with Gaussian filter, D is the binary image using color patterns.

3.1.8 Drop Detachment Frequency

The drop detachment frequency was calculated by the following steps:

1. The images were processed with the filters commented in section 3.1.7.
2. Taking the first image of the process, a square is marked in the area between the electrode and the piece to be welded.
3. For every image in the sequence, the pixels are counted, having in principle that the drop is represented by red pixels the drop identification is performed.
4. It is checked if the drop appears in more than one image so as not to be counted repeatedly by mistake.
5. A mathematical relationship is created between the number of images obtained per second and the number of drops obtained at that time.

The method was tested for the three main modes of transfer. To perform the validation of the proposed method, the waveform of the current was analyzed and the manual analysis of the images obtained was performed. Figure 28 presents an example of the processing carried out,

having as reference the desired area of the image, the presence of drop is analyzed for the next three images, in this specific case a short circuit is detected.

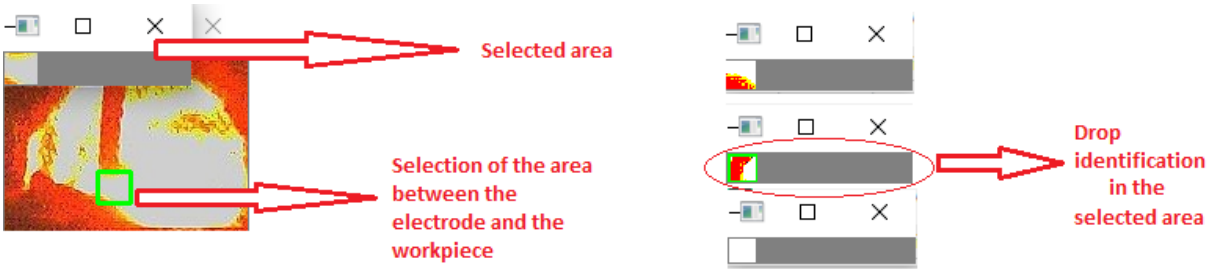

Figure 28 Identification of the drop detachment

3.1.9 Identification of the transfer mode

In our pursuit of defining the transfer mode within the GMAW process, we harnessed the power of a convolutional neural network (CNN) meticulously trained to classify images into the fundamental clusters of globular, spray, and short circuit. This innovative approach enabled us to decipher the intricate characteristics specific to each transfer mode. The methodology behind our CNN implementation involved mathematical operations on the input pixel groups of the images using kernels, also referred to as filters. These filters facilitated the creation of feature maps during each convolution, allowing the network to learn and discern the distinct traits inherent to each transfer mode.

For the configuration of our neural network, we set key parameters as follows: 20 epochs, indicating the number of iterations; image dimensions of 150 by 150 for processing; a batch size of 32, defining the number of images processed in each step; 1000 steps, denoting the frequency of information processing within each iteration; 300 validation steps to monitor the network's learning progress; 32 and 64 filters for the two convolutional layers, respectively, determining the depth of feature extraction; filter sizes of (3, 3) and (2, 2) for the two convolutional layers; a pooling filter size of (2, 2); 2 classes representing the number of cases under consideration; and a learning rate (lr) of 0.0004, indicating the adjustments made by the neural network during the subsampling process. This comprehensive configuration formed the foundation of our innovative approach to classifying and understanding transfer modes in GMAW welding. Appendix 3 and 4 shows the training of the model, including the Python implementation and the execution environment using the PyCharm IDE.

After that, with the information obtained, metallic transfer operational maps were created as shown in Figure 29.

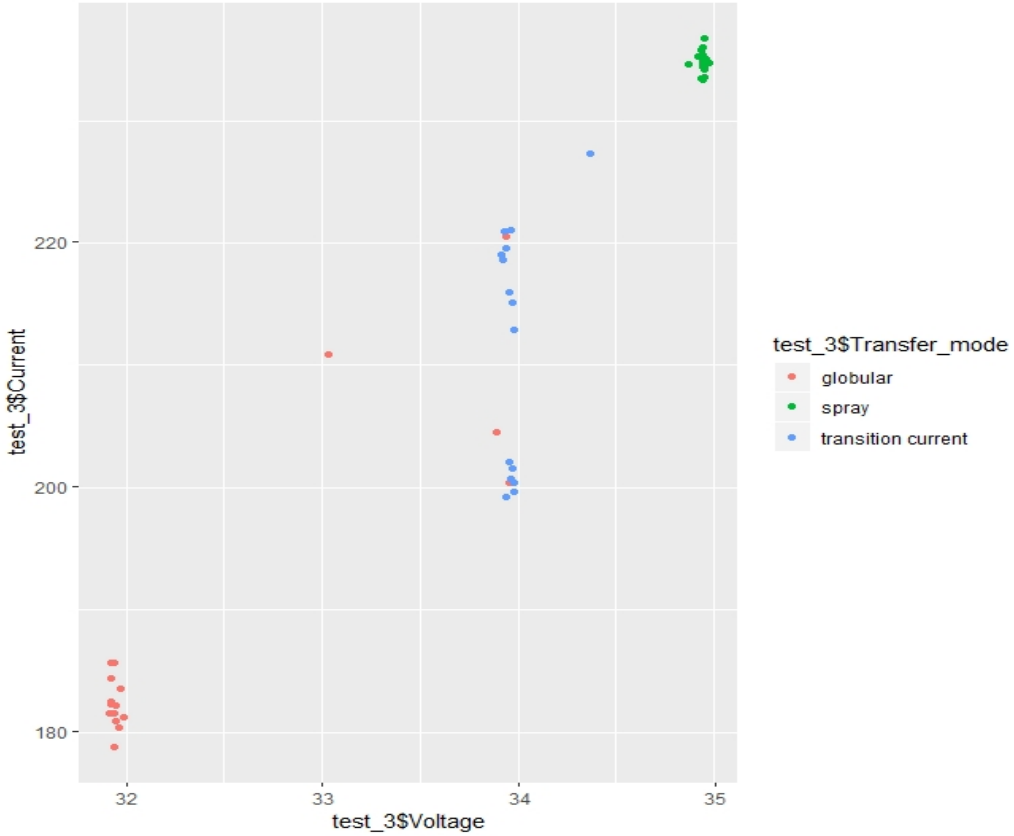

Figure 29 Example of the metallic transference maps

3.2 Fundamentals of statistical analysis

It was decided to use statistical analysis to identify the characteristics of the data and analyze the behavior of the process parameters. Values were obtained with R Studio statistical software.

3.2.1 Mean

The mean of a set of observations is the arithmetic average of the values;

$$\bar{x} = \frac{1}{n}\left(\sum_{i=1}^{n} x_i\right) = \frac{x_1 + x_2 + \cdots + x_n}{n} \tag{13}$$

3.2.2 Standard Deviation (SD)

It is a measure of the amount of variation or dispersion of a set of values. A low standard deviation indicates that the values tend to be close to the mean (also called the expected value) of the set, while a high standard deviation indicates that the values are spread out over a wider range.

$$s = \sqrt{\frac{1}{N-1}\sum_{i=1}^{N}(x_i - \bar{x})^2}, \tag{14}$$

3.2.3 Correlation Matrix

The correlation matrix plays a pivotal role in quantifying the degree of relationship between two random variables by utilizing the covariance measure, as outlined in equation 15. This measurement yields three fundamental coefficients: Pearson, Spearman, and Kendall, each serving as a distinct indicator of the strength and nature of the association between the variables. These coefficients provide valuable insights into the data, with interpretations based on effect size. A correlation coefficient of 0 signifies a null association, while 0.1 denotes a small association, 0.3 indicates a median association, 0.5 represents a moderate association, 0.7 suggests a high association, and 0.9 signifies a very high association. These gradations of association strength help elucidate the relationship between variables and are crucial in various analytical contexts.

$$\boldsymbol{COV(X,Y)} = \frac{\sum_{i=1}^{n}\left(X_i - \bar{X}\right)\left(Y_i - \bar{Y}\right)}{\boldsymbol{n-1}} \tag{15}$$

3.2.4 Background Value and Peak value

Proposed by (Carvalho, 1996)

Background welding current (bkg): the arithmetic average of all the current transient samples less than or equal to the mean of the current (A_mean).

Background welding current (bkg): the arithmetic average of all the voltage transient samples less than or equal to the mean of the voltage (V_mean).

Peak welding current (pkv): the arithmetic average of all the current samples greater than A_mean

Peak welding current (pkv): the arithmetic average of all the voltage samples greater than V_mean

3.3 Machine Learning Algorithms

Machine learning was used to find rules and patterns of behavior in the data. For this, the experiments were carried out and the obtained result went through the data mining process, carrying out the following methodology:

- ✓ Data collection: Recording of the data obtained in carrying out the experiments.
- ✓ Cleaning and normalization of data: The data obtained is analyzed and processed to identify empty fields and anomalous data.
- ✓ Data integration: All data is stored in Xls format and integrated
- ✓ Cluster and Classification: Machine learning (Decision trees) are used to group, classify, and identify data behavior
- ✓ Identification of patterns and rules: From statistical analysis and machine learning methods used, rules for moments of stability and instability are identified.
- ✓ Model development: With the rules created, an artificial intelligence model is developed through a neural backpropagation network capable of predicting instability from the behavioral data of the process.
- ✓ Model validation: New experiments are carried out to validate the behavior of the created model.

3.3.1 Decision Trees

It is a predictive machine-learning model that decides the target value (dependent variable) of a new sample-based on various attribute values of the available data. The internal nodes of a

decision tree denote the different attributes. The branches between the nodes tell us the possible values that these attributes can have in the observed samples, while the terminal nodes tell us the final value (classification) of the dependent variable. (Sumesh, Rameshkumar, Mohandas, & Babu, 2015)

Two different implementations of the decision tree were used, a first model with a classification tree for qualitative variables (transfer mode) and a second model for quantitative variables (geometry) using regression trees. Implementations were done in Knime software, see below (Figure 30):

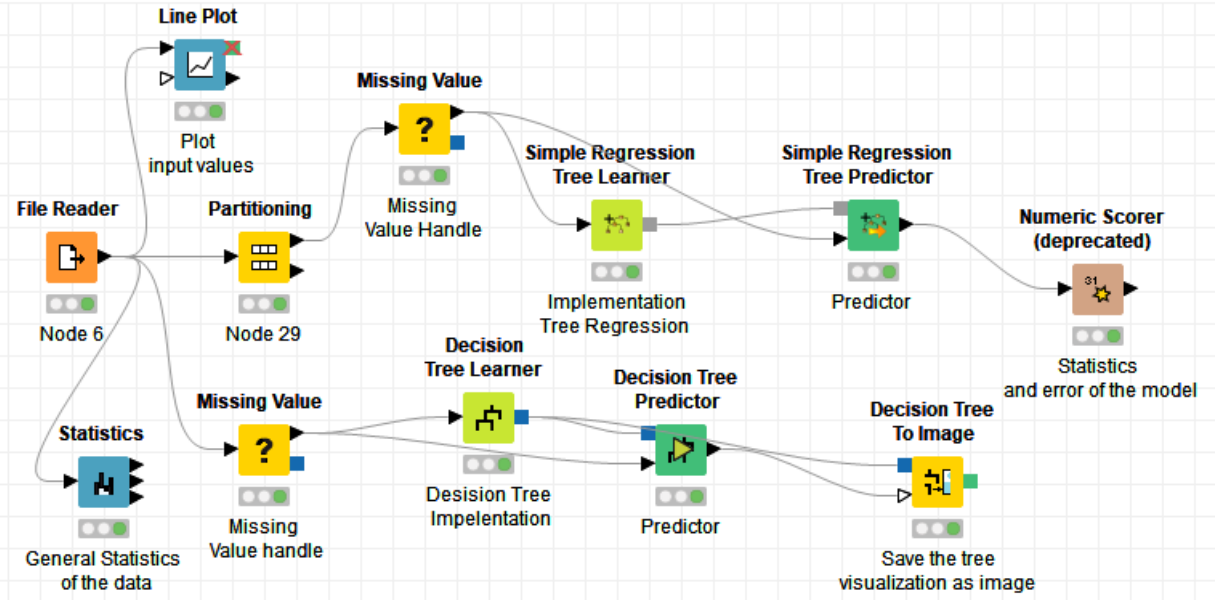

Figure 30 Knime Desition Tree implementation

File reader: Allows reading the data in CSV format.

Missing Value: Helps handle missing values found in cells of the input table

Partitioning: split the input data into two partitions, train and test data (60% of the data was used for training, 20% of the data for validation).

Simple Regression Tree Learner: Is the implementation of the regression tree, follows the algorithm described in CART (Breiman, L., J. Friedman, R. Olshen, 1984), was configured as shown below: Limit number of levels (tree depth, Number of tree levels to be learned.): 3.

Minimum split node size (Minimum number of records in a decision tree node so that another split is attempted.):4, Minimum node size (Minimum number of records in child nodes.):2

Simple regression Tree Predictor: Apply the created model.

Numeric Scorer: computes R^2, mean absolute error, mean squared error, root mean squared error and mean signed difference statistics between the numeric column's values, to see the proportion of the variance in the dependent variable and evaluate the regression model.

The decision tree method was chosen for its classification potential, its easy implementation, and the advantages of a visual representation of the tree that improves the understanding of the patterns found. Other machine learning methods for grouping were also analyzed such as the Kmeans algorithm and self-organizing maps SOM (result presented in previous conference papers by the authors, (Montero Puñales, Elina Mylen; Absi Alfaro, 2018). Being that the decision tree was considered the most convenient method to carry out the model.

The data used for the creation of the trees were the results of the experiments. The four experiments were integrated into an Xls file extension, for a total of 873 records. The parameters collected for each experiment were: voltage reached in the process, process current, welding speed, wire feed speed, sound pressure level, geometry parameters (with and reinforcement), calculated detachment frequency, metal transfer mode (short circuit, spray, globular and transition current)

3.4 Chapter considerations

In conclusion, this chapter has outlined the methodology that serves as the backbone of our data acquisition and analysis process. We have meticulously detailed the various sources from which our data is derived, emphasizing the richness and diversity of our data inputs. Additionally, we have provided a comprehensive exposition of the data processing techniques employed, underscoring the precision and sophistication with which we handle our data. Collectively, these conclusions underscore the rigorous and systematic approach we have adopted in our research, setting the stage for robust data-driven insights and conclusions in the subsequent chapters.

4 Experimental results

This chapter presents the experimental findings derived from the application of the proposed methodology for weld stability assessment in the GMAW process. The objective is to evaluate the relationship between welding parameters and process stability based on multisensory data—including electrical signals, sound pressure, and image-based measurements—collected during controlled tests.

The section begins with a detailed description of the experimental procedure, outlining the configuration of variables such as voltage, current, welding speed, and wire feed speed. Four separate tests were conducted under distinct parameter conditions to investigate their influence on weld bead geometry, process dynamics, and signal behavior.

Subsequent sections present the results of each test individually, highlighting waveform variations, statistical trends, and observed transfer modes. Particular attention is given to the detection of stable and unstable regions, which were identified through acoustic and electrical signal analysis as well as visual inspection of the weld bead.

Following the individual test results, general considerations are provided, synthesizing key patterns and confirming the repeatability of observed behaviors. Finally, the chapter concludes with reflections on the experimental outcomes and how they support the development of intelligent monitoring and classification systems for welding stability.

4.1 Experimental procedure

The results obtained for each experiment are presented below. The experiments were performed by changing the values of the input parameters to study the influence and dependence of those parameters with the resulting welding geometry. The acquisition frequency of current signals is 20 milliseconds and for sound signals, it is 100 milliseconds due to the configuration available in the equipment used.

To perform statistical analysis, the data was divided, each section studied belongs to an area where the input parameters were kept stable when the parameters change a new section is studied independently, allowed to analyze the variations on the outputs parameters. Statistical values corresponding to mean, standard deviation, peak value, background value were

calculated every 200 milliseconds for welding data and 100 milliseconds for sound data. The time registers of the data were used to synchronize both signals by the welded position.
The sheet metal size is 8 mm, welding was from position 5 to 180 mm. The contact tip to work distance used was 18 mm.

4.1.1 Results obtained for test 1

In the first test, the welding speed value was kept constant, varying the wire feed speed and the voltage.

Table 3 Parameter configuration Test 1

Position (mm)	**Voltage(V)**	**Welding Speed (mm/seg)**	**Wire feed speed (m/min)**
5	20	12	5
30	25	12	5
55	25	12	5
80	26	12	7
120	27	12	7
180	27	12	7

Considerations:

It was previously known that the voltage values are directly correlated to the current values, in consequence increasing the value of the voltage the current increases (see Figure 31) and more material is deposited in the piece; as a consequence, the welding geometry changes as shows Figure 35.

The current, voltage and SPL signals have similar behavior (shown in Figures 31, 32, 33 consecutively), the current depending on the voltage supplied to the source and the SPL increasing with increasing current (as shows Figure 34) and the sound pressure levels intensify.

The height (Reinforcement) of the weld bead increased from position 80 due to the increased voltage and wire feed speed (see Figure 34).

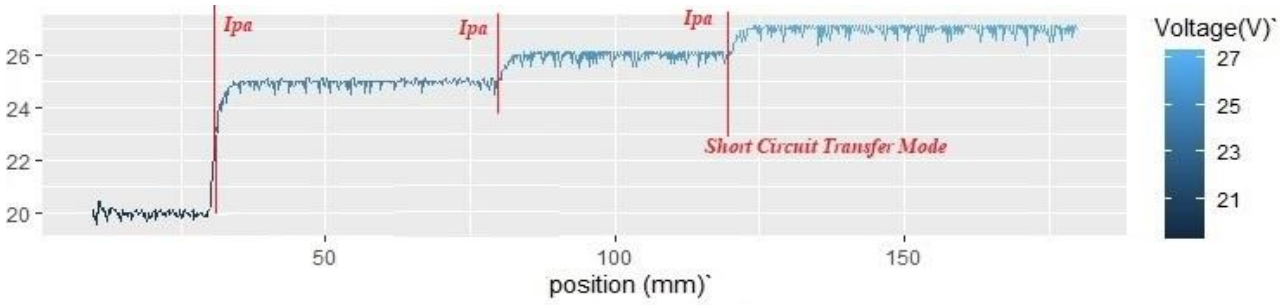

Figure 31 Voltage waveform Test 1

Ipa: Input parameters alteration (Moment when the input parameters are altered)

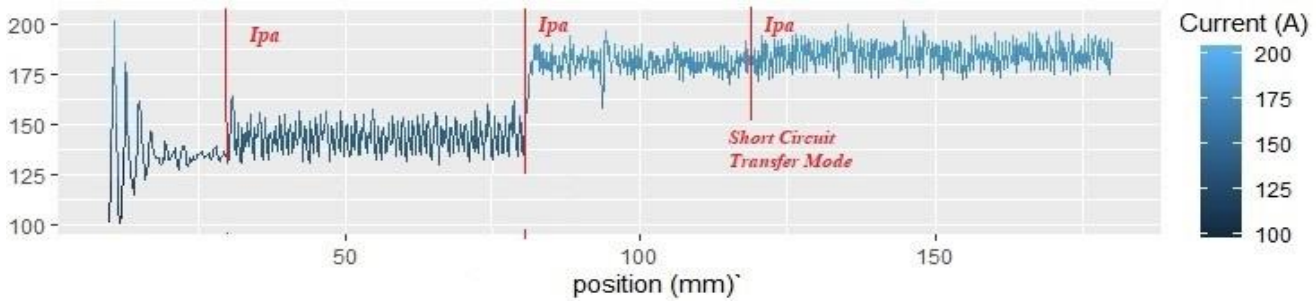

Figure 32 Current waveform Test 1

Figure 33 Sound Pressure level (SPL) Test 1

Figure 34 Reinforcement values Test 1

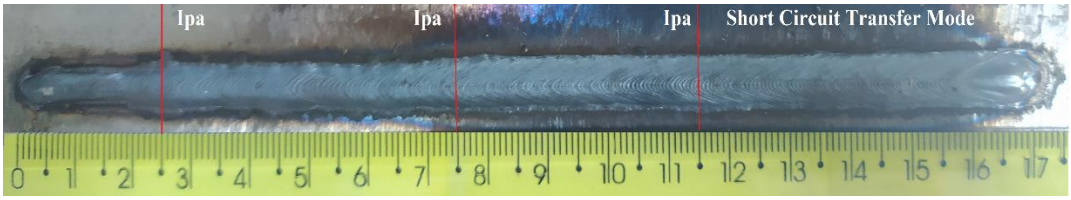

Figure 35 Weld bead geometry Test 1

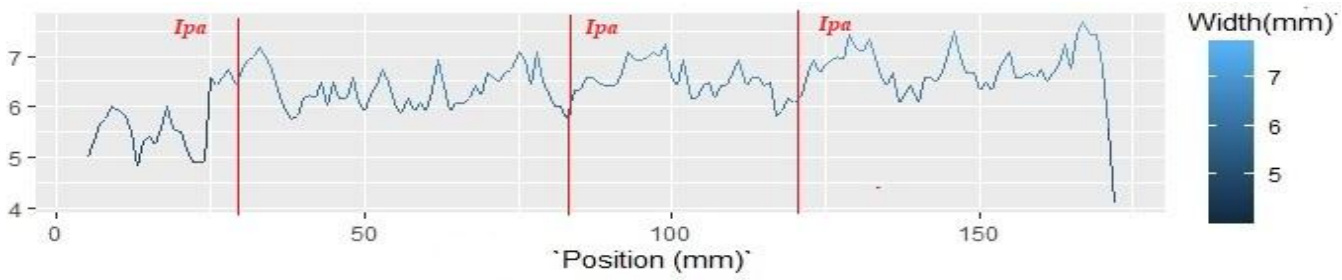

Figure 36 Width values Test 1

The calculated statistical values are presented (see table 4), statistical sequential graphs are presented in Figure 37. The standard deviation of sound pressure values decreases when the current increase and changes in the geometry occur. It is observed that for each welded section, stability states were achieved, at times when the parameters vary the sound signal allows identifying these changes, reaching standard deviation values close to 2.

Table 4 Statistics Test 1

Position (mm)	**SD**					**Mean**				
	A	**V**	**SPL (DB)**	**W (mm)**	**R (mm)**	**A**	**V**	**SPL (DB)**	**W (mm)**	**R (mm)**
0-30	14.51	0.18	1.00	0.35	0.38	135.57	19.96	90.27	5.46	3.09
30-80	7.57	0.39	1.15	0.48	0.22	143.94	24.86	88.53	6.29	2.79
80-180	6.93	0.53	1.25	0.48	0.34	183.03	26.42	91.13	6.60	3.11

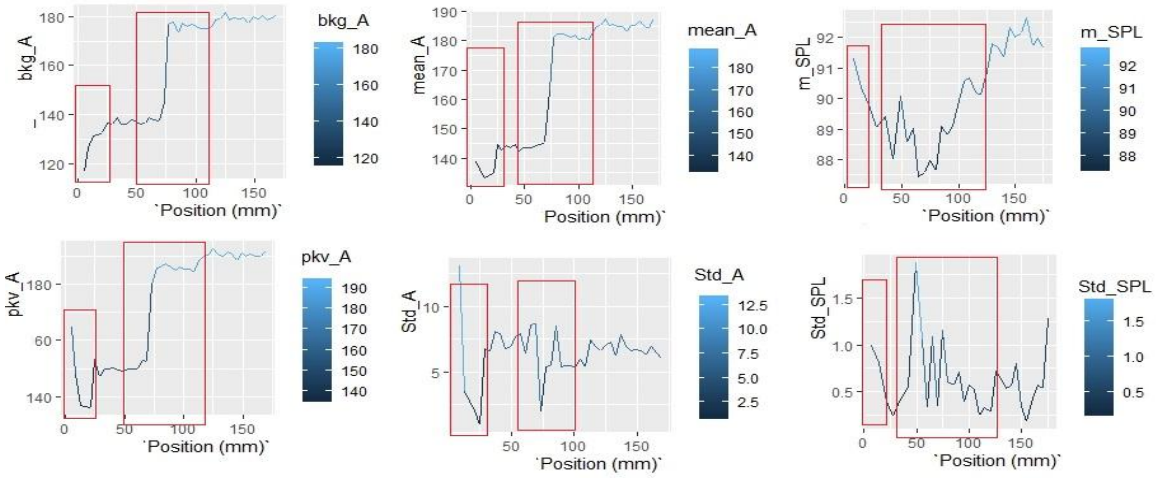

Figure 37 Statistical sequential charts Test 1

Being bkg_A: background value of the current (A), pkv_A: peak value of the current (A), std_A: standard deviation of the current, mean_A: mean of the current, std_SPL: standard deviation of the sound pressure level value, m_SPL means of sound pressure level values (DB).

Transfer mode was identified as a short circuit, with detachment frequency between 25 to 80 drops per second (see Figure 38).

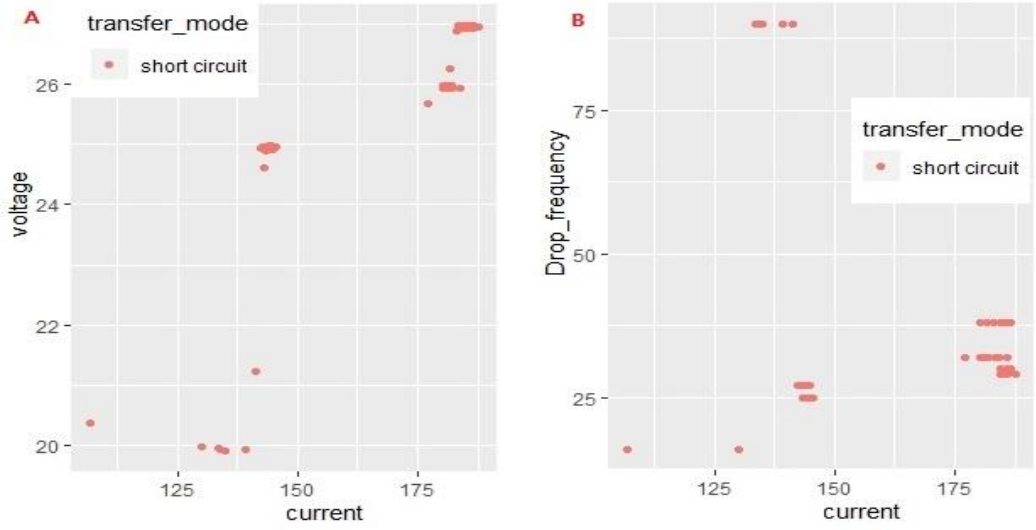

Figure 38 Transfer mode maps (A), detachment frequency map (B) Test 1

A low correlation coefficient for current and voltage is evident in the correlation matrix of this experiment (Figure 39). This result is influenced by the variable wire feed speed, when wire

feed speed is increased instantaneously increases current. If we look closely at Figure 31 that shows the waveform of the current we can deduce that from position 80 the current does not follow the voltage signal.

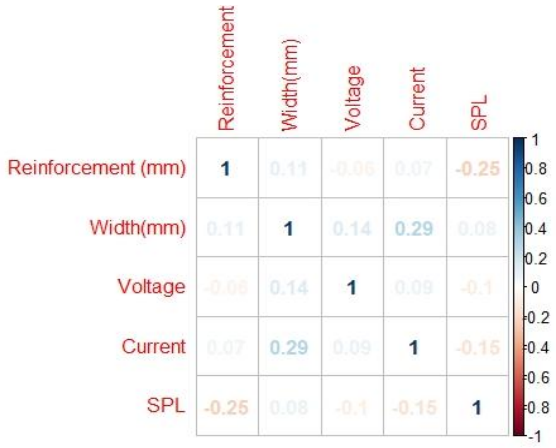

Figure 39 Correlation matrix Test 1

4.1.2 Results obtained for test 2

Experiment two was configured with high voltage values to achieve globular and spray transfer modes. The variable wire feed was also increasing.

Table 5 Parameter configuration test 2

Position (mm)	**Voltage(V)**	**Welding Speed (mm/seg)**	**Wire feed speed (m/min)**
5	32	12	6
30	32	12	6
55	34	12	7
80	34	12	7
120	35	12	8
180	35	12	8

Considerations:

From position 50 to position 100 the presence of transition current was identified (see Figure 40), floats at values from 180 to 220 A and 32 V, changes in the weld geometry (see Figure 44), and a considerable increase in the SPL signal that reached values of 90 Db were reflected (see Figure 42). The sound signal identified for the spray transfer mode is characterized by lower decibels at an average of 88 Db.

The geometry of the weld bead in the area identified for the transition current transfer mode presents irregularities (Figure 44)

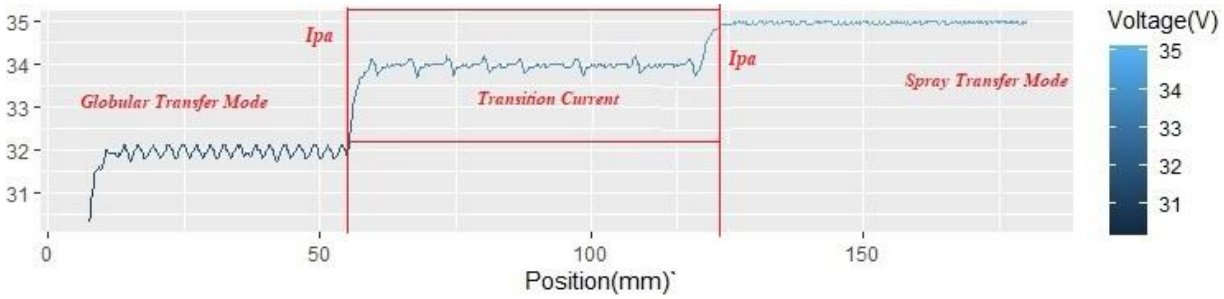

Figure 40 Voltage waveform Test 2

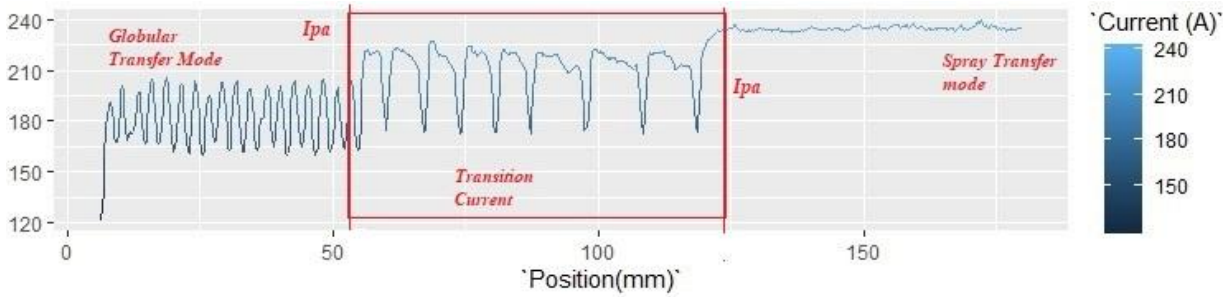

Figure 41 Current waveform Test 2

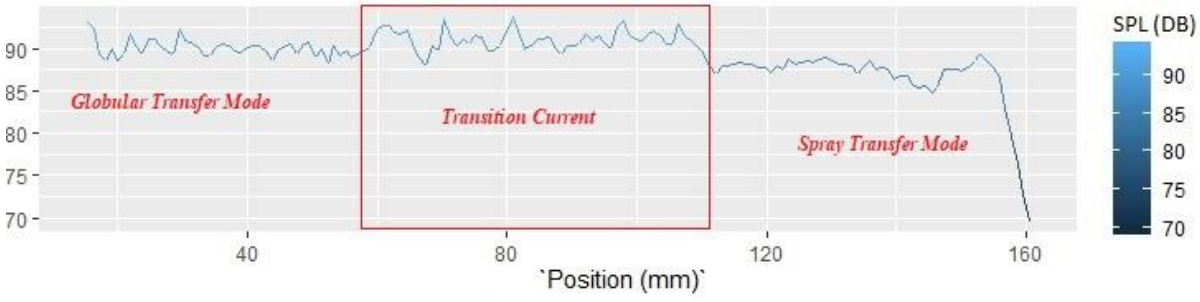

Figure 42 Sound Pressure level (SPL) Test 2

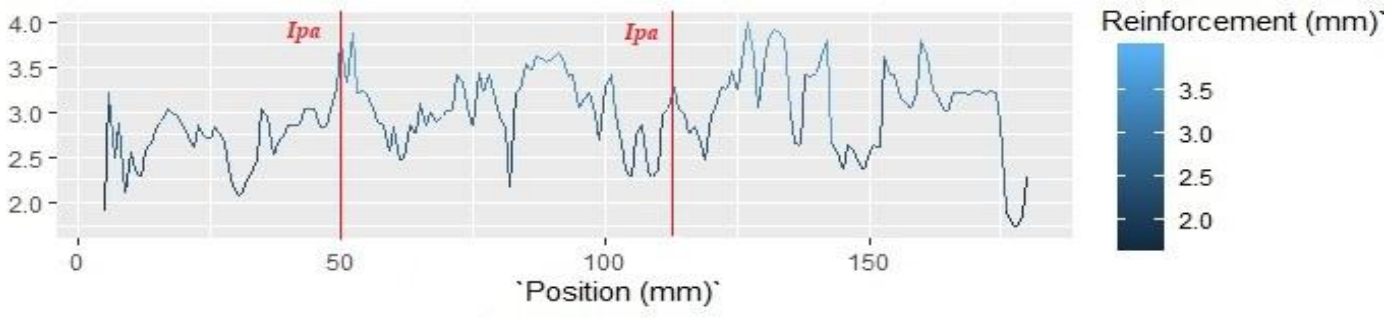

Figure 43 Reinforcement values Test 2

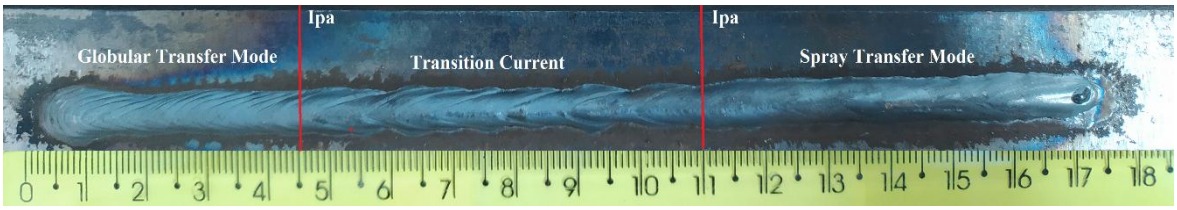

Figure 44 Weld bead geometry Test 2

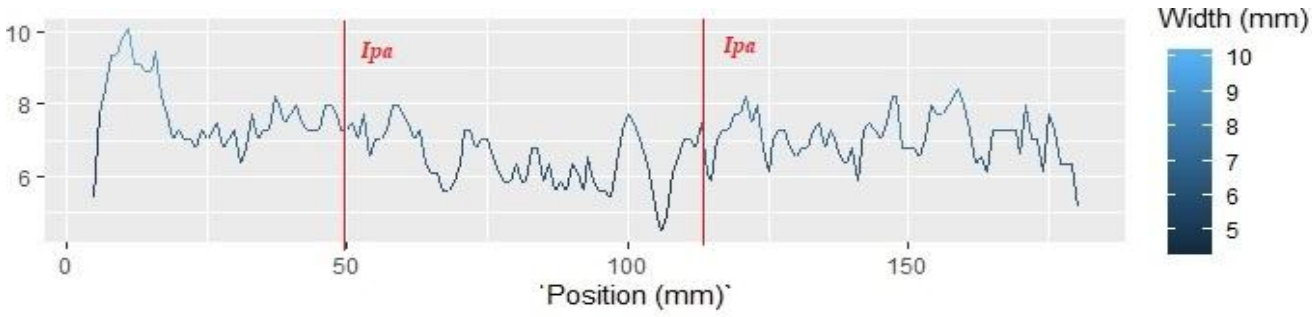

Figure 45 Width values Test 2

Observe in Table 6 that the mean of the current for the area where the transition current was identified has a standard deviation greater than 20.00, which is considered a high value being greater than 15. The increase in sound standard deviation by values close to two is also indicative of changes in geometry. The decrease in the values of the SPL graph at the end of the process corresponds to the closing of the arc.

Table 6 Statistics Test 2

Position (mm)	**SD**					**Mean**				
	A	V	SPL	W	R	A	V	SPL	W	R

			(DB)	(mm)	(mm)			(DB)	(mm)	(mm)
0-55	13.61	0.30	1.31	1.30	0.32	183.08	31.85	90.41	8.08	2.62
55-120	*21.00*	0.99	*2.03*	0.70	0.36	196.71	32.91	90.36	6.99	2.90
122-180	14.38	0.48	1.25	0.81	0.47	225.08	34.53	88.12	6.88	3.05

The sequential graphs (Figure 46) also show in the areas highlighted in red the times when changes and instability in current and voltage signals are detected due to the presence of transition current.

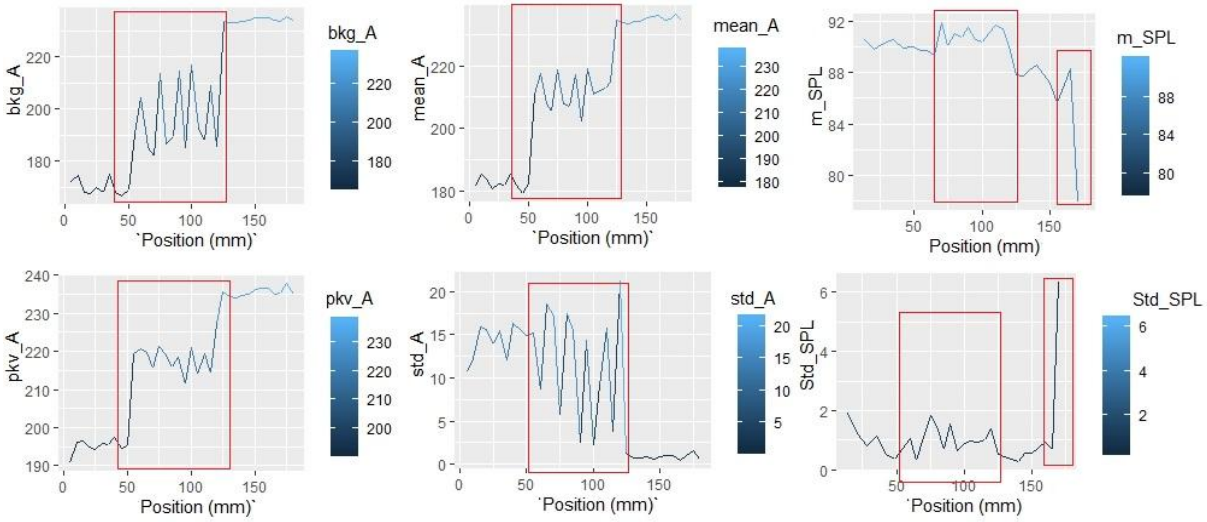

Figure 46 Statistical sequential charts Teste 2

Being bkg_A: background value of the current (A), pkv_A: peak value of the current (A), std_A: standard deviation of the current, mean_A: mean of the current, std_SPL: standard deviation of the sound pressure level value, m_SPL mean of sound pressure level values (DB).

Observing Figure 47 it is possible to verify that the detachment frequency accompanies the increase in current and voltage that generate changes in the transfer mode. For its part, the transition current has a mixture of globular drops that explode and small drops of spray that cause a fluctuation in the values of the sound signal.

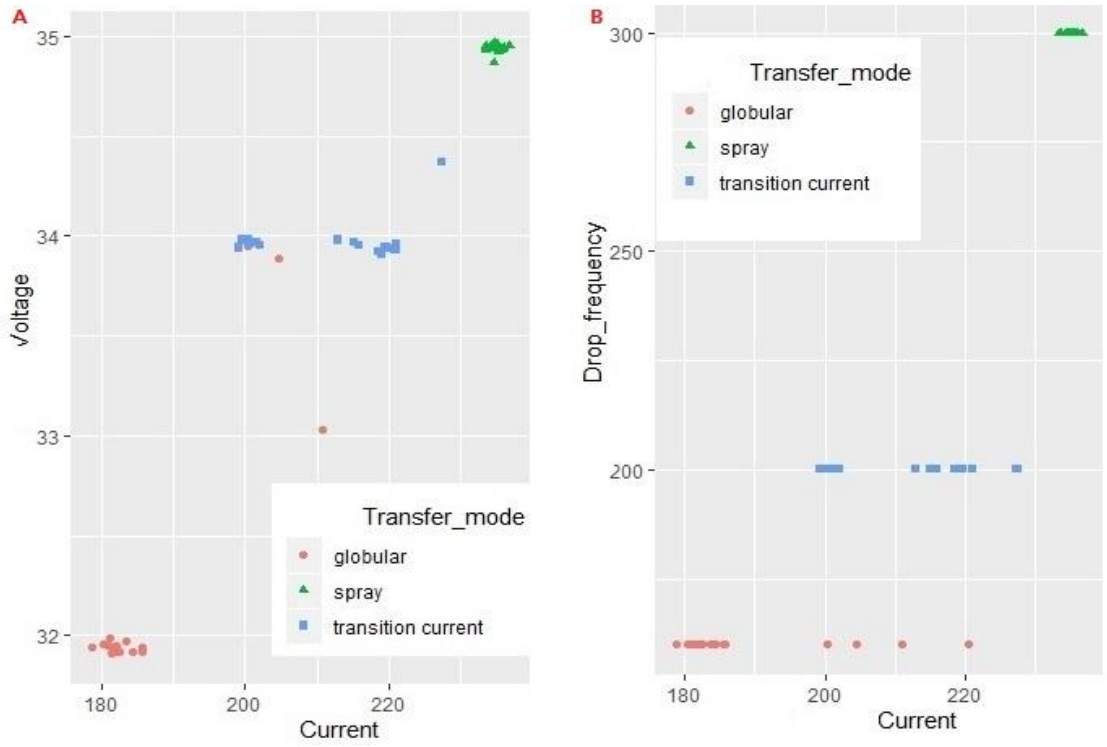

Figure 47 Transfer mode maps (A), detachment frequency map (B) Teste 2

Since the correlation matrix for this experiment (Figure 48) shows a higher negative coefficient for SPL with Voltage and Current, the changes in sound are considerable. For spray transfer mode the sound is quieter and is reflected in lower decibels of the sound pressure level.

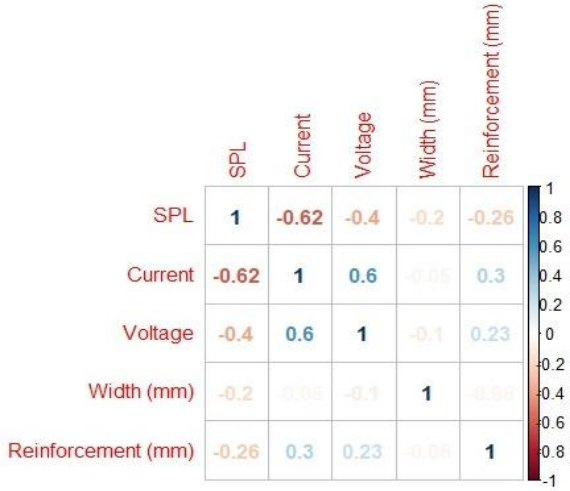

Figure 48 Correlation Matrix Teste 2

4.1.3 Results obtained for test 3

The voltage and wire feed speed are increased and subsequently reduced, the objective is to model the structural difference in deposition and the changes in geometry generated by these two variables.

Table 7 Parameter configuration Test 3

Position (mm)	**Voltage (V)**	**Welding Speed (mm/seg)**	**Wire feed speed (m/min)**
5	20	12	5
30	20	12	5
55	23	12	8
80	23	12	8
120	20	12	5
180	20	12	5

Considerations:

By increasing the wire feeding speed and voltage transfer mode change from short circuit to globular and a higher deposition and reinforcement are obtained in the weld bead. SPL decibels increase in Globular transfer mode.

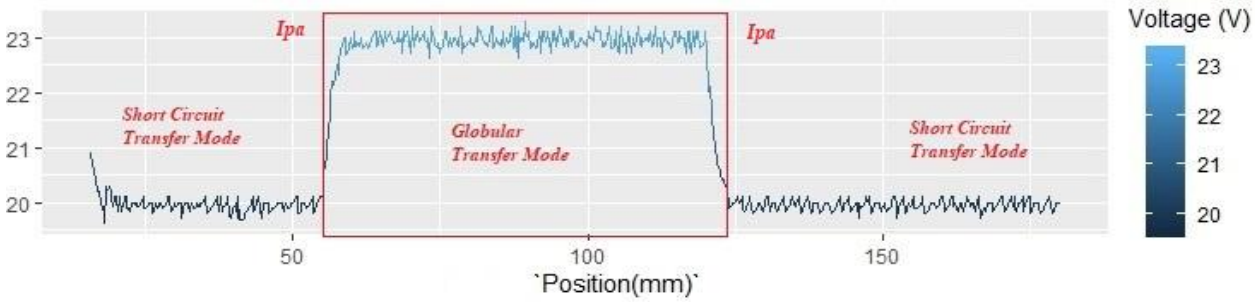

Figure 49 Voltage waveform Test 3

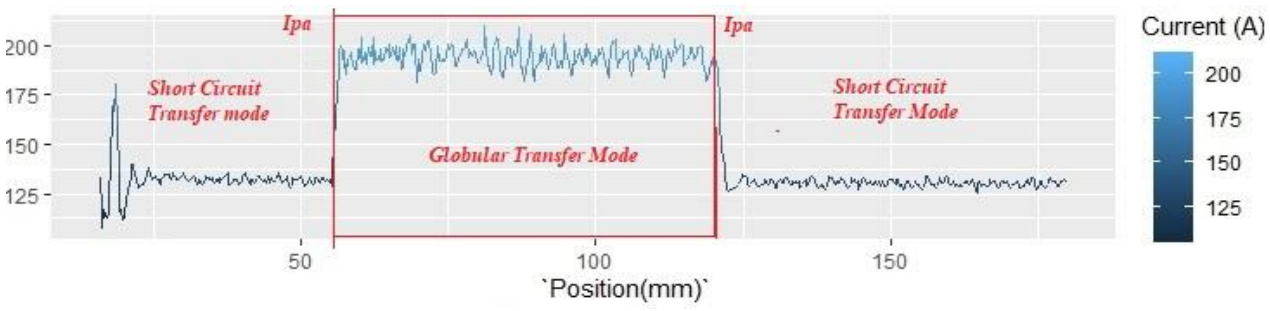

Figure 50 Current waveform Test 3

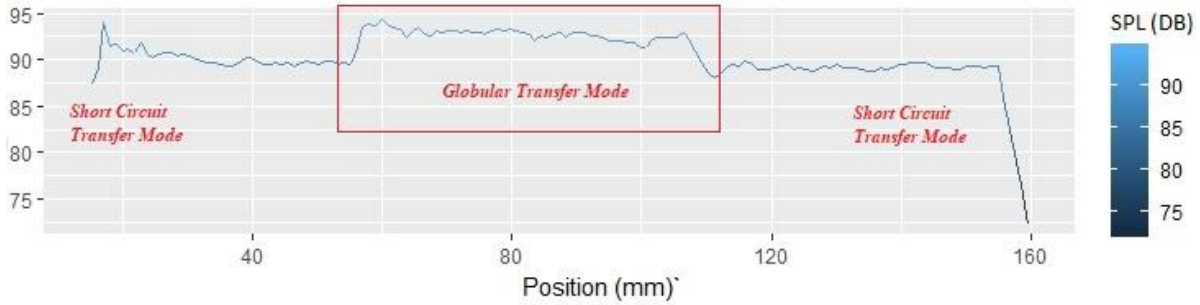

Figure 51 Sound Pressure level (SPL) Test 3

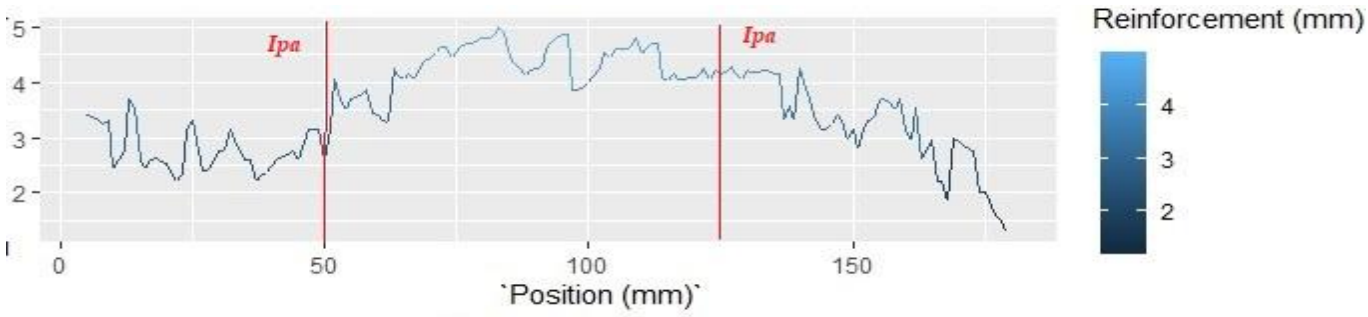

Figure 52 Reinforcement values Test 3

Figure 53 Weld bead geometry Test 3

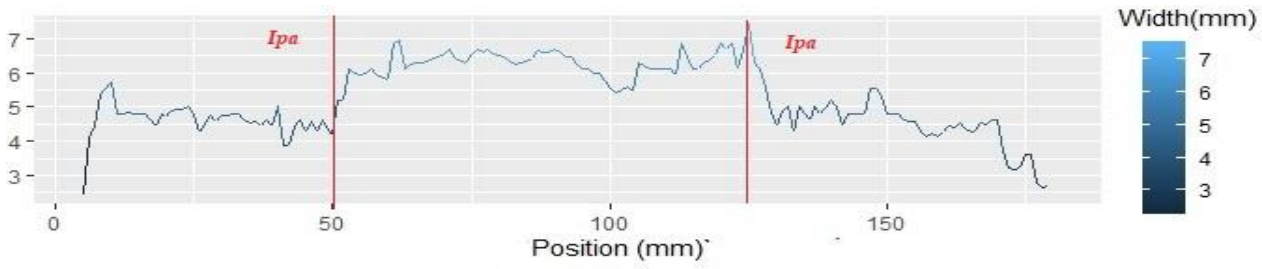

Figure 54 Width values Test 3

Observing the statistics presented in table 8, we find that the standard deviation for the variables is low, the areas present stable values. The variations that appear in the sequential graphs shown in Figure 55, is caused by the variation of the voltage and wire feed speed.

Table 8 Statistics Test 3

Position (mm)	**SD**					**Mean**				
	A	V	SPL (DB)	W (mm)	R (mm)	A	V	SPL (DB)	W (mm)	R (mm)
0-55	7.83	0.17	0.99	0.74	0.57	131.8	19.97	90.12	5.05	2.95
55-120	6.25	0.28	1.58	0.57	0.29	193.9	22.89	91.98	6.16	4.38
120-180	6.53	0.29	2.01	0.71	0.69	131.1	20.006	87.93	4.30	2.92

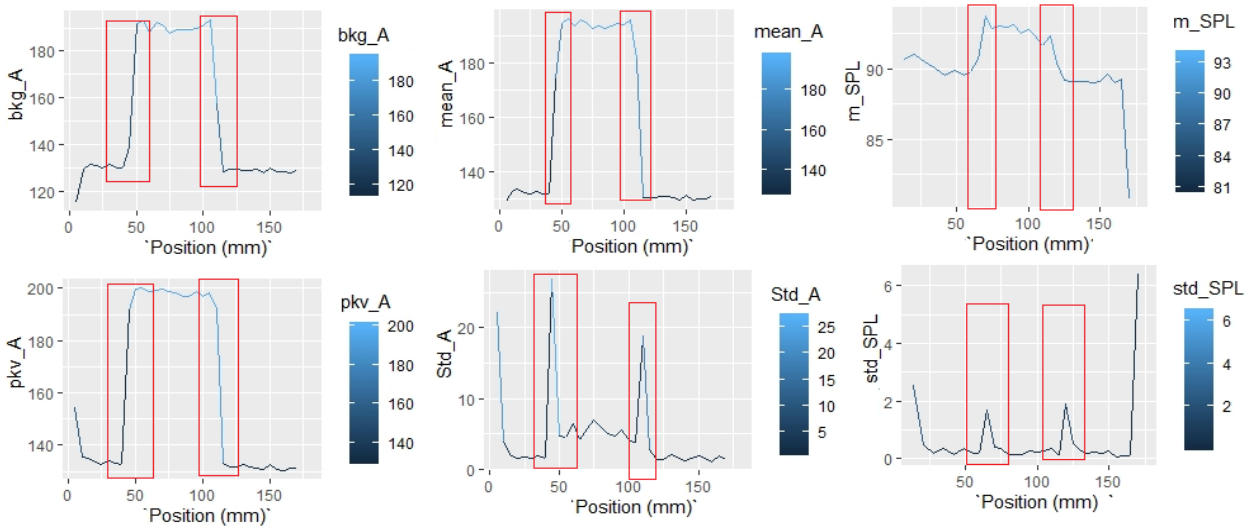

Figure 55 Statistical sequential charts Teste 3

The two transfer modes identified were globular and short circuit as shown in Figure 56.

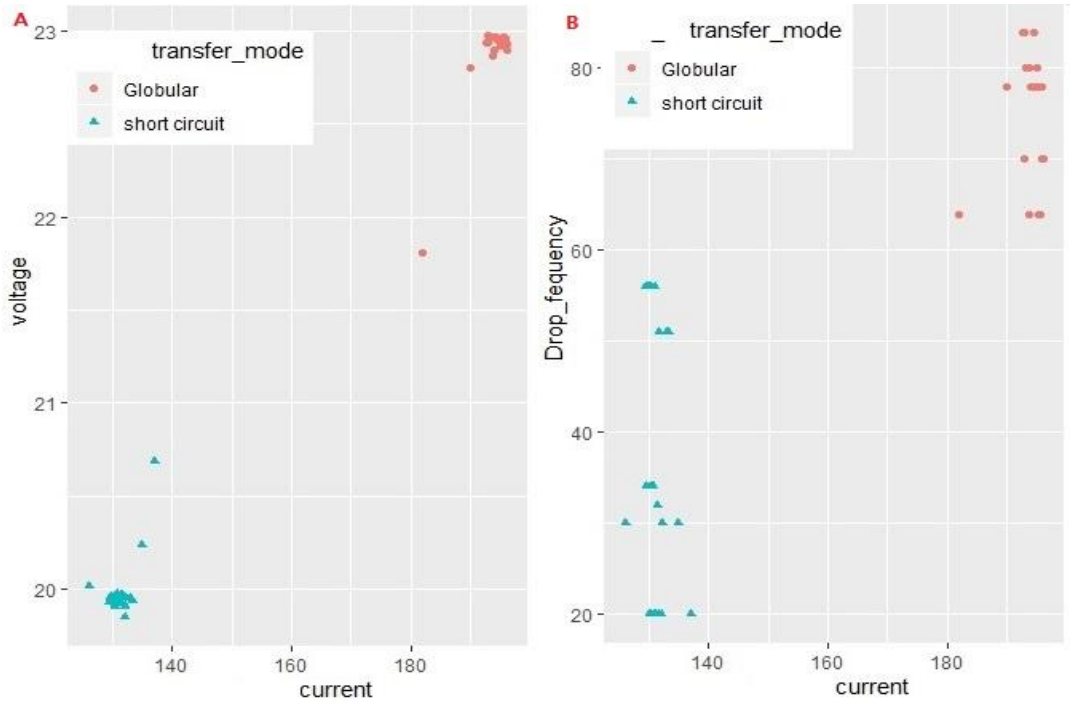

Figure 56 Transfer mode maps (A), detachment frequency map (B) Test 3

This was the test that showed higher correlation indices in its matrix all the variables are correlated.

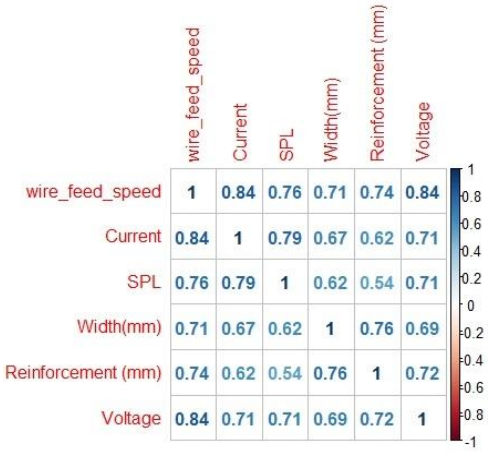

Figure 57 Correlation matrix Test 3

4.1.4 Results obtained for test 4

Configured to see the influence of increased voltage and welding speed.

Table 9 Parameter configuration Test 4

Position (mm)	**Voltage(V)**	**Welding Speed (mm/seg)**	**Wire feed speed (m/min)**
5	23	7	8
30	23	7	8
55	20	10	5
80	20	10	5
120	23	8	8
180	23	8	8
210	23	8	8

Considerations:

The decrease in the welding speed and the voltage increase in the first 60 mm of the weld resulted in an irregular geometry (see Figure 62). It is identified that a welding speed less than 8 causes instability, with highly unstable globular mixed, short-circuit transfer mode.

In the same way with the decrease of the voltage and increase of the welding speed, a thinner bead is obtained to see Figure 62 positions 60-120.

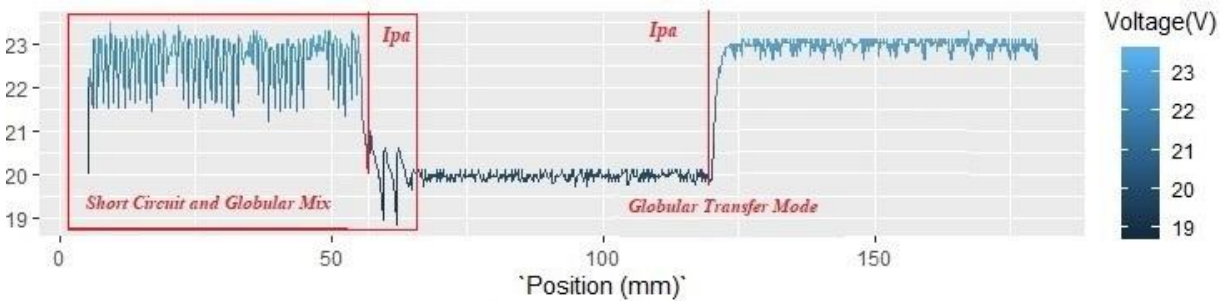

Figure 58 Voltage waveform Test 4

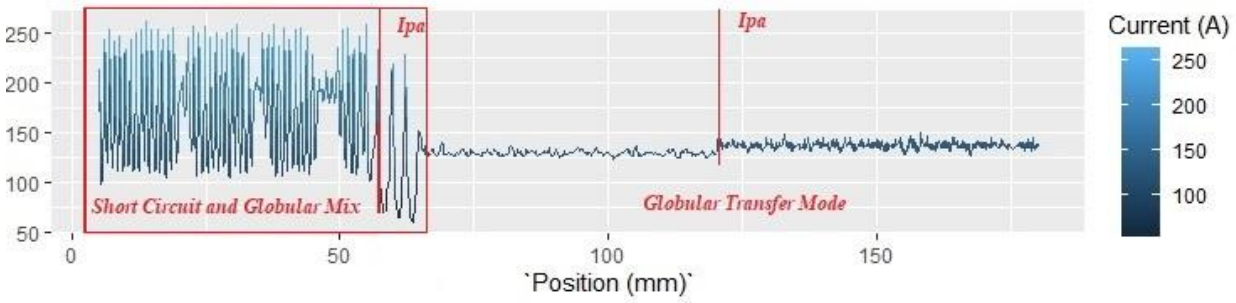

Figure 59 Current waveform Test 4

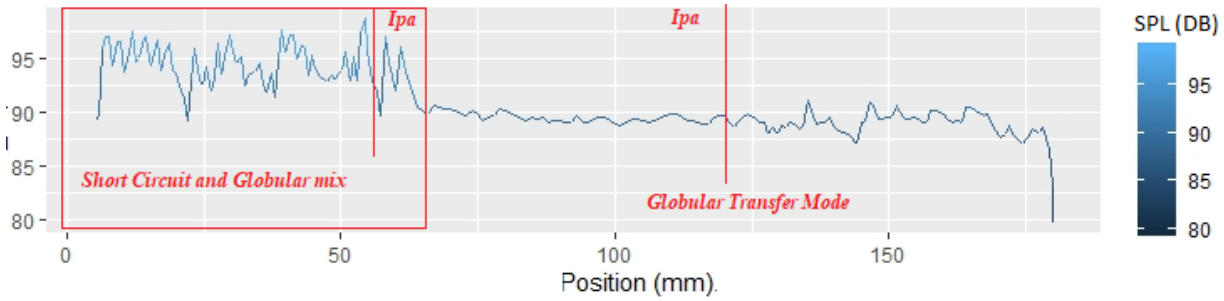

Figure 60 Sound Pressure level (SPL) Test 4

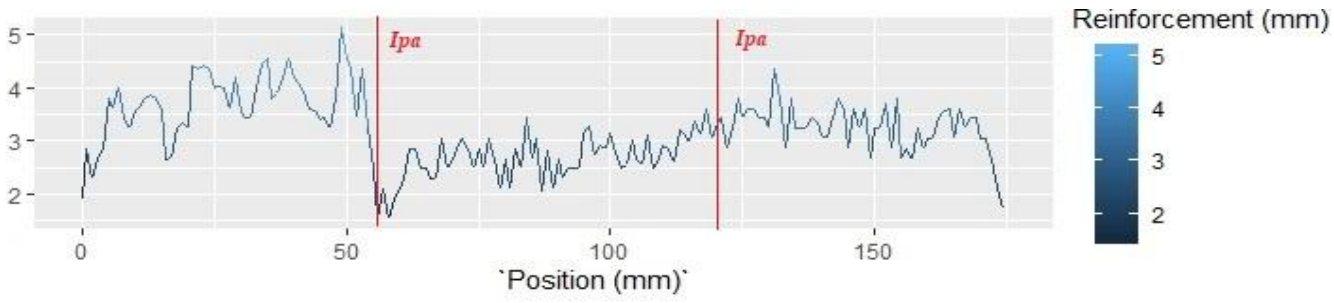

Figure 61 Reinforcement values Test 4

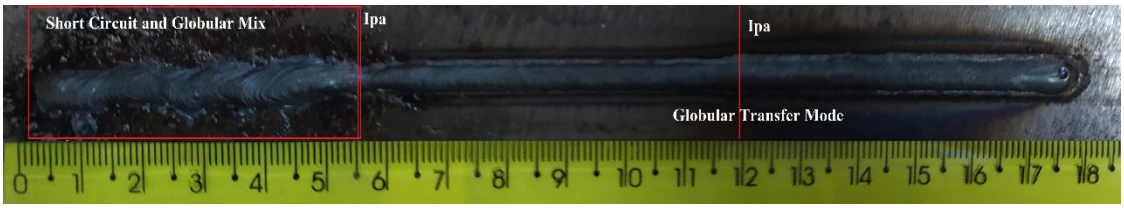

Figure 62 Weld bead geometry Test 4

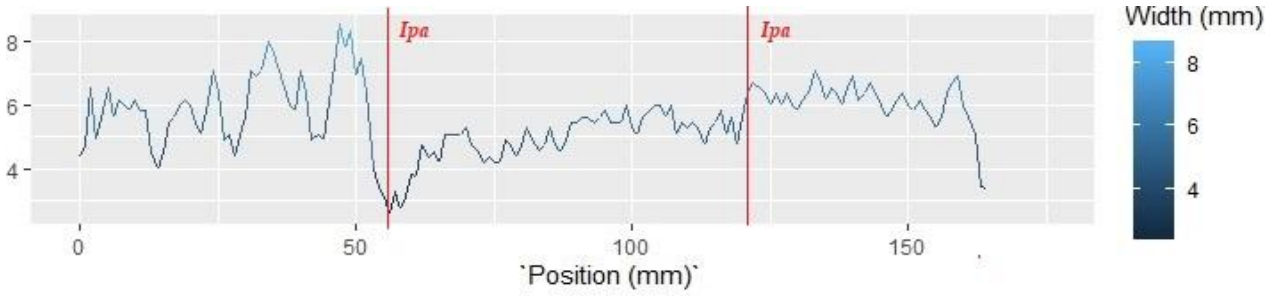

Figure 63 Width values Test 4

For values of voltage in the range of 22 – 23 V and current in the range of 100 – 150 A (position 0 mm to position 60 mm), a mixed globular and short circuit transfer mode is presented (Figure 65 A). The detachment of the drop decreased (see Figure 65 B), a high occurrence of splashes was identified (reflected in the sound pressure level signal, Figure 60) and the geometry presents great irregularity. Note in Table 10 that a high standard deviation for Current and SPL value is obtained (values greater than 2 have been identified for irregularity). Statistical signals are irregular in that position range too, see Figure 64 highlighter area.

Table 10 Statistics Test 4

Position (mm)	**SD**					**Mean**				
	A	V	SPL (DB)	W (mm)	R (mm)	A	V	SPL (DB)	W (mm)	R (mm)
0- 55	44.64	0.55	2.01	1.13	0.62	169.03	22.68	94.41	5.96	3.69
55-120	18.76 *(4.81)*	0.29	1.54	0.80	0.42	129.64	20.00	89.97	4.89	2.67
120-180	4.17	0.21	1.14	0.73	0.43	136.18	22.93	88.72	6.02	3.24

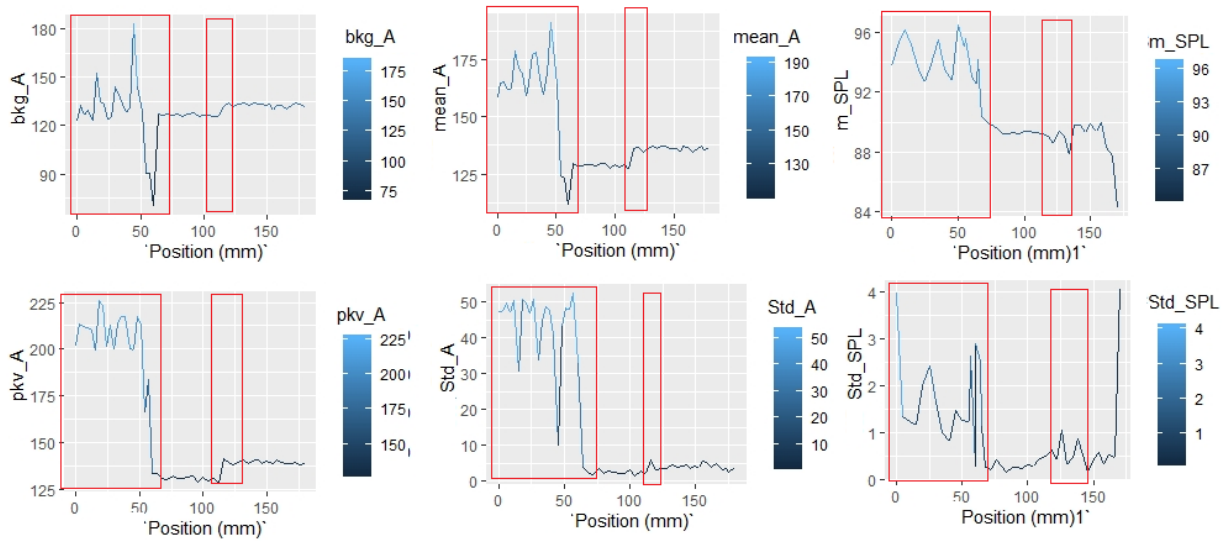

Figure 64 Statistical sequential charts Teste 4

Being bkg_A: background value of the current (A), pkv_A: peak value of the current (A), std_A: standard deviation of the current, mean_A: mean of the current, std_SPL: standard deviation of the sound pressure level value, m_SPL mean of sound pressure level values (DB).

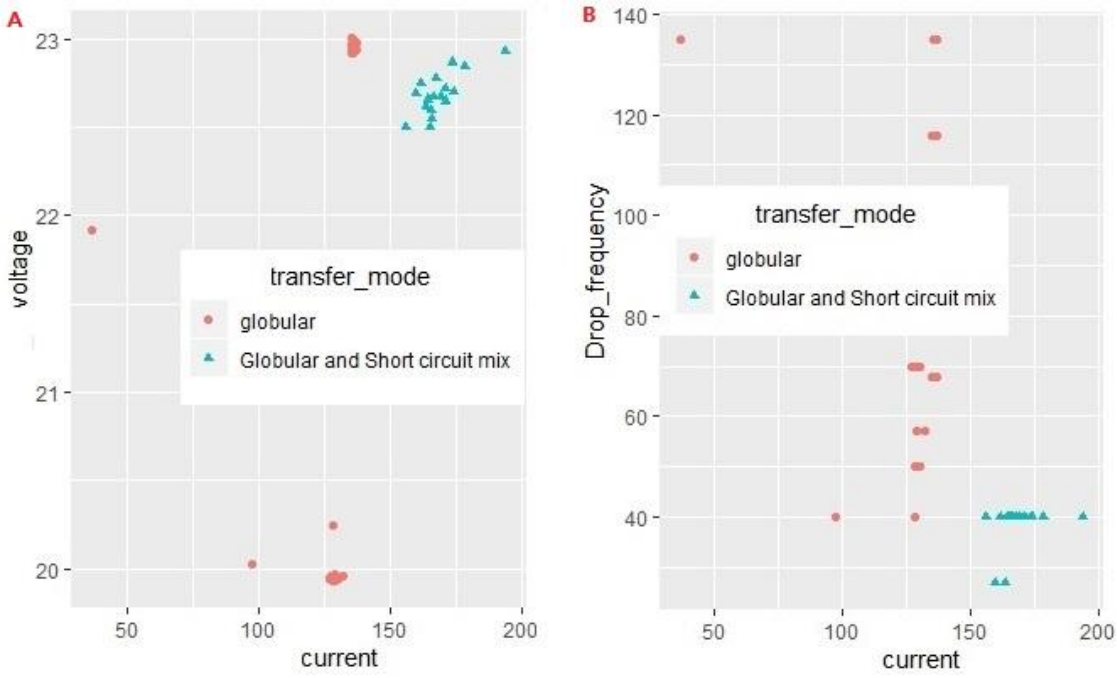

Figure 65 Transfer mode maps (A), detachment frequency map (B) Test 4

A high correlation coefficient for the variable wire feed speed and SPL was obtained. Mixed globular and short circuit transfer mode (transition current) causes a lot of spatters that is reflected in the sound pressure level. This mode of transfer occurred due to the low value of wire feeding speed, therefore the presence of correlation between the two variables. Other relationships known as increased current with higher wire feed speed and higher welding speed were also identified.

Figure 66 Correlation matrix Test 4

4.2 General considerations of the experiments

The experiments were performed with the target that by varying parameters might identify stable and unstable areas. Due to the variation in the parameters, the geometry of the welded bead changes structurally, but there is not necessarily an irregularity in the welded sections, each welded section was analyzed individually. Some characteristics of the experiments carried out are mentioned below:

For each welded section with a certain set of parameters, it is considered instable if: The geometry presents lack of fusion and spatters; Standard deviation of the current greater than 15 and Standard deviation of the SPL greater than 1.0.

The decibels recorded for closed arc, moments before the process begins, and moments after finishing it, is 60 to 70 DB. Already in an open arc the average ranges from 80 to 90 DB. the SPL average is 94 Db for moments of high instability, as shows test 4 position (5 to 55).

The following value ranges cause instability:

Table 11 Value ranges that cause instability

Voltage(V)	**Welding Speed (mm/seg)**	**Wire feed speed (m/min)**
23	7	8
34	12	7

A weak correlation of the variables reinforcement and Sound Pressure level with the coefficient of -0.25 is identified. Making a polynomial regression of both values with the integrated data of the four experiments, a relationship curve is observed between these variables (see Figure 67). This relationship will be analyzed in future works with potentialities to be used in the model for prediction of geometry.

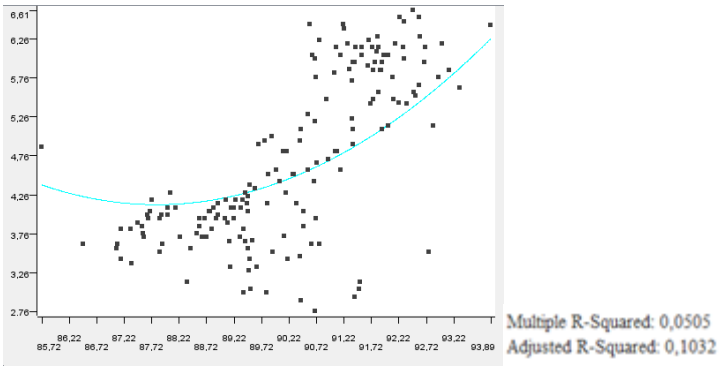

Figure 67 Polynomial regression of SPL and Reinforcement values

Subsequently, indices proposed in the literature by (Carvalho, 1996), (Ogunbiyi & Norrish, 1997) were calculated (see Figure 68) to support the conclusions obtained in our work. Details of the calculated indexes see section 2.9 table 1. Transfer stability Index (TSI), Transfer Index (TI) proposed for classifying the stability based on the current waveform and DCI was based on voltage waveform. Finally, Power Ratio (PR) allows combining current and voltage signal characteristics to monitor stability.

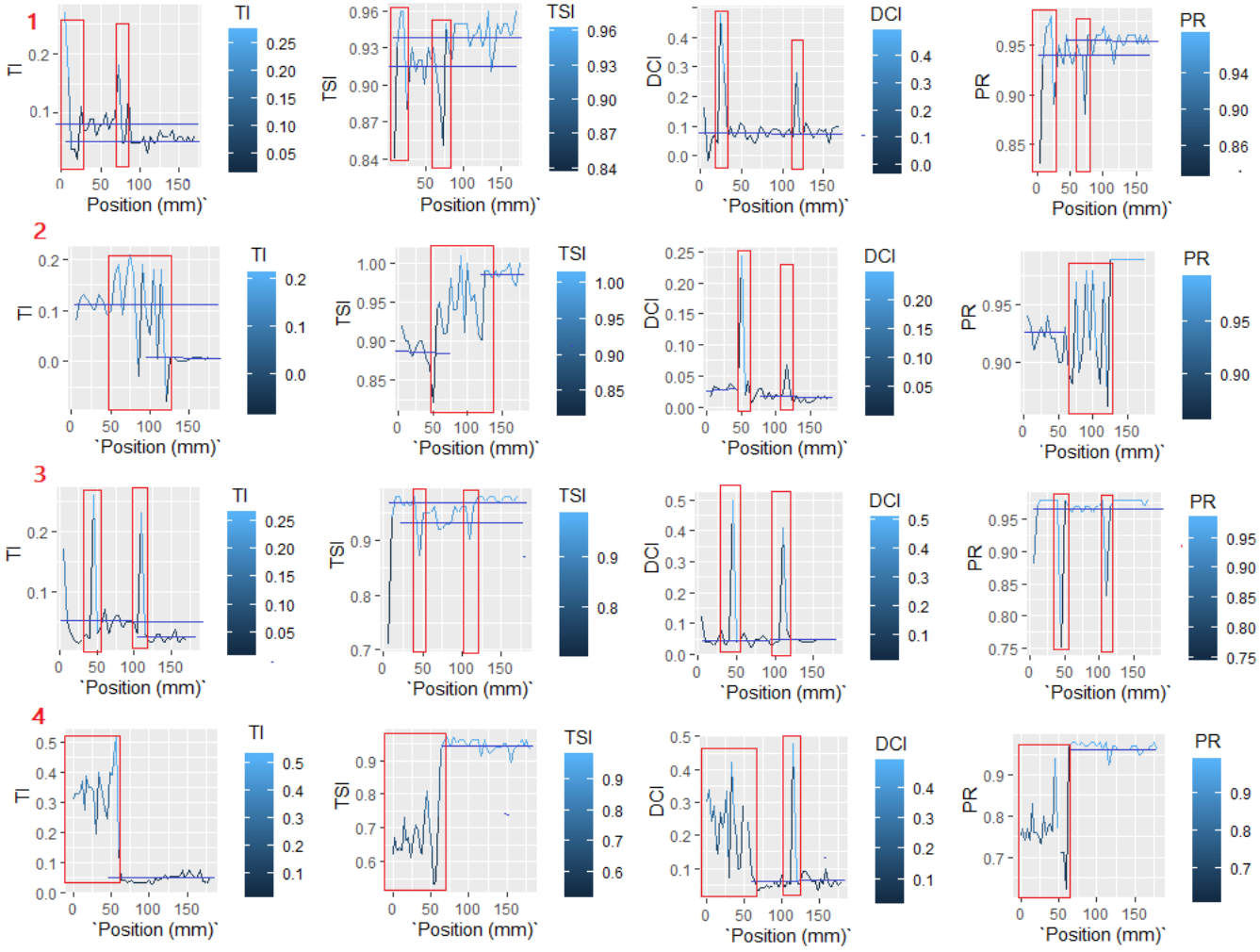

Figure 68 Sequential graphs of TI, TSI, DCI, PR indicators for each experiment

Analyzing the results obtained with the calculated indicators we can conclude that, instances of instability can be identified as shown in the graphs in Figure 68 (instability moments highlighted in red). Note that the DCI value reflects the times when changes in the input voltage values were made. For TI, TSI, and PR values it is possible to identify the moments in which the changes in the input parameters are made and the transition current zones (transition current is presented in experiment 2 position 55 to 125 and experiment 4 position 0 to 60).

The table summarizes the intervals in which stability and instability are presented in the experiments for each indicator.

Table 12 Intervals in which stability and instability are presented for each indicator

Status	TI	TSI	DCI	PR
Stable	0 - 0,10	0,90 - 1	0 - 0,2	0,90 - 1
Unstable	> 0,10	< 0,90	>0,2	<90

The short circuit and globular transfer modes, in addition to being influenced by the process current and voltage, occur depending on variations in the wire feed speed and welding speed. If we look at the general map of the transfer modes for the four experiments (see Figure 69), the globular and short-circuit transfer mode, and the mixture of these two modes can occur in the same ranges of current and voltage. To explore these dependencies, the data were integrated and decision trees were created to separate and classify the data (see image 70). The created decision tree classified with an absolute mean error of 0,243 (see Figure 71).

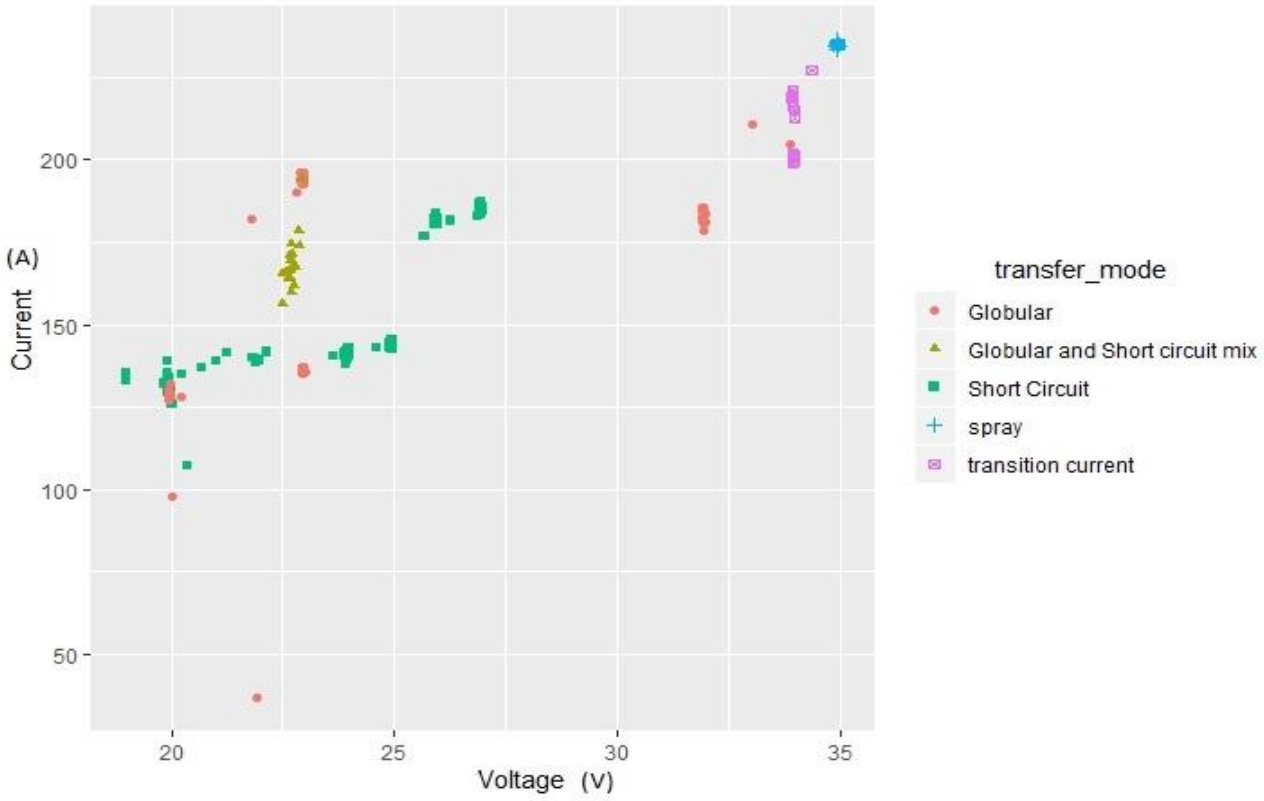

Figure 69 General transfer map (Test 1-4)

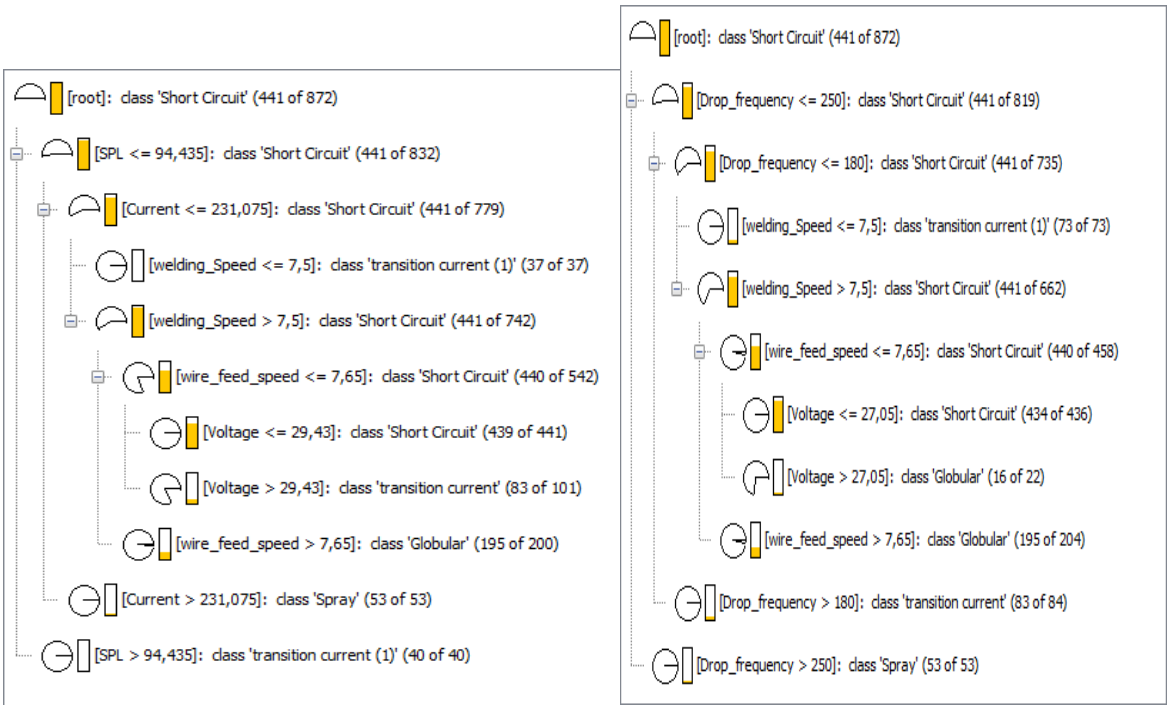

Figure 70 Decision tree for transfer mode classification

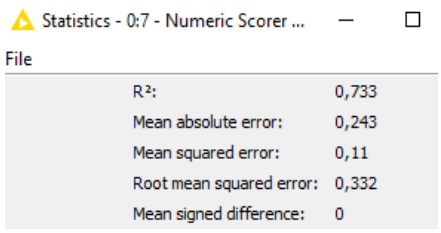

Figure 71 Decision tree classification error

The classification of the metal transfer mode was performed by taking this feature as the target variable in decision tree models. The results indicate that the *spray* transfer mode occurs when the welding current exceeds 231 A, a rule that was satisfied in 100% of the 53 analyzed cases. For current values below 231 A, the *short-circuit* transfer mode predominates, especially when the welding speed is greater than 7.5 mm/s, the wire feed speed is less than or equal to 7.6 mm/s, and the voltage is less than or equal to 29.43 V — this condition was met in 441 out of 889 analyzed cases. When the current is below 231 A and the welding speed is less than 7.5 mm/s, a *globular* or *mixed short-circuit and globular* transfer mode is observed (labeled in the image as “transition current 1”). Within this range, when the welding speed exceeds 7.5 mm/s,

the wire feed speed exceeds 7.65 mm/s, and the voltage is above 27.5 V, *globular* transfer occurs — a pattern observed in 195 of 204 samples.

Additionally, the SPL (Sound Pressure Level) variable was also associated with transfer mode stability. Globular and short-circuit mixed transfer mode — characterized as highly unstable — is observed for SPL values above 94 dB. None of the other transfer modes reached this SPL value.

Decision trees implemented with a regression model for correlation of numerical values were also implemented (see appendix 1 and appendix 2).

Regarding bead geometry, regression trees were used to analyze the influence of process variables on reinforcement and width. For the *reinforcement* variable, when the wire feed speed is greater than 6.81 mm/s, the average reinforcement is 3.30 mm. This value is influenced by both welding speed and SPL. When the SPL is above 91.95 dB, the average reinforcement increases to 3.68 mm, with even higher values observed when the welding speed exceeds 11 mm/s — reaching a mean reinforcement of 4.18 mm. On the other hand, when SPL is below 91.95 dB, the average reinforcement is 3.38 mm. However, if the wire feed speed exceeds 9.4 mm/s, reinforcement decreases to an average of 2.79 mm. For wire feed speeds below 6.8 mm/s, the average reinforcement is 2.4 mm. A particular behavior was noted when the current is below 131 A and SPL is below 90 dB, in which the reinforcement increases to approximately 3.13 mm.

The average *bead width* across the four tests was 5.75 mm. Increasing the wire feed speed has a direct effect on width, reaching an average of 6.62 mm for a wire feed speed of 7.5 mm/s. For wire feed speed values of 8.4 mm/s and current below 136 A, the average width is 5.67 mm. Meanwhile, current values above 136 A are associated with wider beads, with a mean width of 6.46 mm.

In summary, the wire feed speed has a significant impact on both reinforcement and bead width. Welding speed also affects reinforcement, while current strongly influences width. SPL is related to average reinforcement and serves as an auxiliary parameter in assessing transfer stability.

In summary, the analysis revealed key correlations between welding parameters and transfer modes, as well as geometric outcomes of the weld. Spray transfer mode was consistently observed at currents above 231 A, while short-circuit and globular modes appeared below this threshold, depending on voltage, wire feed speed, and welding speed. SPL levels above 94 dB were linked to highly unstable mixed transfer modes. In terms of bead geometry, wire feed speed emerged as the most influential variable, directly affecting both reinforcement and width. Reinforcement increased with SPL and welding speed, while excessive wire feed speed caused a decrease. Similarly, higher current levels promoted wider beads. These findings provide a solid foundation for understanding the relationships among process parameters, stability, and resulting weld quality.

4.3 Proposal of stability indicator based on the characteristics extracted from the data.

In our pursuit of understanding and classifying stability in the welding process, we undertook a multifaceted approach. Initially, we processed the results obtained from our experiments, identifying specific characteristics that enabled the delineation of stable and unstable areas within the process. Subsequently, we embarked on creating a predictive model harnessing artificial neural network technology, implemented using the Knime platform.

The modeling phase involved a meticulous exploration of the neural network's architecture, aiming to optimize its performance. For this purpose, we employed the Knime RProp algorithm, an optimization technique that adapts weight updates according to the error function's behavior. This local adaptation, as described by (Riedmiller & Braun, 1993), allowed us to fine-tune the network's learning process for more precise stability classification. Figure 72 shows the implementation made in Knime environment.

The training data for our neural network model comprised a range of parameters obtained during data processing, encompassing various metrics related to current, voltage, sound, and other critical factors. These inputs were fed into the network, with outputs defined as binary values, representing stable (0) and unstable (1) processes.

The model's implementation extended beyond Knime into the Python programming language, where we harnessed the capabilities of TensorFlow for neural network development. We

leveraged popular libraries such as NumPy and Pandas for data preprocessing and analysis, OpenCV for image processing, and the Keras API for constructing and training the neural network architecture.

For training, the values obtained in the processing were used as inputs: mean of the current obtained in the process (mean_A), the standard deviation of the current obtained in the process (std_A), peak value of the current and voltage obtained in the process (pkv_A, pkv_V), background value of the current and voltage obtained in the process (bkg_A, bkg_V), calculated values of Transfer Index (TI), Transfer Stability Index (TSI), Power Ratio (PR), Dip Consistency Index (DCI), mean Sound Pression level (m_SPL), the standard deviation of Sound Pression level (std_SPL), the standard deviation of the geometry values reinforcement and width (std_R, std_W). The network outputs were defined in binary values being 0 stable processes, and 1 unstable process. The values of all experiments were integrated into an Xls document as shown in appendix 5, with a total of 165 records for each parameter.

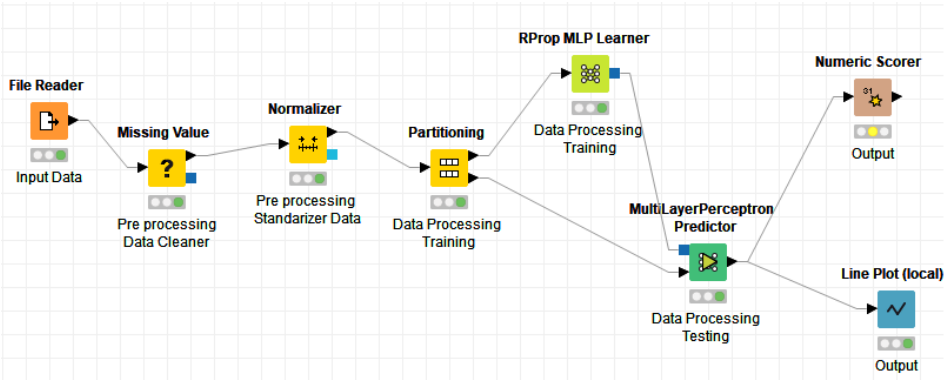

Figure 72 Multilayer perceptron feedforward artificial neural network Knime implementation

Subsequently, we validated the model with data from new experiments, deliberately introducing challenges such as rust and paint application to the welding surfaces. These irregularities were strategically incorporated to test the model's robustness and its ability to identify issues in adverse welding conditions. The impact of rust and paint on welding parameters, as well as the corresponding sound level variations, were meticulously analyzed to evaluate the model's performance under these challenging circumstances.

In these experiments, the test was conducted with the voltage and current configuration of Test 2, while intentionally subjecting the test specimens to oxidation and paint application to generate irregularities in the GMAW welding process. The presence of paint and rust on the welding surfaces introduces additional complexities and challenges to the welding process. Paint can negatively impact the adhesion of the welding material, resulting in decreased weld quality. Moreover, the emission of gases and particles from the paint during welding can affect the stability of the arc and the overall weld quality. Rust on the welding surfaces can impede proper fusion of the materials, leading to compromised structural integrity of the weld. By incorporating these intentional irregularities, the model's performance was further evaluated, specifically in its ability to accurately identify and predict issues in the welding process under adverse conditions.

As As shown in the images 73,74, a significant change can be observed in the sound level signal when the welding process passes through areas affected by rust and paint. The presence of rust and paint introduces disturbances that impact the welding process. Additionally, the results of current and voltage variations obtained in Test 2 were compared with the results obtained when these disturbances were present. These comparisons allow us to evaluate the effects of rust and paint on the welding parameters and further assess the performance of the model under these challenging conditions.

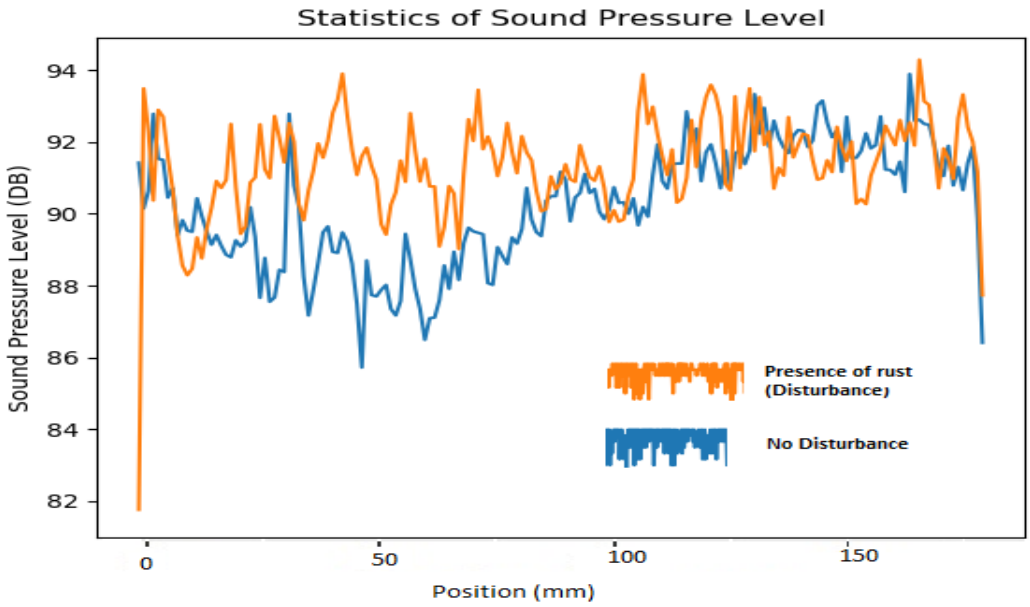

Figure 73 Sound Pressure Signal Comparison - Original Test 2 vs Test with Disturbances

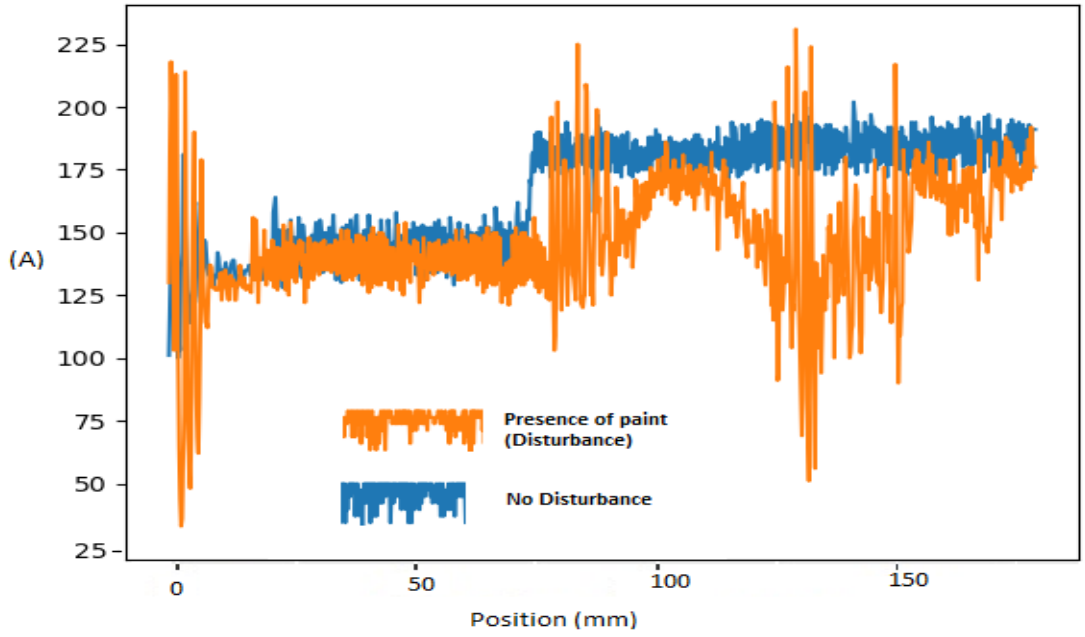

Figure 74 Amperage Signal Comparison - Original Test 2 vs Test with Disturbances

Figure 75 illustrates the classification results obtained for all tests based on the calculated indices. The red line represents the stability classification, with a value of 1 indicating unstable areas and a value of 0 indicating moments of stability. It is important to note that there are some values that fall outside the expected range (highlighted in orange in the image), particularly in the DCI parameter. These values were not identified in the model due to the experiments involving changes in the reference voltage values supplied to the source. The presence of these out-of-range values highlights the need for further analysis and refinement of the model to account for such variations in the experimental setup.

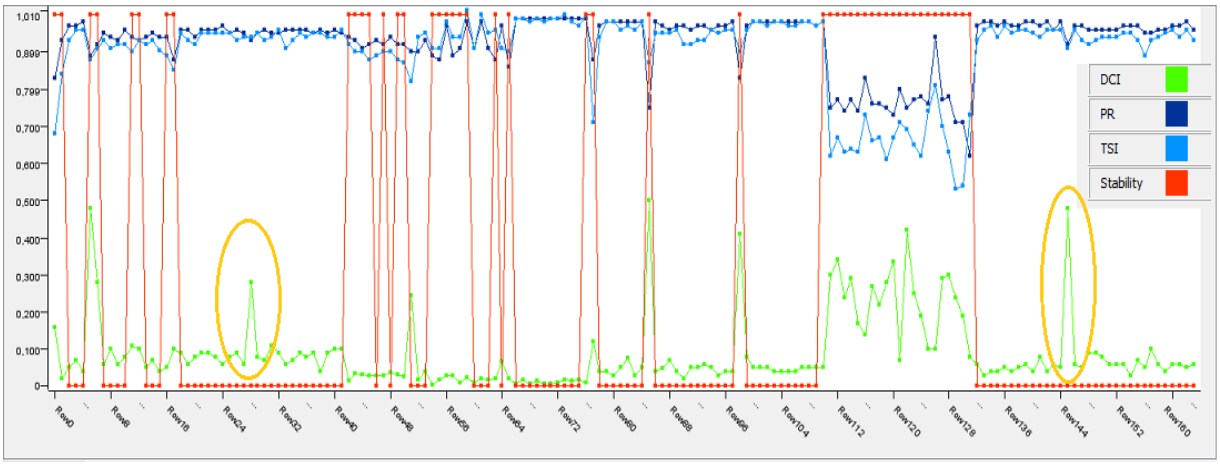

Figure 75 Classification Performance Considering Computed Stability Indices and Experimental Disturbances.

In Figure 76, the pink line represents the prediction obtained from the neural network for the target variable of stability. The neural network's prediction closely aligns with the initial classification line in blue, demonstrating its accuracy. Through the learning process, the model was able to identify areas of instability that were not initially detected in the classification due to the introduced disturbances, as indicated by the orange-highlighted regions. These disturbances, such as oxidation and paint application, had a noticeable impact on the sound pressure signal, and the neural network successfully captured these changes to predict the stability of the welding process.

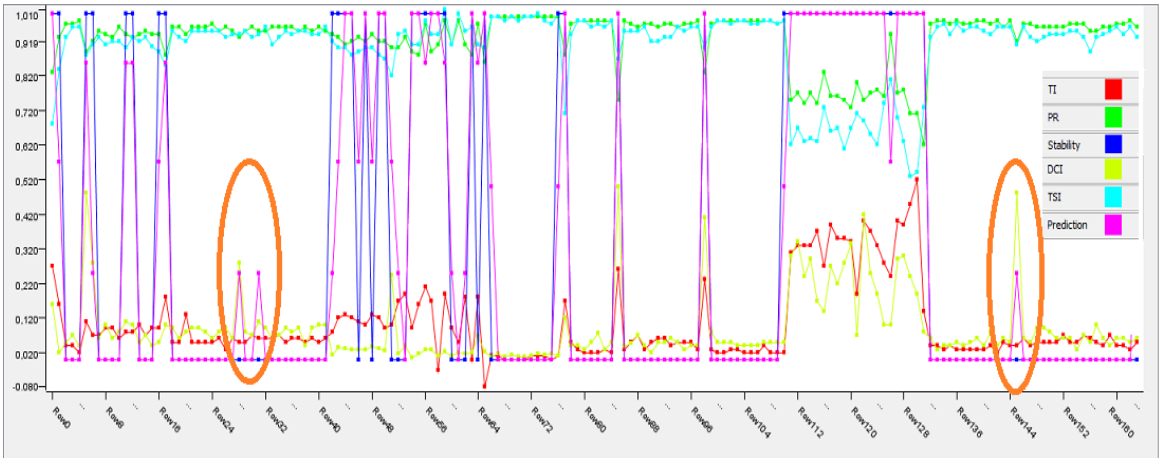

Figure 76 Prediction obtained with the neural network.

4.4 Chapter considerations

Analyzing the results obtained with the calculated indices, it can be concluded that statistical analysis played a crucial role in the classification of stability in the GMAW welding process. By calculating and evaluating various indices such as Dip Consistency Index (DCI), Power Ratio (PR), Transfer Stability Index (TSI), and Transfer Index (TI), it was possible to assess the stability of the process. These indices provided valuable insights into the variations and deviations in current, voltage, and sound pressure level (SPL) values.

The experimental setup played a crucial role in obtaining accurate and reliable signals for analysis. The specially designed welding workstation and data acquisition system provided a controlled environment for signal acquisition. The welding parameters, including voltage, current, welding speed, and wire feed speed, were precisely controlled and monitored. This ensured the consistency and accuracy of the collected data, allowing for robust statistical analysis.

Moreover, the presence of disturbances such as oxidation and paint on the welding surfaces significantly influenced the welding process and its stability. These disturbances resulted in noticeable changes in the sound pressure level signal. The model successfully identified and classified the instability associated with these altered values of DCI, which were not initially accounted for in the classification. This highlights the importance of considering external factors and their statistical impact in ensuring stable welding processes.

5 Conclusions

This thesis presented a comprehensive methodology for evaluating stability in the Gas Metal Arc Welding (GMAW) process, combining statistical indicators, data fusion, and machine learning techniques. Through the integration of acoustic, visual, and electrical data, it was possible to identify critical parameters and patterns that influence weld quality in real time.

The experimental results demonstrated that specific ranges of voltage, wire feed speed, and welding speed are strongly correlated with unstable metal transfer modes, such as globular or mixed modes. By applying statistical methods—including standard deviation, kurtosis, and peak/background signal values—key stability metrics were extracted and validated across multiple experiments. These metrics enabled the classification of welding segments into stable or unstable regions with a high degree of reliability.

A machine learning model based on artificial neural networks was successfully trained to predict process stability using these extracted features. The model proved capable of identifying not only expected instability zones but also unforeseen disturbances, such as those caused by surface oxidation and paint contamination. This highlights the system's robustness and potential for deployment in industrial environments where real-time monitoring and control are essential.

Overall, the proposed methodology advances the field by offering a data-driven, non-intrusive, and scalable solution for welding stability assessment. It paves the way for the development of intelligent quality control systems capable of adapting to complex process dynamics. Furthermore, the use of sensory fusion and artificial intelligence contributes to reducing material waste, improving safety, and enhancing production efficiency.

6 Future works

Future work will focus on enhancing the predictive capabilities of the proposed model by incorporating penetration as a key variable, enabling a more comprehensive assessment of weld quality. To achieve greater accuracy in geometric measurements and reduce modeling errors, a laser scanner will be employed. Additionally, data collected from unstable welding conditions will be used to define intelligent rule sets for a real-time artificial intelligence system capable of detecting instability with high precision. These developments will be combined with mechanical performance tests—such as tensile strength and hardness—and improved sensor integration, thus supporting the implementation of robust, fully automated control strategies for the GMAW process.

To promote transparency and reproducibility, all data collected in this research has been stored in an open-access repository: osf.io/j2swb.

To complement the technical evaluation of the proposed methodology, a strategic analysis was conducted to assess both internal capabilities and external conditions that may influence its implementation.

- Strengths:
  The system offers real-time monitoring using a non-intrusive sensor fusion approach, enabling simultaneous acquisition and interpretation of acoustic, visual, and electrical signals. The integration of artificial intelligence and machine learning enhances the model's ability to classify stable and unstable conditions accurately, making it a highly adaptable solution.

- Weaknesses:
  Although effective in laboratory environments, the model has not yet been deployed in industrial production settings. Its performance remains dependent on sensor calibration and environmental conditions, which may limit scalability in real-world applications.

- Opportunities:
  There is substantial potential for extending this system across different welding processes and industrial sectors. Aligned with the goals of Industry 4.0, the

methodology contributes to process automation, predictive maintenance, and quality control. It also serves as a powerful tool for welder training and academic research.

- Threats:

  Resistance to technological change, especially in industries with established protocols, may slow adoption. Additionally, high initial implementation costs and interference in complex industrial environments pose risks to the widespread integration of the system.

- Challenges:

  Major challenges include scaling the model from laboratory to production environments, ensuring its adaptability to varied metal transfer modes, and maintaining consistent performance when faced with inconsistent material surfaces or adverse conditions such as oxidation or contamination.

- Economic Analysis:

  From a financial standpoint, the methodology presents significant benefits by enabling early detection of instabilities, thus reducing defect rates, material waste, and the need for manual rework. Over time, this contributes to cost savings, greater production efficiency, and a strong return on investment (ROI), making it a viable solution for smart manufacturing.

7 Acknowledgments

This work has been supported by the Brasilia University (UnB), the government research CAPES foundation and CNPQ.

I would like to extend my heartfelt gratitude to my advisor Sadek for their invaluable guidance and unwavering support throughout this journey. Their mentorship has been an inspiration and a driving force in the completion of this work.

I would also like to express my deep appreciation to Guillermo for placing his trust in me and providing me with a remarkable opportunity that significantly contributed to the success of this endeavor.

My heartfelt thanks go to my family for their unflagging support and encouragement. To my mother, who has always been a relentless source of motivation, and to my son, whose unwavering belief in me has been my greatest strength.

Lastly, I am profoundly thankful to my husband for his unwavering belief in my dreams and for steadfastly encouraging me to pursue my goals, even in the face of challenges. His unwavering support has been my rock, and I am immensely grateful for it.

8 References

Adolfsson, S., & Bahrami, A. (1999). On-line quality monitoring in short-circuit gas metal arc welding. *Welding Journal*, *78*(2), 59S-73S. Retrieved from http://www.aws.org/wj/supplement/WJ_1999_02_s59.pdf

Agapkin, O. A., Orlov, Y. V., Persiantsev, I. G., & Dolenko, S. A. (2003). Preprocessing ultrasonic scanning data with the help of Hopfield-style neural network. *Nuclear Instruments and Methods in Physics Research, Section A: Accelerators, Spectrometers, Detectors and Associated Equipment*, *502*(2–3), 520–522. https://doi.org/10.1016/S0168-9002(03)00488-1

Ates, H. (2007). Prediction of gas metal arc welding parameters based on artificial neural networks. *Materials & Design*, *28*(2007), 2015–2023. https://doi.org/10.1016/j.matdes.2006.06.013

Breiman, L., J. Friedman, R. Olshen, and C. S. (1984). Classification and regression trees. In *Wadsworth Books* (Vol. 103). https://doi.org/10.1023/A

Carvalho. (1996). *AN ADAPTIVE CONTROL SYSTEM FOR OFF-LINE PROGRAMMING IN ROBOTIC GAS METAL ARC WELDING*. CRANFIELD UNWERSITY SCHOOL.

Cayo, & Alfaro. (2008). *WELDING QUALITY MEASUREMENT BASED ON ACOUSTIC SENSING.pdf* (Proceedings of COBEM 2007, Ed.). COBEM, ABCM, Brazil.

Cayo, E. (2008). Weld transference modes identification through sound pressure level in GMAW process. *Journal of Achievements in Materials And*, *29*(1), 57–62. Retrieved from http://www.journalamme.org/papers_vol29_1/2918.pdf

CAYO, E. H. (2008). *Monitoramento, Detecção E Localização De Defeitos Na Solda Baseada No Sensoriamento Da Pressão Acústica Do Arco Elétrico No Processo Gmaw-S Eber*. 124.

Cayo, E. H., & Alfaro, S. C. A. (2009). A Non-Intrusive GMA Welding Process Quality Monitoring System Using Acoustic Sensing. *Sensors (Basel, Switzerland)*, *9*(9), 7150–7166. https://doi.org/10.3390/s90907150

CHÁVEZ, J. J. M. (2014). *Uma Metodologia Para Obtenção E Validação De Parâmetros Ótimos Em Soldagem Gmaw Pulsado*. UNB, Brazil.

Correia, D. S., Gonçalves, C. V., Da Cunha, S. S., & Ferraresi, V. A. (2005). Comparison between genetic algorithms and response surface methodology in GMAW welding optimization. *Journal of Materials Processing Technology*, *160*(1), 70–76. https://doi.org/10.1016/j.jmatprotec.2004.04.243

Costa, T. F. (2014). *Avaliação De Critérios De Estabilidade Do Processo Mig / Mag Curto-Circuito Na Soldagem De Aços Inoxidáveis Austenítico E Duplex*. UNIVERSIDADE FEDERAL DE UBERLÂNDIA, Brazil.

Cruz, J. G., Torres, E. M., & Absi Alfaro, S. C. (2015). A methodology for modeling and control of weld bead width in the GMAW process. *Journal of the Brazilian Society of Mechanical Sciences and Engineering*, *37*(5), 1529–1541. https://doi.org/10.1007/s40430-014-0299-8

De Meneses, V. A., Gomes, J. F. P., & Scotti, A. (2014). The effect of metal transfer stability (spattering) on fume generation, morphology and composition in short-circuit MAG welding. *Journal of Materials Processing Technology*, *214*(7), 1388–1397. https://doi.org/10.1016/j.jmatprotec.2014.02.012

de Rezende, G. M. C., Liskévych, O., Vilarinho, L. O., & Scotti, A. (2011). Um critério para determinar a regulagem da tensão em soldagem MIG/MAG por curto-circuito. *Soldagem e Inspecao*, *16*(2), 98–103.

Di, L., Yonglun, S., & Feng, Y. (2000). On line monitoring of weld defects for short-circuit gas metal arc welding based on the Self-Organize feature Map neural networks. *Proceedings of the International Joint Conference on Neural Networks*, *5*, 239–244.

Fan, C., Xie, W., Yang, C., Lin, S., & Fan, Y. (2017). Process Stability of Ultrasonic-Wave-Assisted Gas Metal Arc Welding. *Metallurgical and Materials Transactions A*, *48*(10), 4615–4621. https://doi.org/10.1007/s11661-017-4226-3

Fernandes, D. B., de Menezes Júnior, L. C., Vilarinho, L. O., & Scotti, A. (2010). Ensaio para

medição de nível e alcance de respingos em soldagem MIG/MAG. *Soldagem e Inspecao*, *15*(2), 150–151.

FIGUEIREDO, K. M. DE. (2000). *MAPEAMENTO DOS MODOS DE TRANSFERÊNCIA METÁLICA NA SOLDAGEM MIG DE ALUMÍNIO*. Universidade Federal de Uberlândia, Brazil.

Franco, F. D. (2008). *Real Time Welding Defects Monitoriment Using Spectrometry*. *3*, 784–792.

Ghetiya, N. D., & Patel, K. M. (2014). Prediction of Tensile Strength in Friction Stir Welded Aluminium Alloy Using Artificial Neural Network. *Procedia Technology*, *14*, 274–281. https://doi.org/10.1016/j.protcy.2014.08.036

Grad, L., Grum, J., Polajnar, I., & Slabe, J. M. (2004). Feasibility study of acoustic signals for on-line monitoring in short circuit gas metal arc welding. *International Journal of Machine Tools and Manufacture*, *44*(5), 555–561. https://doi.org/10.1016/j.ijmachtools.2003.10.016

Grum, J., Bergant, Z., & Polajnar, I. (2012). *MONITORING THE GMAW PROCESS BY DETECTION OF WELDING CURRENT , LIGHT INTENSITY AND SOUND*. DEFEKTOSKOPIE 2012, Czech Society for Nondestructive Testing, Czech Republic.

Guillermo Alvarez Bestard. (2017). *SENSOR FUSION AND EMBEDDED DEVICES TO ESTIMATE AND CONTROL THE DEPTH AND WIDTH OF THE WELD BEAD IN REAL TIME*. Universidade de Brasília - UnB, Brazil.

Hermans, M., & Ouden, G. Den. (1999). Process behavior and stability in short circuit gas metal arc welding. *Welding Journal-New York-*, *78*, 137–141. Retrieved from https://app.aws.org/wj/supplement/Hermans/ARTICLE4.pdf%0Ahttp://files.aws.org/wj/supplement/Hermans/ARTICLE4.pdf

Huang, Y., Wang, K., Zhou, Z., Zhou, X., & Fang, J. (2017). Stability evaluation of short-circuiting gas metal arc welding based on ensemble empirical mode decomposition. *Measurement Science and Technology*, *28*(3), 12pp. https://doi.org/10.1088/1361-

6501/aa5746

Igel, C., & Husken, M. (2003). *Empirical evaluation of the improved Rprop learning algorithms*. *50*, 105–123.

Kang, M. J., Kim, Y., Ahn, S., & Rhee, S. (2003). Spatter rate estimation in the short-circuit transfer region of GMAW. *Welding Journal*, *82*(9), 238s-247s.

Kang, & Rhee. (2001). The Statistical Models for Estimating the Amount of Spatter in the Short Circuit Transfer Mode of GMAW. *THE WELDING JOURNAL*, *80*(January), 1–8.

Kim, I. S. J., Son, J. S., Park, C. E., Kim, I. S. J., & Kim, H. H. (2005). An investigation into an intelligent system for predicting bead geometry in GMA welding process. *Journal of Materials Processing Technology*, *159*(1), 113–118. https://doi.org/10.1016/j.jmatprotec.2004.04.415

Kulkarni, S. D., Mallya, U. D., & Chaturvedi, R. C. (1998). Droplet Detachment and Plate Fusion Characteristics in Pulsed Current Gas Metal Arc Welding. *Welding Journal*, *6*(June), 254-s-269-s.

Lopera, J. E. P., Alfaro, S. C. A., & Motta, J. M. S. T. (2012). Modelagem empírica da transferência goticular projetada em processos de soldagem GMAW. *Soldagem e Inspecao*, *17*(4), 335–346. https://doi.org/10.1590/S0104-92242012000400008

Luksa, K. (2006). Influence of weld imperfection on short circuit GMA welding arc stability. *Journal of Materials Processing Technology*, *175*(1–3), 285–290. https://doi.org/10.1016/j.jmatprotec.2005.04.053

Macías, E. J., Roca, A. S., Fals, H. C., Fernández, J. B., & de la Parte, M. P. (2010). Time–frequency diagram applied to stability analysis in gas metal arc welding based on acoustic emission. *Science and Technology of Welding and Joining*, *15*(3), 226–232. https://doi.org/10.1179/136217110X12665778348588

Malviya, R., & Pratihar, D. K. (2011). Tuning of neural networks using particle swarm optimization to model MIG welding process. *Swarm and Evolutionary Computation*,

1(4), 223–235. https://doi.org/10.1016/j.swevo.2011.07.001

Margarita, E., Torres, M., Andrés, J., Cruz, G., Emilio, J., Lopera, P., & Alfaro, S. C. A. (2013). Parameter Optimization in Gmaw Process With Solid and Metal-Cored Wires. *Cobem*, 5256–5266.

Meneses, L. Y. H. (2013). *Modelagem E Simulação Da Transferência Metálica No Processo Gmaw-S Em Soldagem Orbital*. UNB, Brasilia.

Mirapeix, J., García-Allende, P. B., Cobo, A., Conde, O. M., & López-Higuera, J. M. (2007). Real-time arc-welding defect detection and classification with principal component analysis and artificial neural networks. *NDT & E International*, *40*(4), 315–323. https://doi.org/10.1016/j.ndteint.2006.12.001

Mita, Sakabe, & Yokoo. (1988). Quantitative estimates of arc stability for CO 2 gas shielded arc welding. *Welding International*, *2*(2), 152–159. https://doi.org/10.1080/09507118809447460

Moinuddin, S. Q., & Sharma, A. (2015). Arc stability and its impact on weld properties and microstructure in anti-phase synchronised synergic-pulsed twin-wire gas metal arc welding. *Materials and Design*, *67*, 293–302. https://doi.org/10.1016/j.matdes.2014.11.052

Montero Puñales, Elina Mylen; Absi Alfaro, S. C. F. E. G. R. T. (2018). Memorias 6. In I. IV (Ed.), *PREPROCESSING OF DATA OBTAINED IN THE GMAW WELDING PROCESS USING MACHINE LEARNING TECHNIQUES* . (p. 10). Retrieved from https://repositorio.unb.br/bitstream/10482/34346/1/EVENTO_HerramientasAdquisicionDatos.pdf

Mota, C. P., Mendes, R., Neto, F., & Vilarinho, L. O. (2013). *Do Por Curto-Circuito*.

Mousavi, M., & Haeri, M. (2011). Welding current and arc voltage control in a GMAW process using ARMarkov based MPC. *Control Engineering Practice*, *19*(12), 1408–1422. https://doi.org/10.1016/j.conengprac.2011.07.015

Ogunbiyi, B., & Norrish, J. (1997). Monitoring indices for metal transfer in the GMAW process. *Science and Technology of Welding and Joining*, *2*(1), 33–35. https://doi.org/10.1179/stw.1997.2.1.33

P.J. Modenesi, R. C. de A. (1997). The influence of small variations of wire characteristics on gas metal arc welding process stability. *Journal of Materials Processing Technology*, *86*, 226–232. https://doi.org/10.1016/S0924-0136(98)00315-X

Pal, K., & Pal, S. K. (2011). Effect of pulse parameters on weld quality in pulsed gas metal arc welding: A review. *Journal of Materials Engineering and Performance*, *20*(6), 918–931. https://doi.org/10.1007/s11665-010-9717-y

Pinto Lopera, J. E. (2016). *Uso de agentes inteligentes no controle simultâneo da largura e do reforço dos cordões de solda no processo GMAW-S*.

Ponomarev, A. (1997). *Arc welding process statistical analysis. Methodical Approaches, Analysis Conceptions, Experiences.* Denmark: DTU-Helsingor.

Riedmiller, M., & Braun, H. (1993). A direct adaptive method for faster backpropagation learning: the RPROP algorithm. *IEEE International Conference on Neural Networks*, 586–591 vol.1. https://doi.org/10.1109/ICNN.1993.298623

Roca, A. S., Fals, H. C., Fernández, J. B., Macías, E. J., & De La Parte, M. P. (2009). Artificial neural networks and acoustic emission applied to stability analysis in gas metal arc welding. *Science and Technology of Welding and Joining*, *14*(2). https://doi.org/10.1179/136217108X382981

S. W. Campbell, Galloway, A. M., & McPherson, N. A. (2012). Artificial Neural Network Prediction of Weld Geometry Performed Using GMAW with Alternating Shielding Gases. *Welding Journal*, *91*(6), 174–181.

Shao, Y., Wang, Z., & Zhang, Y. (2011). Monitoring of liquid droplets in laser-enhanced GMAW. *International Journal of Advanced Manufacturing Technology*, *57*(1–4), 203–214. https://doi.org/10.1007/s00170-011-3266-x

Silva, C. R., Ferraresi, V. A., & Scotti, A. (2000). A quality and cost approach for welding process selection. *Journal of the Brazilian Society of Mechanical Science and Engineering*, *22*(3), 389–398. https://doi.org/http://dx.doi.org/10.1590/S0100-73862000000300002

Simpson, S. W. (2008). Signature image stability and metal transfer in gas metal arc welding. *Science and Technology of Welding and Joining*, *13*(2), 176–183. https://doi.org/10.1179/174329307x251871

Soderstrom, E. J., & Mendez, P. F. (2008). Metal Transfer during GMAW with Thin Electrodes and Ar-CO 2. *Welding Research*, *87*(May), 124–133.

Souza, Albuquerque, Filho, S., Paula, G. de, Sotero, R. T. M., & Farias. (2012). *IDENTIFICAÇÃO DE DEFEITOS EM JUNTAS SOLDADAS INSPECIONADAS POR ULTRASSOM ATRAVÉS DE REDES NEURAIS ARTIFICIAIS COM PRÉ-PROCESSAMENTO PELA TRANSFORMADA DISCRETA DO COSSENO*. (June 2016).

Souza, D. (2010). *Levantamento de Mapas Operacionais de Transferência Metálica para Soldagem MIG/MAG de Aço ao Carbono na Posição Plana*. Universidad Federal de Uberlândia, Brazil.

Suban, M. (2001). Determination of stability of MIG/MAG welding processes. *Quality and Reliability Engineering International*, *17*(5), 345–353. https://doi.org/10.1002/qre.414

Sumesh, A., Rameshkumar, K., Mohandas, K., & Babu, R. S. (2015). Use of machine learning algorithms for weld quality monitoring using acoustic signature. *Procedia Computer Science*, *50*, 316–322. https://doi.org/10.1016/j.procs.2015.04.042

Sun, H., Yang, J., & Wang, L. (2017). Resistance spot welding quality identification with particle swarm optimization and a kernel extreme learning machine model. *International Journal of Advanced Manufacturing Technology*, *91*(5–8), 1879–1887. https://doi.org/10.1007/s00170-016-9944-y

Wang, Y. C. Z. Y. J. D. D. S. Z. (2019). A Rprop-Neural-Network-Based PV Maximum Power Point Tracking Algorithm with Short-Circuit Current Limitation. *IEEE ISGT NA*

2019, *1*.

Weglowski, M. (2008). Modeling and Analysis of the Arc Light Spectrum in GMAW. *Welding Journal*, *87*(August), 212–218.

Węglowski, M. S., Huang, Y., & Zhang, Y. M. (2008). Relationship between wire feed speed and metal transfer in GMAW. *Journal of Achievements in Materials and Manufactruring Engineering*, *29*(2), 191–194.

Wu, C., Polte, T., & Rehfeldt, D. (2001). A fuzzy logic system for process monitoring and quality evaluation in GMAW. *Welding Journal*, *80*(February), 33–38. Retrieved from http://ww.aws.org/wj/supplement/WJ_2001_02_s33.pdf

Wu, C. S., Gao, J. Q., & Hu, J. K. (2007). Real-time sensing and monitoring in robotic gas metal arc welding. *Measurement Science and Technology*, *18*(1), 303–310. https://doi.org/10.1088/0957-0233/18/1/037

Xiong, J., Zhang, G., Hu, J., & Wu, L. (2014). Bead geometry prediction for robotic GMAW-based rapid manufacturing through a neural network and a second-order regression analysis. *Journal of Intelligent Manufacturing*, *25*(1), 157–163. https://doi.org/10.1007/s10845-012-0682-1

Y.X.Chu, S.J.Hu, W.K.Hou, P.C.Wang, S. P. M. (2004). Signature analysis for quality monitoring in short-circuit GMAW. *Welding Journal*, *83*(12), 336S-343S. Retrieved from http://files.aws.org/wj/supplement/WJ_2004_12_s336.pdf

Yamamoto, E., Yamazaki, K., Suzuki, K., & Koshiishi, F. (2013). Effect of Flux Ratio in Flux-Cored Wire on Wire Melting Behaviour and Fume Emission Rate. *Welding in the World*, *54*(5–6), R154–R159. https://doi.org/10.1007/BF03263501

9 Appendix

Apendix 1

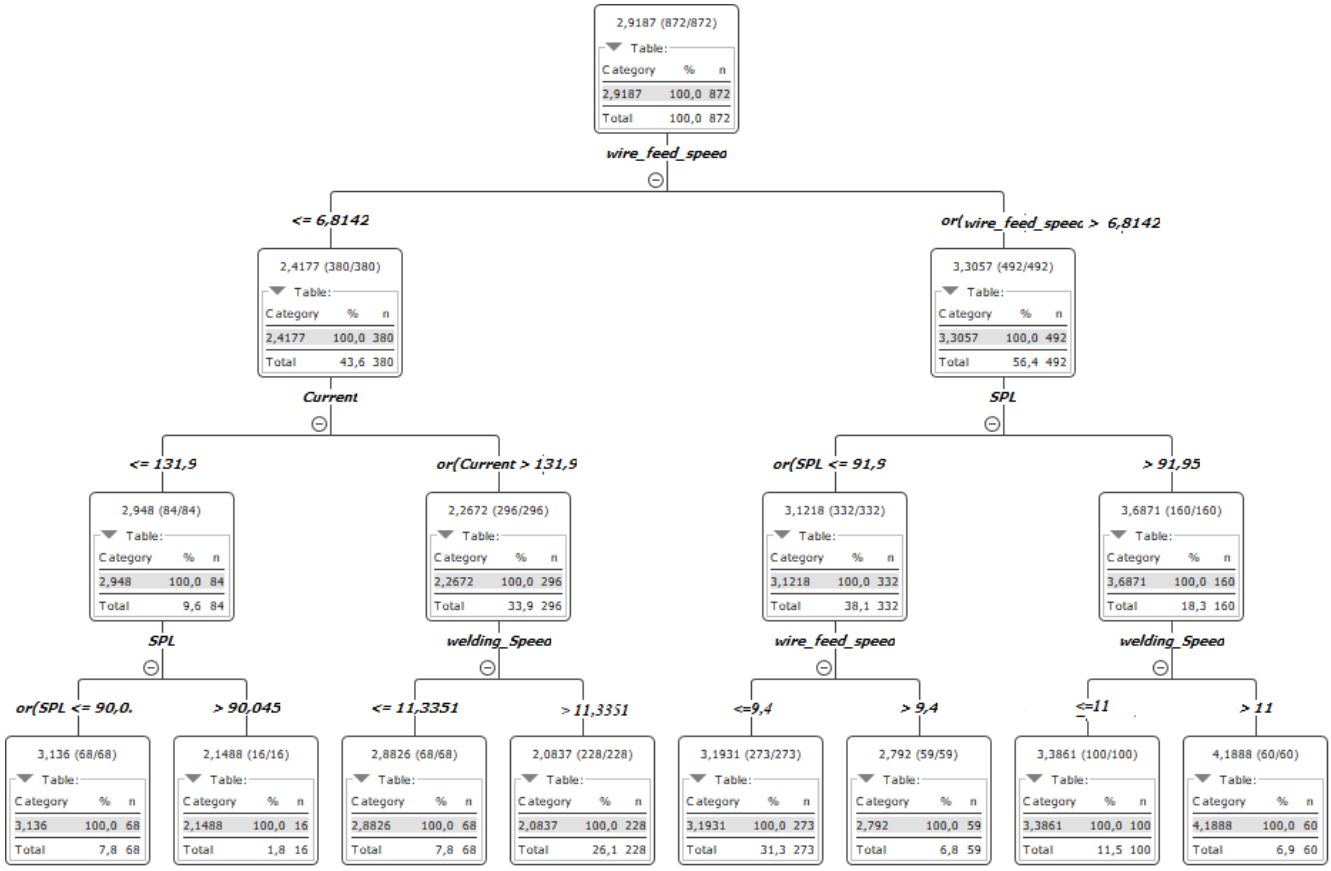

Apendix 2

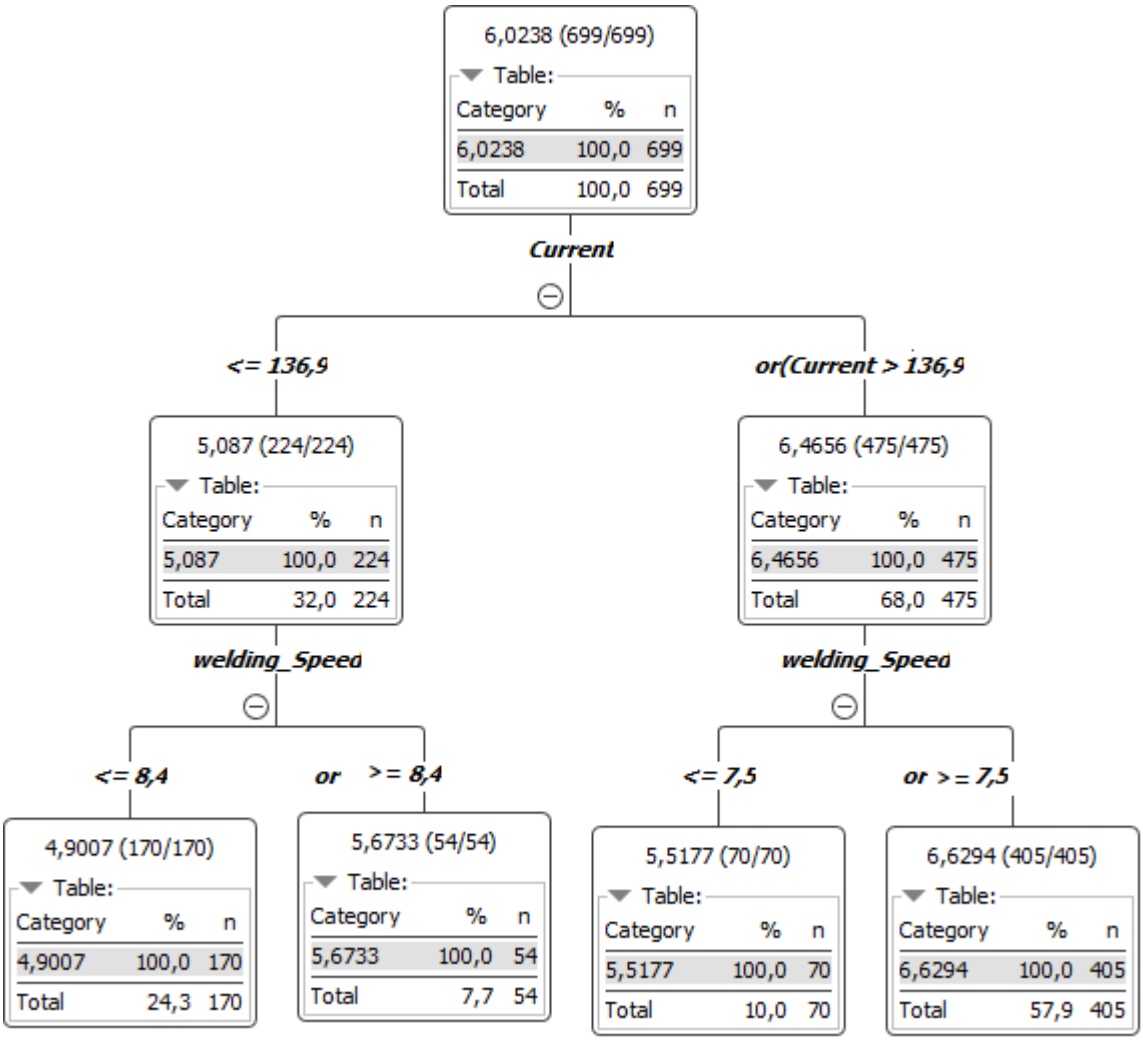
6,0238 (699/699)
Table:
Category % n
6,0238 100,0 699
Total 100,0 699
Current
<= 136,9
or(Current > 136,9
5,087 (224/224)
Table:
Category % n
5,087 100,0 224
Total 32,0 224
6,4656 (475/475)
Table:
Category % n
6,4656 100,0 475
Total 68,0 475
welding_Speed
welding_Speed
<= 8,4
or >= 8,4
<= 7,5
or >= 7,5
4,9007 (170/170)
Table:
Category % n
4,9007 100,0 170
Total 24,3 170
5,6733 (54/54)
Table:
Category % n
5,6733 100,0 54
Total 7,7 54
5,5177 (70/70)
Table:
Category % n
5,5177 100,0 70
Total 10,0 70
6,6294 (405/405)
Table:
Category % n
6,6294 100,0 405
Total 57,9 405

Apendix 3

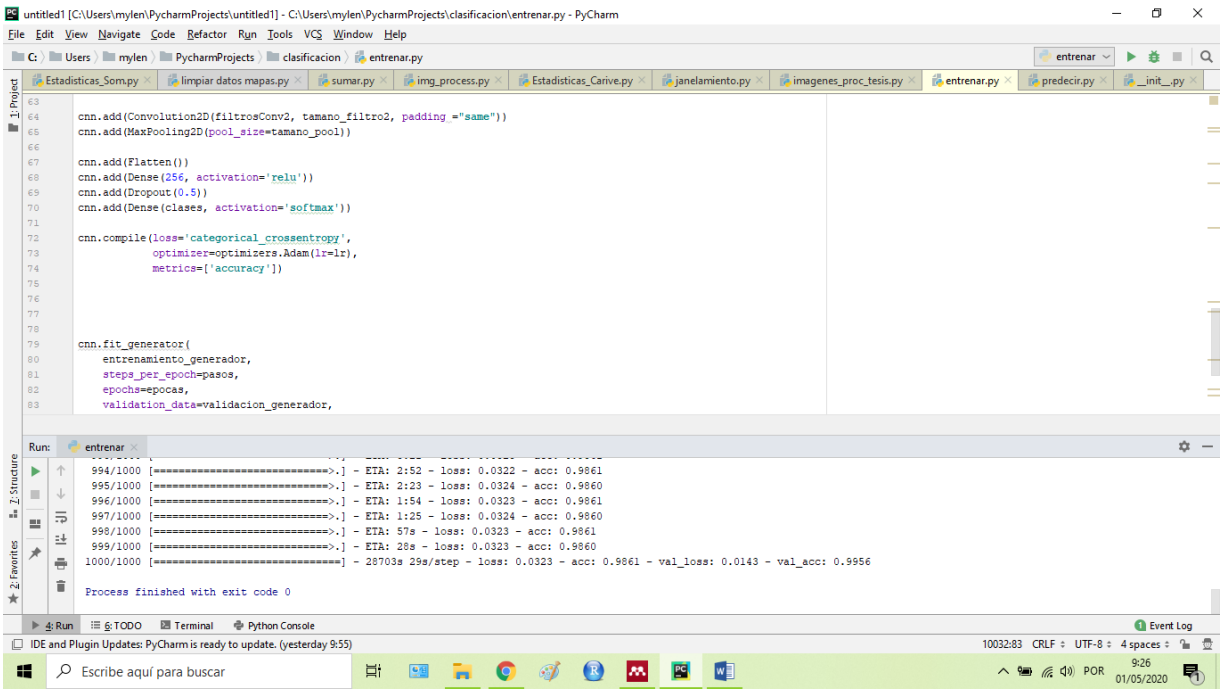

Apendix 4

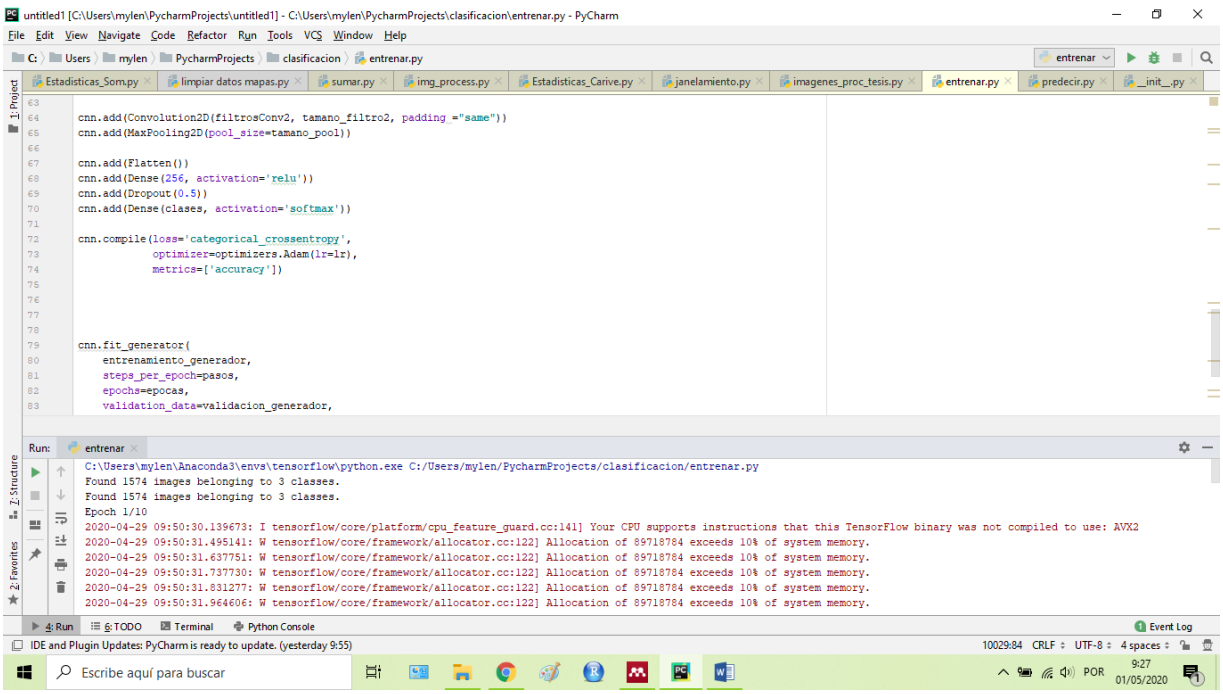

Appendix 5

	A	B	C	D	E	F	G	H	I	J	K	L	M
110	129.90	1.09	130.46	128.5	19.93	19.83	0,02	0.05	0.98	0.98	80.83	0.12	0
111	129.9	1.83	131.08	128.12	19.96	19.85	0,02	0.05	0.97	0.97	80.84	0.09	0
112	mean_A	Std_A	pkv_A	bkg_A	mean_V	bkg_V	TI	DCI	PR	TSI	m_SPL	Std_SPL	Stability
113	130.52	1.40	131.4	129.0	19.93	19.82	0,02	0.05	0.98	0.98	80.85	6.43	1
114	158.15	47.33	201.77	122.45	22.68	21.98	0,31	0.30	0.75	0.62	93.77	3.97	1
115	164.9	47.29	213.37	132.58	22.70	21.92	0,33	0.34	0.77	0.67	95.33	1.34	1
116	165.15	49.85	212.33	126.54	22.64	22.08	0,33	0.24	0.74	0.63	96.12	1.23	1
117	161.95	47.14	211.12	129.16	22.68	22.0	0,33	0.29	0.77	0.64	96.13	1.17	1
118	161.95	50.57	209.88	122.72	22.71	22.32	0,37	0.17	0.74	0.63	95.19	2.00	1
119	179.04	30.62	199.0	152.44	22.86	22.53	0,27	0.14	0.83	0.73	93.51	2.01	1
120	171.4	50.83	225.87	135.08	22.74	22.12	0,39	0.27	0.76	0.66	92.71	2.42	1
121	169.15	49.74	223.12	133.16	22.62	22.1	0,35	0.22	0.76	0.67	93.88	1.65	1
122	158.75	46.76	201.0	124.18	22.57	21.92	0,35	0.28	0.75	0.61	93.88	1.66	1
123	164.35	50.71	212.77	124.72	22.65	21.88	0,34	0.336	0.73	0.67	95.51	1.00	1
124	177.35	33.68	199.41	144.25	22.85	22.67	0,19	0.07	0.80	0.71	93.52	0.81	1
125	178.42	44.78	213.54	139.8	22.68	21.72	0,40	0.42	0.75	0.69	92.79	1.48	1
126	166.95	48.74	217.25	133.41	22.53	21.96	0,37	0.25	0.77	0.65	92.79	1.49	1
127	159.4	47.85	217.57	128.07	22.66	22.22	0,33	0.19	0.78	0.62	96.48	1.26	1
128	169.15	40.63	200.36	131.0	22.80	22.56	0,28	0.10	0.76	0.74	95.03	1.23	1
129	191.2	9.81	199.4	183.0	22.95	22.72	0,24	0.10	0.94	0.81	93.11	0.26	1
130	180.45	43.27	217.1	143.8	22.64	21.98	0,40	0.29	0.77	0.70	93.12	0.27	1
131	164.47	48.38	212.55	128.41	22.49	218.62	0,39	0.30	0.78	0.63	94.20	1.14	1
132	124.4	47.84	165.55	90.72	20.23	19.74	0,45	0.24	0.71	0.53	95.55	2.62	1
133	122.95	52.45	183.57	90.30	20.08	19.68	0,52	0.19	0.71	0.54	93.03	2.89	1
134	111.45	32.94	133.76	70.0	19.94	19.77	0,14	0.08	0.62	0.73	92.49	2.52	1
135	129.5	3.76	133.12	127.08	19.95	19.83	0,04	0.06	0.97	0.93	90.35	0.26	0
136	128.75	2.55	130.8	126.7	19.94	19.87	0,04	0.03	0.98	0.96	89.98	0.22	0
137	128.71	1.95	130.4	127.18	19.94	19.85	0,03	0.04	0.98	0.97	89.77	0.41	0
138	128.9	3.52	132.37	126.58	19.95	19.87	0,04	0.04	0.97	0.94	89.78	0.42	0
139	129.05	2.18	130.9	127.2	19.94	19.84	0,03	0.05	0.98	0.97	89.59	0.28	0
140	128.45	2.99	131.0	125.9	19.94	19.86	0,03	0.04	0.97	0.95	89.26	0.17	0
141	129.65	2.58	131.33	127.12	19.94	19.84	0,03	0.05	0.97	0.96	89.20	0.26	0
142	129.5	2.32	132.14	128.07	19.96	19.84	0,03	0.06	0.98	0.96	89.20	0.27	0